THE APPLICATION OF HERMITE POLYNOMIALS TO TURBULENT DIFFUSION

Thesis submitted in accordance with the requirements of the University of Liverpool for the degree of Doctor in Philosophy

by Deborah Anne Perrin

March 1988

Abstract

This thesis examines the use of an infinite series of orthogonal polynomials to represent the concentration field of a finite quantity of material dispersing in a turbulent flow. The polynomials concerned are generalised, three dimensional Hermite polynomials. The series is used to represent the instantaneous distribution of concentration of material and several of its ensemble mean properties.

Chapter 1 reviews the complete probabilistic description of the distribution of a finite quantity of material dispersing in a turbulent flow. The complexity of the description and the resulting problems associated with investigating the development of the distribution in space and time are highlighted. The chapter concludes with an explanation of the purpose and aims of the thesis.

Chapter 2 outlines some of the previous uses of Hermite series representations. Using a framework of relative diffusion, the generalised Hermite series to be investigated is introduced. An explanation is given of how the series can be used to represent the distribution of concentration and several of its ensemble mean properties for an arbitrary flow field and initial distribution of material.

Chapters 3 and 4 develop the use of Hermite series representations in frameworks of relative and absolute diffusion, respectively, for particular models of dispersion. Chapter 3 applies a three dimensional series to dispersion in a uniform strain velocity field. All possible orientations of the principal strain axes are assumed equiprobable so that the flow is isotropic. A Hermite series is used to represent (a) the instantaneous

concentration field, and (b) the ensemble mean concentration. The effect on the coefficients of the series of the molecular diffusivity, the initial distribution of material and the rate of strain tensor is examined. The effect of particular choices for the arbitrary tensor of each series is also investigated.

Chapter 4 is concerned with a particular model of dispersion in the atmospheric surface layer. Working in a framework of absolute diffusion, a one dimensional Hermite series - analogous to that investigated in chapters 2 and 3 - is used to represent the crosswind integrated mean concentration of material released from an instantaneous point source. The analysis focusses on the use of the first few terms of the series to approximate the expected deviations from the Gaussian of the horizontal downwind distribution of mean concentration. Various choices for the arbitrary functions of the series are investigated. A numerical scheme is applied to calculate higher order coefficients, and hence terms, of the series. The results of the scheme are validated by comparing (a) various numerically calculated measures of quantity, location and spread of material, and (b) the numerically calculated lower order approximations to the horizontal distribution of material, with the corresponding exact results. The numerical results are used to establish the development with height and time of the skewness and kurtosis of the horizontal downwind distribution of material.

Acknowledgements

First and foremost I would like to thank Professor Philip Chatwin, my supervisor, for his willing help and encouragement during this work. It is impossible for me to do justice here to his infectious enthusiasm which was, and remains, an invaluable motivating force.

Special thanks are due to several other people who have helped me during the period of writing up. Dr. Gary Walker and Professor C. Michael of the Department of Applied Mathematics must be mentioned for their kind support and understanding. To Dr. James Irwin and Dr. David Hall of Warren Spring Laboratory, Stevenage, I would like to express my gratitude for their moral and intellectual support.

I am indebted to my family, especially my mother, for their interest in the progress of this work, and in particular for the concern they have shown for me.

I thank Gillian Hannaby for the speed and skill with which she has typed this thesis.

Finally, I acknowledge the receipt of a postgraduate studentship from the University of Liverpool.

Contents

Page

Page

CHAPTER ONE

The Mathematical Description of Turbulent Diffusion

1.1 Introduction

Most flows are turbulent, the flow of the oceans, of blood in the human body and of the atmosphere are all turbulent. Therefore the study of turbulent diffusion is vital to many important practical problems. For example, when a cloud of toxic contaminant is released into the atmosphere, depending on the nature of the contaminant and of its effects, interest may lie in

(a) the likelihood of a known lethal concentration or dosage being exceeded

(b) the concentration of contaminant at any location (usually ground level) averaged over a given period of time

(c) the rate at which the contaminant is removed from the atmosphere by, for example, chemical conversion or deposition.

Consider the following, a situation fundamental to many of these problems. A finite quantity, Q, of material is released from a known initial distribution into an incompressible turbulent velocity field. Assume that the material is passive, so that the material does not influence the behaviour of the velocity field, and that Q is conserved throughout the realisation of the dispersion, so that, for example, no material is absorbed by or deposited on the boundaries of the flow field. Let $\Gamma(\underline{X},t)$ and $\underline{\Upsilon}(\underline{X},t)$ denote the

distribution of concentration of material and of velocity, respectively, a time t after release. Since Q is conserved

$$\int \Gamma(\underline{X},t)\, dV(\underline{X}) = Q \qquad (1.1)$$

and because the flow is incompressible

$$\nabla.\underline{\Upsilon} = 0. \qquad (1.2)$$

Now consider the execution of any number of similar realisations, in each one of which the quantity Q, the initial distributions $\Gamma(\underline{X},0)$ and $\underline{\Upsilon}(\underline{X},0)$, and the origin relative to which $\underline{X}$ is measured are identical. Since the flow is turbulent, the value of $\Gamma(\underline{X},t)$ for each fixed $\underline{X}$ and t will vary from realisation to realisation. In other words, there is an infinite ensemble (i.e. set) of possible realisations of the dispersion.

A description of the variation of $\Gamma(\underline{X},t)$ with $\underline{X}$ and t in any one realisation is not only theoretically impossible - since that of $\underline{\Upsilon}(\underline{X},t)$ is not known - it is also useless from a practical point of view. The only practically useful description is the probabilistic or statistical description of the infinite ensemble of realisations:

$$\{\Gamma^{(n)}(\underline{X},t)\ ; \qquad n=1,2,3,\ldots\} \qquad (1.3)$$

where $\Gamma^{(n)}(\underline{X},t)$ denotes the distribution of concentration in the nth realisation. The problem then is to determine the behaviour of the statistical properties of $\Gamma(\underline{X},t)$ in terms of those of $\underline{\Upsilon}(\underline{X},t)$.

It is worth pointing out that in most problems, because of practical considerations, the ensemble of realisations is defined somewhat differently to that above and, typically, includes all realisations in which the statistical properties of the velocity field $\underline{\Upsilon}(\underline{X},t)$, rather than the initial velocity field $\underline{\Upsilon}(\underline{X},0)$, satisfy certain conditions. For example, when material is to be released into the atmosphere from an industrial plant, the detailed meteorology cannot be predetermined and interest lies in the behaviour of the concentration field in all possible meteorological conditions. In this case the meteorological conditions may be divided into various subsets, for example Pasquill stability class (Pasquill and Smith 1983), and the behaviour of the concentration field in each subset determined. The main point is that the ensemble of realisations must constitute a statistical ensemble (Monin and Yaglom 1971, p.210).

As is illustrated in the next section, the full statistical description of any statistical ensemble, such as (1.3), is extremely complex. In this thesis, attention is focussed on the use of a Hermite series representation for some of the simpler components of the description, viz. the ensemble mean properties of $\Gamma(\underline{X},t)$. Before introducing the Hermite series in Chapter 2, in order to explain the motivation behind and aims of the thesis, it is important in this chapter to review briefly the principles involved in investigating the ensemble mean properties of $\Gamma(\underline{X},t)$ and to outline the information about the concentration field afforded by particular ensemble mean properties. The chapter is not intended to be an exhaustive account, rather use is made of references where appropriate.

Section 1.2 begins with an introduction to probability density functions (p.d.fs) and an explanation of the relationships between the p.d.fs and the ensemble mean properties of $\Gamma(\underline{X},t)$. The concepts of relative and absolute diffusion are also outlined. Section 1.3 introduces both the governing equations for the ensemble mean properties and some definitions of relevance to Chapters 2 and 3. The chapter concludes in Section 1.4 with an outline of the purpose of the thesis.

1.2 The Statistical Description of the Ensemble

1.2.1. Probability Density Functions vs. Ensemble Mean Properties

The statistical description of the infinite ensemble of possible realisations, (1.3), is completely defined in terms of an infinite set of multi-point p.d.fs. Knowing these p.d.fs it is possible to obtain all the information required about the dispersion (Lumley 1970; Monin and Yaglom 1971). For example, in most practical problems interest lies in the probability - or likelihood - of the occurrence of a particular event in any one realisation. In particular, if the contaminant is toxic, interest may lie in the probability of a known toxic level of concentration, θ_T say, being exceeded at $(\underline{X},t)$. Denoting this probability by $p(\theta_T;\underline{X},t)$

$$p(\theta_T;\underline{X},t) = \int_{\theta_T}^{\infty} p(\theta;\underline{X},t)\, d\theta \qquad (1.4)$$

where $p(\theta;\underline{X},t)$ is the one-point p.d.f. defined such that

$p(\theta;\underline{X},t)\delta\theta$ ($\delta\theta$ small and positive) represents the probability that $\Gamma(\underline{X},t)$ lies between θ and $(\theta+\delta\theta)$ i.e.

$$p(\theta;\underline{X},t)\delta\theta = \lim_{M\to\infty}\left\{\frac{1}{M}\ (\text{no. of measurements where } \theta<\Gamma(\underline{X},t)<\theta+\delta\theta)\right\}.$$

Since $\Gamma(\underline{X},t)$ must lie between zero and infinity

$$\int_0^\infty p(\theta;\underline{X},t)\ d\theta = 1. \qquad (1.5)$$

From (1.4) we see that knowing $p(\theta;\underline{X},t)$, $p(\theta_T;\underline{X},t)$ can be determined. Note that for generality, the upper limits of the integrals in (1.4) and (1.5) have been set to infinity and the lower limits to θ_T and zero respectively. However, in practice, for each $(\underline{X},t)$ there will be maximum and minimum attainable concentrations, θ_{max} and θ_{min} say, such that for $\theta>\theta_{max}$ or $\theta<\theta_{min}$, $p(\theta;\underline{X},t)=0$. Therefore (1.4) and(1.5) may be written

$$p(\theta_T;\underline{X},t) = \int_{\theta_T}^{\theta_{max}} p(\theta;\underline{X},t)\ d\theta$$

and

$$\int_{\theta_{min}}^{\theta_{max}} p(\theta;\underline{X},t)\ d\theta = 1$$

respectively.

Generalising (1.4) somewhat and by way of another example, consider a flammable gas which will only combust within a limited range of concentration in air, $\theta_1 < \Gamma(\underline{X},t) < \theta_2$ say. Then the probability that ignitable conditions exist at $(\underline{X},t)$ is given by

$$\text{probability that } (\theta_1 < \Gamma(\underline{X},t) < \theta_2) = p(\theta_1,\theta_2;\underline{X},t) = \int_{\theta_1}^{\theta_2} p(\theta;\underline{X},t)\, d\theta.$$

As an example of a higher order p.d.f. consider the two-point p.d.f. $p(\theta,\phi;\underline{X},\underline{Y},t)$ defined such that $p(\theta,\phi;\underline{X},\underline{Y},t)\delta\theta\delta\phi$ represents the probability that $\Gamma(\underline{X},t)$ lies between θ and $(\theta+\delta\theta)$ if $\Gamma(\underline{Y},t)$ lies between ϕ and $(\phi+\delta\phi)$. Knowing $p(\theta,\phi;\underline{X},\underline{Y},t)$, we can find the probability, $p(\theta_T,\phi_S;\underline{X},\underline{Y},t)$, that $\Gamma(\underline{X},t)$ will exceed θ_T if $\Gamma(\underline{Y},t)$ exceeds ϕ_S since

$$p(\theta_T,\phi_S;\underline{X},\underline{Y},t) = \int_{\theta_T}^{\infty}\int_{\phi_S}^{\infty} p(\theta,\phi;\underline{X},\underline{Y},t)\, d\phi d\theta.$$

Unfortunately the investigation of the p.d.fs is a complex problem both theoretically and practically (Lumley 1970; Monin and Yaglom 1971) and, as discussed below, although it is receiving increased attention, in the past - following the seminal work of people such as Reynolds (1894) and Taylor (1921) - most workers have focussed on a simpler set of parameters associated with the statistical description of the ensemble, viz. the ensemble mean properties of $\Gamma(\underline{X},t)$ (see Monin and Yaglom 1971, 1975 and Pasquill

and Smith 1983 for reviews of the literature).

There are an infinite number of ensemble mean properties of $\Gamma(\underline{X},t)$, each is a mean of a function of $\Gamma(\underline{X},t)$. In order to illustrate how each is defined, consider a subset of the infinite ensemble of realisations (1.3)

$$\{\Gamma^{(n)}(\underline{X},t) \; ; \qquad n=1,2,3,\ldots M\}. \tag{1.6}$$

Since (1.3) is a statistical ensemble, for large enough M and for each fixed $\underline{X}$ and t, the mean value of $\Gamma(\underline{X},t)$ derived from the subset (1.6) varies little as M is increased. That is, letting

$$\gamma = \frac{1}{M} \sum_{r=1}^{M} \Gamma^{(r)}(\underline{X},t)$$

and

$$\overline{\Gamma}(\underline{X},t) = C(\underline{X},t) = \lim_{N\to\infty} \left\{\frac{1}{N} \sum_{r=1}^{N} \Gamma^{(r)}(\underline{X},t)\right\} \tag{1.7}$$

then

$$E\,\{(\gamma - C)^2\}(\underline{X},t) \to 0 \quad \text{as} \quad M \to \infty$$

where an overbar has been used to denote the taking of the mean of an infinite ensemble of values and E represents the expected (or mean) value. Equation (1.7) defines $C(\underline{X},t)$, the ensemble mean concentration and the simplest ensemble mean property of $\Gamma(\underline{X},t)$.

Similarly, for any function of $\Gamma(\underline{X},t)$, $f(\Gamma)$ say, it is possible to define an ensemble mean $\overline{f(\Gamma)}(\underline{X},t)$ by

$$\overline{f(\Gamma)}(\underline{X},t) = \lim_{N\to\infty} \left\{\frac{1}{N} \sum_{r=1}^{N} f(\Gamma^{(r)})(\underline{X},t)\right\}. \tag{1.8}$$

Expressing $\Gamma(\underline{X},t)$ as the sum of its mean and deviation from the mean, $c(\underline{X},t)$ say, we have

$$\begin{aligned} &\Gamma(\underline{X},t) = C(\underline{X},t) + c(\underline{X},t) \\ &\bar{\Gamma}(\underline{X},t) = C(\underline{X},t) \; ; \; \bar{c}(\underline{X},t) = 0. \end{aligned} \tag{1.9}$$

Some elementary properties of $C(\underline{X},t)$ and $c(\underline{X},t)$ now follow. Taking the ensemble mean of (1.1) and using (1.9b and c)

$$\int C(\underline{X},t)\, dV(\underline{X}) = Q \; ; \qquad \int c(\underline{X},t)\, dV(\underline{X}) = 0. \tag{1.10}$$

In other words, for any fixed t, the total amount of "C-stuff" is conserved and is equal to Q whilst the sum of the fluctuations from the mean is identically zero so that $c(\underline{X},t)$ must take on both positive and negative values. Since $\Gamma(\underline{X},0)$ is fixed from realisation to realisation, using (1.9)

$$\Gamma(\underline{X},0) = C(\underline{X},0) \; ; \qquad c(\underline{X},0) = 0. \tag{1.11}$$

It is important to emphasise that, in general, without making simplifying assumptions (Birch, Brown, Dodson and Thomas 1978; Hanna

1984a; Lockwood and Naguib 1975; Sawford and Stapountzis 1986), the ensemble mean properties cannot be used to calculate the probability of the occurrence of a particular event in any one realisation, such as $p(\theta_T;\underline{X},t)$ defined by (1.4). However each ensemble mean property can be expressed in terms of the moments of $p(\theta;\underline{X},t)$ and therefore gives information about the distribution of $p(\theta;\underline{X},t)$ with θ (Lumley 1970; Monin and Yaglom 1971). For example, $C(\underline{X},t)$ is the first moment of $p(\theta;\underline{X},t)$ i.e.

$$C(\underline{X},t) = \overline{\Gamma}(\underline{X},t) \int_0^\infty \theta\, p(\theta;\underline{X},t)\, d\theta. \tag{1.12}$$

Therefore for each fixed $\underline{X}$ and t, $C(\underline{X},t)$ locates the position of the centroid of the distribution of $p(\theta;\underline{X},t)$. The shape of the distribution of $p(\theta;\underline{X},t)$ is given by its higher order moments about $C(\underline{X},t)$. For example, the mean square fluctuation, $\overline{c^2}(\underline{X},t)$, is the variance of $p(\theta;\underline{X},t)$ and gives information on the spread of $p(\theta;\underline{X},t)$ about $C(\underline{X},t)$ i.e.

$$\overline{c^2}(\underline{X},t) = \overline{(\Gamma - C)^2}(\underline{X},t) = (\overline{\Gamma^2} - C^2)(\underline{X},t) = \int_0^\infty (\theta - C)^2\, p(\theta;\underline{X},t)\, d\theta. \tag{1.13}$$

$C(\underline{X},t)$ and $\overline{c^2}(\underline{X},t)$, especially $C(\underline{X},t)$, are the most studied of the ensemble mean properties of $\Gamma(\underline{X},t)$. However $\overline{c^2}(\underline{X},t)$ is of fundamental importance to most problems, for example assessing the effect of the release of a toxic material, since it gives information on the spread of concentration levels about the mean. The ratio

$$I = \frac{\sqrt{\overline{c^2}(\underline{X},t)}}{C(\underline{X},t)} \qquad (1.14)$$

is commonly used as a measure of the variability between realisations (Csanady 1973; Hanna 1984a; Wilson, Robins and Fackrell 1985). If I is much less than one, the fluctuations can be considered negligible and knowledge of $C(\underline{X},t)$ alone is adequate. However, as discussed by Chatwin (1982) and Carn and Chatwin (1985), there is plenty of experimental evidence of values of I of the order of 1-10, so knowledge of $C(\underline{X},t)$ alone is often inadequate. Recently, in recognition of the significance of $\overline{c^2}(\underline{X},t)$, more work has been devoted to developing and assessing appropriate models, in particular in the context of modelling plume dispersal in the atmospheric boundary layer (see Hanna 1984b for a review also Carn and Chatwin 1985; Sawford and Hunt 1986). Such work has also been prompted by the developments of better theoretical and practical techniques for studying p.d.fs, in particular $p(\theta;\underline{X},t)$. It is not the purpose of this work to detail these developments, rather just to indicate that the study of p.d.fs is accelerating and is likely, eventually, to receive as much attention as has the study of $C(\underline{X},t)$ in the past. Detailed references to the pioneering papers in the study of p.d.fs and to subsequent developments are given by Birch, Brown, Dodson and Thomas (1978), Fackrell and Robins (1982) and Kowe and Chatwin (1985).

1.2.2 The Choice of Coordinate Framework

Finally in this section, it is important to describe briefly one aspect of the ensemble of realisations (1.3) which has profound

implications, in particular for the value of the ensemble mean properties.

So far the only restriction that has been placed on the choice of coordinate framework is that it is well defined and does not vary from realisation to realisation. For a long time it has been recognised that there are at least two distinct types of framework which can be used profitably to study turbulent diffusion

(a) absolute diffusion

and (b) relative diffusion.

These are also known as Eulerian and Lagrangian frameworks respectively. In a framework of absolute diffusion, the identifying property of the material - such as its temperature or concentration - is measured relative to a point either fixed in space or moving with a uniform velocity. For example, the concentration of the cloud considered above could be measured relative to the initial position ($t=0$) of the centre of mass of the cloud. In a framework of relative diffusion, the identifying property is measured relative to a point which moves with the material, for example the instantaneous position of the centre of mass of the cloud.

The implications of, and advantages associated with evaluating the ensemble mean properties in this latter framework have been discussed in detail by several authors (Batchelor 1952; Chatwin 1982; Chatwin and Sullivan 1979a; Csanady 1973; Monin and Yaglom 1975). The essential point to recognise is that with $\underline{X}$ measured relative to the centre of mass of the cloud, as is evident from (1.7) and (1.8), at any time t after release, the distribution of $C(\underline{X},t)$ or any ensemble mean property is only evaluated once the centres of mass

of each instantaneous distribution $\Gamma^{(n)}(\underline{X},t)$, n=1,2,..., have been made coincident. Now in many practical problems, at least in the early stages of dispersion, the displacement of the centre of mass of the cloud in a given time, predominates the distortion of the material about its centre of mass in the same time. That is, because the linear dimensions of the cloud are much smaller than those of the energy containing eddies of the flow, the cloud of material meanders through the flow with the shape of its distribution changing relatively slowly. Ensemble mean properties evaluated within a framework of relative diffusion are not subject to the smearing effects of this meandering which are inherent in, and often dominate, the distributions of those evaluated in any framework of absolute diffusion. In particular, the magnitude of the ensemble mean concentration in relative diffusion is often much closer to the actual concentration than that evaluated in a framework of absolute diffusion (Chatwin 1982; Csanady 1973, p.82). In spite of this advantage of relative diffusion, it must be acknowledged that in many problems the distribution of concentration relative to a fixed structure, such as a gas storage container, or a particular topographical feature, is the main concern. In these cases a framework of absolute diffusion is obviously appropriate.

In this thesis, and for the reasons explained later in the text, both types of framework are considered. The analyses of Chapters 2 and 3 are performed in a framework of relative diffusion whilst the problem considered in Chapter 4 uses a framework of absolute diffusion. For clarity, in the remainder of this Chapter and in Chapters 2 and 3, lower case characters, such as $\underline{x}$ and $\underline{y}$, will be used to denote vectors measured in a framework of relative diffusion and upper case characters, such as $\underline{X}$ and $\underline{Y}$, will be

reserved for denoting an arbitrary framework.

1.3 Equations and Definitions

1.3.1 The Governing Equations of the Ensemble Mean Properties

The problems involved in the theoretical investigation of each of the ensemble mean properties of $\Gamma(\underline{X},t)$ are typified by those of $C(\underline{X},t)$.

Using the summation convention over repeated subscripts, the governing equation for $\Gamma(\underline{X},t)$ may be written (Monin and Yaglom 1971, p.581)

$$\frac{\partial \Gamma}{\partial t} + \tau_i \frac{\partial \Gamma}{\partial X_i} = K \frac{\partial^2 \Gamma}{\partial X_j \partial X_j} \tag{1.15}$$

where K is the molecular diffusivity. Let $\underline{\tau}(\underline{X},t)$ be expressed as the sum of its ensemble mean, $\underline{U}(\underline{X},t)$, and its deviation from this mean, $\underline{u}(\underline{X},t)$, so that (compare (1.9))

$$\begin{aligned} \tau_i &= U_i + u_i \\ \bar{\tau}_i &= U_i \; ; \quad \bar{u}_i = 0 \end{aligned} \tag{1.16}$$

Then, substituting (1.16a) and (1.9a) into (1.15), taking the ensemble mean and using (1.2), (1.16b and c) and (1.9b and c) leads to

$$\frac{\partial C}{\partial t} + \frac{\partial}{\partial X_i}(U_i C + \overline{u_i c}) = K \frac{\partial^2 C}{\partial X_j \partial X_j} \; . \tag{1.17}$$

This is the governing equation for $C(\underline{X},t)$. Since it involves $c(\underline{X},t)$ it is not closed, nor is any finite subset of the infinite set of equations which govern the ensemble mean properties of $\Gamma(\underline{X},t)$. For example, subtracting (1.17) from (1.15), multiplying by (2c) and taking the ensemble mean leads to the governing equation for $\overline{c^2}(\underline{X},t)$

$$\frac{\partial \overline{c^2}}{\partial t} + U_i \frac{\partial \overline{c^2}}{\partial X_i} + \frac{\partial}{\partial X_i}(\overline{u_i c^2}) + 2\overline{u_i c}\frac{\partial C}{\partial X_i} = K\frac{\partial^2 \overline{c^2}}{\partial X_j \partial X_j} - 2K\overline{\left[\frac{\partial c}{\partial X_j}\right]^2} \qquad (1.18)$$

which includes $(\overline{\underline{u}c})$ and (∇c). This fundamental problem has led to a substantial amount of literature devoted to the analyses of closure hypotheses (Monin and Yaglom 1971, 1975). The majority of this work has been devoted to investigating closure hypotheses for the equation for $C(\underline{X},t)$, (1.17), although recently more attention has been paid to closure hypotheses for (1.18) (see discussions by Hanna 1984b and Sykes, Lewellen and Parker 1984). The application of many of these hypotheses can only be justified for simplified flows, in particular homogeneous or stationary flows. One major advantage of the Hermite series representation to be examined in this thesis is that its applicability is not restricted to simplified flows. This point is discussed further in Section 1.4.

1.3.2 Properties and Definitions of Ensemble Mean Properties in Relative Diffusion

By definition, the concentration field of a cloud of contaminant measured relative to the centre of mass of the cloud,

$\Gamma(\underline{x},t)$, satisfies

$$\int x_i \, \Gamma(\underline{x},t) \, dV(\underline{x}) = 0. \tag{1.19}$$

Therefore, using (1.9) and (1.19)

$$\int x_i \, C(\underline{x},t) \, dV(\underline{x}) = 0; \qquad \int x_i \, c(\underline{x},t) \, dV(\underline{x}) = 0. \tag{1.20}$$

As well as $C(\underline{x},t)$ and $\overline{c^2}(\underline{x},t)$, two other ensemble mean properties of $\Gamma(\underline{x},t)$ will also be discussed in Chapter 2, namely the distance-neighbour function $p(\underline{y},t)$ (Batchelor 1952; Chatwin and Sullivan 1979a, 1980a; Richardson 1926; Sullivan 1971, 1975, 1976) and the correlation function $r(\underline{y},t)$ (Chatwin and Sullivan 1978, 1979b, 1980a) defined by

$$p(\underline{y},t) = Q^{-2} \int \overline{\Gamma(\underline{x},t) \, \Gamma(\underline{x}+\underline{y},t)} \, dV(\underline{x})$$

$$= Q^{-2} \int \{C(\underline{x},t) \, C(\underline{x}+\underline{y},t) + \overline{c(\underline{x},t) \, c(\underline{x}+\underline{y},t)}\} \, dV(\underline{x}) \tag{1.21}$$

$$r(\underline{y},t) = p(\underline{y},t) - Q^{-2} \int C(\underline{x},t) \, C(\underline{x}+\underline{y},t) \, dV(\underline{x})$$

$$= Q^{-2} \int \overline{c(\underline{x},t) \, c(\underline{x}+\underline{y},t)} \, dV(\underline{x}). \tag{1.22}$$

In order to interpret $p(\underline{y},t)$ and $r(\underline{y},t)$ consider $Q^{-1} \, \Gamma(\underline{x},t)dV(\underline{x})$ and $Q^{-1} \, \Gamma(\underline{x}+\underline{y},t)dV(\underline{y})$. These represent the proportions of contaminant in volume elements of size $dV(\underline{x})$ and $dV(\underline{y})$ surrounding $\underline{x}$ and $(\underline{x}+\underline{y})$ respectively. Thus when molecular diffusion, K, is negligible $p(\underline{y},t)dV(\underline{y})$ is the average of the proportion of the volume of contaminant within which the origin of

the vector $\underline{y}$ must lie so that a volume $dV(\underline{y})$ surrounding the other end of $\underline{y}$ will also contain contaminant. $r(\underline{y},t)$ is the contribution to $p(\underline{y},t)$ from the fluctuations in concentration. Its Fourier transform is the energy spectrum of $\int \overline{c^2}(\underline{x},t)\, dV(\underline{x})$.

1.4 Purpose of the Thesis

The purpose of this thesis is to show how a series of generalised Hermite polynomials can be used to represent $\Gamma(\underline{X},t)$ and several of its ensemble mean properties, and investigate the use of the representations.

The previous sections have given an overview of the complete mathematical description of a cloud of material dispersing in turbulent flow. Some of the problems associated with examining the development of the distribution of the material in space and time have been highlighted. The aim of doing this was to identify several points which emphasise the advantages of the Hermite series representations to be investigated here. Before introducing the representations in Chapter 2, it is useful to summarise these advantages.

First, the representations can be applied in frameworks of absolute or relative diffusion (Section 1.2.2). Second, the applicability of the representations is not restricted to simplified flows. Rather, in theory the representations can be applied to any flow although, in practice, their use may be more suited to particular types of flow (Section 1.3.1). Finally, the use of the general representation is not restricted to $C(\underline{X},t)$, rather it can be applied to $\Gamma(\underline{X},t)$ or any one of its ensemble mean properties

which satisfies some fairly simple rules. Many of the ensemble mean properties satisfy these rules, including $\overline{c^2}(\underline{X},t)$.

It is not worth elaborating further on these points at this stage since they will be justified in subsequent chapters. As will become clear in Chapter 2, a comprehensive investigation of the use of the representations is beyond the scope of this work. However, the work does attempt to develop various, selected strands of the investigation in a way that accentuates the advantages of the representations.

CHAPTER TWO

A Three Dimensional Hermite Series Representation for $\Gamma(\underline{x},t)$ and its Ensemble Mean Properties

2.1 Introduction

The aim of this chapter is threefold. First, to show how $\Gamma(\underline{x},t)$ and a number of its ensemble mean properties, for example $C(\underline{x},t)$, $\overline{c^2}(\underline{x},t)$ and $p(\underline{y},t)$, can be represented by a generalised three dimensional Hermite series. Secondly, to explain why it appears worthwhile to investigate the use of these representations. Thirdly, to explain the rationale behind the approach adopted in the rest of the thesis to beginning this investigation.

A Hermite series representation, in the form of a Gram-Charlier series or Edgeworth series, is conventionally used in turbulence to analyse deviations from the Gaussian of a non-random function. However, Chatwin and Sullivan (1980a) have shown how a generalised three dimensional Hermite series can be used to represent a correlation function of the cloud $(r(\underline{y},t))$, which by virtue of its invariant properties can never be Gaussian, not even approximately so. Their results suggest the representation should be of practical value. In Sections 2.3-2.5, the use of this representation is extended to $\Gamma(\underline{x},t)$ and several of its other ensemble mean properties.

Initially, in Section 2.2, in order to emphasise both the naturalness of the representations and the ease with which they can be handled, brief descriptions are given of the one dimensional Gram-Charlier and Edgeworth series. Some simple examples are used

to illustrate their conventional use and the analogous three dimensional series are defined.

2.2 The Gram-Charlier and Edgeworth Series Representations

2.2.1 The One Dimensional Series

The Gaussian distribution is the solution to many simplified models of problems in turbulence (Batchelor 1952; Pasquill and Smith 1983; Taylor 1953, 1954a). For example, in one of the simplest models of dispersion in the atmospheric surface layer, the ensemble mean concentration, $\chi(x,y,z,t)$, of a quantity, Q, of passive, conserved material released from a ground-level point source is given by the three dimensional Gaussian distribution (Csanady 1973)

$$\chi(x,y,z,t) = \frac{Q}{(2\pi)^{3/2}\,\sigma_x\,\sigma_y\,\sigma_z} \exp\left\{-\frac{1}{2}\left[\frac{x^2}{\sigma_x^2}+\frac{y^2}{\sigma_y^2}+\frac{z^2}{\sigma_z^2}\right]\right\} \qquad (2.1)$$

where the x,y,z axes are taken in the horizontal downwind, horizontal crosswind and vertical directions, respectively, with the origin fixed at the centre of mass of the cloud. σ_x, σ_y and σ_z represent the root mean square deviations of the distributions in the appropriate directions. For example

$$\sigma_x^2 = \frac{\int x^2 \chi\, dxdydz}{\int \chi\, dxdydz} = Q^{-1} \int x^2 \chi\, dxdydz.$$

Integrating (2.1) over y and t, the corresponding one dimensional Gaussian model of diffusion from an infinite, continuous, crosswind

line source is obtained i.e.

$$\chi_{\ell}(x,z) = \frac{Q_{\ell}}{\sqrt{2\pi}\, U\, \sigma_z} \exp\left[-\frac{1}{2}\frac{z^2}{\sigma_z^2}\right]$$

where the axes are now taken fixed at the source, the mean velocity, U, is assumed constant and parallel to the x axis and Q_{ℓ} represents the quantity of material released per unit length per unit time.

In many of these problems (Chatwin 1970, 1980; Chatwin and Sullivan 1981; Lupini and Tirabassi 1983; Smith 1978, 1982a, 1982b, 1982c, 1985) the deviations from the Gaussian have been investigated by representing the actual property by the first few terms of its Gram-Charlier series (type A) - hereafter referred to simply as the Gram-Charlier series - or Edgeworth series (Cramer 1946; Kendall and Stuart 1969; Mihaila 1968).

In order to illustrate the main features of each series it is sufficient to consider their one dimensional forms. Higher dimensional Gram-Charlier series and Edgeworth series are considered in depth elsewhere (Chambers 1967; Kampé de Fériet 1966; Kendall and Stuart 1969; Mihaila 1968) and are therefore defined in Section 2.2.2 without detailed consideration.

First, consider an arbitrary well-defined function $f(z)$ (the conditions $f(z)$ must satisfy to be represented by a Gram-Charlier series or Edgeworth series are discussed by Kendall and Stuart 1969). For simplicity, let $f(z)$ be expressed in standard measure i.e.

$$\int_{-\infty}^{\infty} f(z)\, dz = 1; \quad \int_{-\infty}^{\infty} z\, f(z)\, dz = 0; \quad \int_{-\infty}^{\infty} z^2\, f(z)\, dz = 1. \qquad (2.2)$$

The Gram-Charlier series of $f(z)$ may be written

$$f(z) = \frac{1}{\sqrt{2\pi}} \sum_{n=0}^{\infty} F_n H_n(z) \exp\left[-\frac{1}{2} z^2\right] \tag{2.3}$$

where the one dimensional Hermite polynomials $H_n(z)$, $n=1,2,\ldots,$ are defined by (Kendall and Stuart 1969)

$$H_n(z) \exp\left[-\frac{1}{2} z^2\right] = (-1)^n \frac{d^n}{dz^n} \left\{\exp\left[-\frac{1}{2} z^2\right]\right\}.$$

For example,

$$H_0(z) = 1; \qquad H_1(z) = z; \qquad H_2(z) = z^2 - 1.$$

Using the orthogonality property of the polynomials

$$\frac{1}{\sqrt{2\pi}} \int_{-\infty}^{\infty} H_n(z)\, H_m(z) \exp\left[-\frac{1}{2} z^2\right] dz = n!\, \delta_{nm}$$

the following expression for the coefficients of the series is obtained

$$F_n = \frac{1}{n!} \int_{-\infty}^{\infty} H_n(z)\, f(z)\, dz \qquad n = 1,2,\ldots . \tag{2.4}$$

In other words, if n is odd, F_n is dependent on all the odd moments of $f(z)$ of order $\leq n$ and, if n is even, F_n is dependent on all the even moments of $f(z)$ of order $\leq n$. For

example, using (2.2) and (2.4)

$$F_0 = 1$$

$$F_1 = F_2 = 0$$

$$F_3 = \frac{1}{3!}\int_{-\infty}^{\infty} H_3(z)\, f(z)\, dz = \frac{1}{3!}\int_{-\infty}^{\infty} z^3\, f(z)dz$$

$$F_4 = \frac{1}{4!}\int_{-\infty}^{\infty} H_4(z)\, f(z)\, dz = \frac{1}{4!}\left\{\int_{-\infty}^{\infty} z^4\, f(z)\, dz - 3\right\}.$$

Thus the first few terms of (2.3) may be written

$$f(z) = \frac{1}{\sqrt{2\pi}}\left\{1 + F_3H_3(z) + F_4H_4(z) + \ldots\right\}\exp\left[-\frac{1}{2}z^2\right]$$

so that the first term of the Gram-Charlier series of $f(z)$ is the Gaussian distribution with the same mean and variance as $f(z)$, subsequent terms represent the deviation of $f(z)$ from the Gaussian.

In many practical and theoretical problems it is not possible to determine completely the behaviour of the function $f(z)$ but the behaviour of the lower order moments of $f(z)$ can be determined, hence so can the approximation to $f(z)$ afforded by the corresponding initial terms of (2.3). In these problems therefore, interest lies in whether the initial terms of (2.3) give a better approximation to $f(z)$ than the Gaussian, in particular whether (2.3) is an asymptotic representation for $f(z)$. In most practical problems interest lies in the approximation to $f(z)$ afforded by the first five terms of (2.3) viz.

$$f_G(z) = \frac{1}{\sqrt{2\pi}} \left\{1 + \frac{\beta_3}{3!} H_3(z) + \frac{\beta_4}{4!} H_4(z)\right\} \exp\left[-\frac{1}{2} z^2\right] \qquad (2.5)$$

since moments of order higher than four calculated from measurements are usually subject to large errors (Kendall and Stuart 1969). In (2.5) the dimensionless parameters β_3 and β_4 represent the skewness and kurtosis of $f(z)$ respectively (Kendall and Stuart 1969; Lumley 1970) i.e.

$$\beta_3 = 3!\, F_3 = \int_{-\infty}^{\infty} z^3 f(z)\, dz; \qquad \beta_4 = 4!\, F_4 = \int_{-\infty}^{\infty} z^4 f(z)\, dz - 3.$$

If $f(z)$ is Gaussian, β_3 and β_4 are identically zero.

An example application of (2.5) is shown in Fig. 2.1 where $f(z)$ has been taken equal to the normalised gamma function expressed in standard measure

$$f(z) = \frac{\sqrt{p}}{(p-1)!} \exp(-s)\, s^{(p-1)}, \quad z = \frac{(s-p)}{p}, \quad s > 0, \quad p \text{ a constant} > 0. \qquad (2.6)$$

It is seen that for $p=16$ (Fig. 2.1a), β_3 and β_4 are both fairly close to zero (0.5 and 0.375 respectively) and (2.5) appears to give a satisfactory approximation to $f(z)$. However, for $p=2$ (Fig. 2.1b), $\beta_3 (=\sqrt{2})$ and $\beta_4 (=3)$ are further from the Gaussian values and the approximation is unsatisfactory.

For a class of frequency functions often encountered in statistical theory, the Gram-Charlier series (2.3) is not an asymptotic representation. Edgeworth has proposed an alternative

series which is an asymptotic representation for this class (Cramer 1946; Kendall and Stuart 1969). The important point to make here is that the Edgeworth series is in fact a rearrangement of the terms of the Gram-Charlier series (2.3). The first few terms of the Edgeworth series are

$$f_E(z) = \frac{1}{\sqrt{2\pi}} \left\{1 + \frac{\beta_3}{3!} H_3(z) + \frac{\beta_4}{4!} H_4(z) + \frac{10}{6!} (\beta_3)^2 H_6(z)\right\} \exp\left[-\frac{1}{2} z^2\right]. \tag{2.7}$$

For the same reasons as for the Gram-Charlier series, only these terms are considered in most practical problems.

In Figs. 2.1c and 2.1d, the approximation given by (2.7) to the previous example function, (2.6), is compared with the corresponding Gram-Charlier series approximation and with the exact function. For both $p=16$ and $p=2$, the Edgeworth series approximation is more satisfactory than the Gram-Charlier series approximation.

2.2.2 Higher Dimensional Series

Higher dimensional Gram-Charlier and Edgeworth series may also be defined (Chambers 1967; Kampé de Fériet 1966; Kendall and Stuart 1969; Lumley 1970; Mihaila 1968). In particular, the three dimensional Gram-Charlier series of a function $F(\underline{z})$ where

$$\int F(\underline{z})\, dV(\underline{z}) = 1; \quad \int z_i\, F(\underline{z})\, dV(\underline{z}) = 0;$$

$$\int z_i z_j\, F(\underline{z})\, dV(\underline{z}) = s_{ij} \tag{2.8}$$

may be written

$$F(\underline{z}) = n(\underline{\sigma}) \sum_{m=0}^{\infty} F^{(m)}_{ij\ldots k} H^{(m)}_{ij\ldots k}(\underline{z}, \underline{\sigma}) \exp\left[-\frac{1}{2}\sigma_{pq} z_p z_q\right]. \quad (2.9)$$

In (2.9) the summation convention over repeated subscripts has been used, $n(\underline{\sigma})$ is given by equation (A5) of Appendix A, m represents the number of subscripts $ij\ldots k$ and the positive-definite, symmetric tensor σ_{ij} is such that

$$s_{ij}\,\sigma_{jk} = \delta_{ik}$$

where s_{ij} is given by (2.8c).

The Hermite polynomials of three variables $H^{(n)}_{ij\ldots k}(\underline{z}, \underline{\sigma})$, $n=1,2,\ldots,$ are defined by

$$H^{(n)}_{ij\ldots k}(\underline{z}, \underline{\sigma}) \exp\left[-\frac{1}{2}\sigma_{pq} z_p z_q\right] = (-1)^n \frac{\partial^n}{\partial z_i \partial z_j \ldots \partial z_k} \exp\left[-\frac{1}{2}\sigma_{pq} z_p z_q\right].$$

Some properties of the polynomials are given in Appendix A along with further references. Using equations (A10)-(A12), (2.8) and (2.9)

$$F^{(0)} = 1; \qquad F^{(1)}_i = F^{(2)}_{ij} = 0.$$

Thus (2.9) may be written

$$F(\underline{z}) = n(\underline{\sigma}) \left\{ F^{(0)} + \sum_{m=3}^{\infty} F^{(m)}_{ij\ldots k} H^{(m)}_{ij\ldots k}(\underline{z}, \underline{\sigma}) \right\} \exp\left[-\frac{1}{2} \sigma_{pq} z_p z_q \right]. \tag{2.10}$$

2.3 The Hermite Series Representations

In Section 2.2 evidence was given of the practical and theoretical value of two particular Hermite series representations, the Gram-Charlier series and Edgeworth series. It is now possible to appeal to this evidence and other results to suggest general representations for $\Gamma(\underline{x},t)$ and several of its ensemble mean properties, in particular $C(\underline{x},t)$, $\overline{c^2}(\underline{x},t)$, $p(\underline{y},t)$ and $r(\underline{y},t)$. Here, the word 'general' is used to signify a representation which requires no assumptions to be made about the turbulent nature of the flow or the initial distribution of material.

Before introducing the representations, it is important to emphasise the point made in Section 1.4, namely that the arguments below can be extended to derive analogous Hermite series representations for a concentration field measured in an arbitrary framework, $\Gamma(\underline{X},t)$, and its ensemble mean properties. This extension is discussed in Chapter 4. However, because of the importance of relative diffusion and in order, in the first instance, to justify the representations as clearly as possible, it is sensible initially to focus on relative diffusion.

First, consider the conditions which must or should preferably be satisfied by a general representation for $C(\underline{x},t)$. Any representation must decay to zero as $|\underline{x}| \to \infty$. Observations suggest that in some flows $C(\underline{x},t)$ decays to zero like $\exp(-A\,|\underline{x}|^2)$ for

some constant A. In addition, there is evidence that under certain conditions $C(\underline{x},t)$ is Gaussian (Batchelor 1952; Csanady 1973; Monin and Yaglom 1975, p.577; Sullivan 1971).

As a second condition, it is at the least preferable that any representation is mathemtically easy to handle and has interpretable coefficients. Whilst a representation in wave-number (or frequency) space using Fourier integrals would be possible, such a representation is of most value in the special case of homogeneous (or stationary) turbulence (Frost and Moulden 1977; Monin and Yaglom 1975) and, furthermore, would not explicitly reflect the observed exponential decay of $C(\underline{x},t)$. On the other hand, the Gram-Charlier series of $C(\underline{x},t)$ (see (2.9)) viz.

$$C(\underline{x},t) = n(\underline{\mu}) \sum_{m=0}^{\infty} B^{(m)}_{ij\ldots k}(t) H^{(m)}_{ij\ldots k}(\underline{x},\underline{\mu}) \exp\left[-\frac{1}{2}\mu_{pq}(t)x_p x_q\right] \tag{2.11}$$

where

$$\mu_{ij} N_{jk} = \delta_{ik}$$

and

$$N_{ij}(t) = Q^{-1} \int x_i x_j \, C(\underline{x},t) \, dV(\underline{x})$$

satisfies both conditions and reflects this exponential decay but evidence suggests its practical value is restricted to near Gaussian $C(\underline{x},t)$ (Chatwin 1980; Kendall and Stuart 1969). Theoretical evidence of a Gaussian or near Gaussian $C(\underline{x},t)$ depends on certain simplifying assumptions, in particular that the flow is homogeneous

and that molecular diffusion may be ignored (Batchelor 1952; Monin and Yaglom 1971, p.540 and 1975, p.567-578). These assumptions are sufficient for many problems for several reasons. For example, the eddies responsible for relative diffusion often lie within the equilibrium range - or even in the inertial subrange - so that local isotropy and therefore homogeneity can be assumed (Monin and Yaglom 1975, p.337). If the same eddies lie within the inertial-convective subrange (Monin and Yaglom 1975, p.383) or if only the large scale statistical structure of $\Gamma(\underline{x},t)$ is of interest (Chatwin and Sullivan 1979a; Monin and Yaglom 1971, p.591) there is evidence to show that molecular diffusion may be neglected. However, most naturally occurring flows are inhomogeneous and evidence of non-Gaussian $C(\underline{x},t)$ is available (Chatwin and Sullivan 1979b; Monin and Yaglom 1975, p.578; Pasquill and Smith 1983). For these reasons, and since we are seeking a general representation for $C(\underline{x},t)$, (2.11) must be regarded as unsuitable.

However, it is possible to generalise (2.11) and represent $C(\underline{x},t)$ by the series

$$C(\underline{x},t) = Q\, n(\underline{\beta}) \sum_{m=0}^{\infty} B^{(m)}_{ij\ldots k}(t) H^{(m)}_{ij\ldots k}(\underline{x},\underline{\beta}) \exp\left[-\frac{1}{2}\beta_{pq}(t)x_p x_q\right] \qquad (2.12)$$

where $\beta_{ij}(t)$ is now an arbitrary, positive-definite, symmetric, non-random tensor and Q has been taken out of the summation for later convenience. The choice of $\beta_{ij}(t)$ is discussed in Section 2.5. For now it is important to stress that, given the evidence outlined above and in Section 2.2, for any well-behaved $\beta_{ij}(t)$,

(2.12) appears to be a natural representation for $C(\underline{x},t)$.

Granted this naturalness and granted that the conditions specified above for $C(\underline{x},t)$ typify those which must be satisfied by a general representation for many ensemble mean properties of $\Gamma(\underline{x},t)$ it is now natural to propose that each of these ensemble mean properties be represented by series like (2.12). In particular, using $\rho_{ij}(t)$, $\eta_{ij}(t)$ and $\lambda_{ij}(t)$ to denote arbitrary, non-random, positive-definite, symmetric tensors $\overline{c^2}(\underline{x},t)$, $p(\underline{y},t)$ and $r(\underline{y},t)$ may be represented by the series

$$\overline{c^2}(\underline{x},t) = Q^2\, n(\underline{\rho}) \sum_{m=0}^{\infty} D^{(m)}_{ij\ldots k}(t) H^{(m)}_{ij\ldots k}(\underline{x},\underline{\rho}) \exp\left[-\frac{1}{2}\rho_{pq}(t)x_p x_q\right] \tag{2.13}$$

$$p(\underline{y},t) = n(\underline{\underline{\eta}}) \sum_{m=0}^{\infty} E^{(m)}_{ij\ldots k}(t) H^{(m)}_{ij\ldots k}(\underline{y},\underline{\underline{\eta}}) \exp\left[-\frac{1}{2}\eta_{pq}(t)y_p y_q\right] \tag{2.14}$$

$$r(\underline{y},t) = n(\underline{\underline{\lambda}}) \sum_{m=0}^{\infty} L^{(m)}_{ij\ldots k}(t) H^{(m)}_{ij\ldots k}(\underline{y},\underline{\underline{\lambda}}) \exp\left[-\frac{1}{2}\lambda_{pq}(t)y_p y_q\right]. \tag{2.15}$$

Similar representations for other ensemble mean properties of $\Gamma(\underline{x},t)$ could be defined. Attention will be focussed on (2.12)-(2.15) because evidence of the behaviour of $C(\underline{x},t)$ $\overline{c^2}(\underline{x},t)$, $p(\underline{y},t)$ and $r(\underline{y},t)$ is available.

The evidence for $C(\underline{x},t)$ has already been discussed. As might be expected, there is less evidence for the other ensemble mean

properties. First, for $\overline{c^2}(\underline{x},t)$, whilst there are no known measurements from clouds, measurements of the appropriate analogue of $\overline{c^2}(\underline{x},t)$ in a steady plume have shown an approximately Gaussian distribution, except near the centre of the plume (Chatwin and Sullivan 1979b). Assuming these results generalise to clouds, they support the use of the general representation (2.13). Further support can be drawn from the theoretical investigation of the particular velocity field

$$\tau_j = \tau_{ij} x_i \tag{2.16}$$

where by (1.2)

$$\tau_{ii} = 0$$

i.e. $\underline{\tau}(\underline{x},t)$ a pure straining motion. The sole random feature of this $\underline{\tau}(\underline{x},t)$ is that the direction of the principal strain axes vary from realisation to realisation. This velocity field is considered in detail in Chapter 3, all that will be noted here is that the results suggest that in <u>some</u> flows $\overline{c^2}(\underline{x},t)$ decays like $\exp(-B\,|\underline{x}|^2)$ for some constant B.

As for $\overline{c^2}(\underline{x},t)$, there are no known measurements of $p(\underline{y},t)$ in clouds. However (2.14) is consistent with measurements of the analogue of $p(\underline{y},t)$ in steady plumes which show a Gaussian distribution in the bulk of the plume (Sullivan 1971). A Gaussian distribution for $p(\underline{y},t)$ in homogeneous turbulence is also proposed by Batchelor (1952).

Evidence from the measurements of plumes is also available for the representation for $r(\underline{y},t)$, (2.15). Indeed, the representation has already been suggested by Chatwin and Sullivan (1980a) following

an examination of such measurements and the use of the analogue of (2.15) to represent the one dimensional analogue of $r(\underline{y},t)$ in a plume. Their results suggest (2.15) will be of practical use and are discussed in more detail in Section 2.4.5.

Finally, to complete the mathematical representations to be investigated in this thesis, it remains to introduce one further extension of the generalised Hermite series, namely that the random concentration field, $\Gamma(\underline{x},t)$, be represented by the series

$$\Gamma(\underline{x},t) = Q\, n(\underline{\alpha}) \sum_{m=0}^{\infty} A^{(m)}_{ij\ldots k}(t) H^{(m)}_{ij\ldots k}(\underline{x},\underline{\alpha}) \exp\left[-\frac{1}{2}\alpha_{pq}(t)x_p x_q\right] \quad (2.17)$$

where $\alpha_{ij}(t)$ is an arbitrary, positive-definite, symmetric tensor which may now be chosen random. The reasons for introducing (2.17) are obvious. The conditions specified earlier for $C(\underline{x},t)$, $\overline{c^2}(\underline{x},t)$, $p(\underline{y},t)$ and $r(\underline{y},t)$ typify those which should be satisfied by any representation for $\Gamma(\underline{x},t)$. The series (2.17) is therefore a natural representation to investigate. It provides, in conjunction with (2.12)-(2.15), a more complete mathematical representation for the concentration field and its ensemble mean properties and is therefore of inherent interest.

The aim of this thesis is:

(a) to investigate the use of the representations (2.12)-(2.15) and (2.17),

and (b) to generalise the investigation to frameworks other than frameworks of relative diffusion.

For the reasons given at the beginning of this section, (b) is considered in Chapter 4. To achieve (a), it is essential in the first instance to outline the basic properties of (2.12)-(2.15) and (2.17). This is done in the next section, Section 2.4. In Section 2.5, by way of discussing the practical and theoretical value of (2.12)-(2.15) and (2.17), the important questions to be addressed in this thesis are raised.

2.4 Properties of the Representations for $\Gamma(\underline{x},t)$, $C(\underline{x},t)$, $\overline{c^2}(\underline{x},t)$, $p(\underline{y},t)$ and $r(\underline{y},t)$.

Continuing to make no artificial or restrictive assumptions about the nature of the turbulent flow or the initial distribution of material, in this section

(a) the expressions for the first few coefficients of each of the representations (2.17), (2.12)-(2.15) are derived in terms of the moments of $\Gamma(\underline{x},t)$, $C(\underline{x},t)$, $\overline{c^2}(\underline{x},t)$, $p(\underline{y},t)$ and $r(\underline{y},t)$,

(b) the relationships between the coefficients of each representation are illustrated.

The results of Appendix A are used throughout the section.

2.4.1 The Representation for $\Gamma(\underline{x},t)$

Let $a_{ij}(t)$ denote the inverse of the symmetric tensor $\alpha_{ij}(t)$ in (2.17), i.e.

$$a_{ij}\,\alpha_{jk} = \delta_{ik}$$

(so that $a_{ij}(t)$ is also symmetric) and let $M^{(n)}_{ij\ldots k}(t)$ denote the nth order moment of $\Gamma(\underline{x},t)$

$$M^{(n)}_{ij\ldots k}(t) = Q^{-1}\int x_i x_j \ldots x_k\,\Gamma(\underline{x},t)\,dV(\underline{x}). \tag{2.18}$$

Hence, using (1.1) and (1.19)

$$M^{(0)}(t) = 1; \qquad M^{(1)}_i(t) = 0. \tag{2.19}$$

Using (A10)-(A13) (with $C^{(n)}_{ij\ldots k}$, $S^{(n)}_{ij\ldots k}$ and Ψ_{ij} replaced by $A^{(n)}_{ij\ldots k}(t)$, $M^{(n)}_{ij\ldots k}(t)$ and $a_{ij}(t)$ respectively)

$$A^{(0)}(t) = 1$$

$$A^{(1)}_i(t) = 0$$

$$A^{(2)}_{ij}(t) = \frac{1}{2}\,(M^{(2)}_{ij} - a_{ij})$$

$$A^{(3)}_{ijk}(t) = \frac{1}{3!}\,M^{(3)}_{ijk} \tag{2.20}$$

$$A^{(4)}_{ijk\ell}(t) = \frac{1}{4!}\left\{M^{(4)}_{ijk\ell} - (a_{ij}M^{(2)}_{k\ell} + a_{ik}M^{(2)}_{j\ell} + a_{i\ell}M^{(2)}_{jk} + a_{jk}M^{(2)}_{i\ell} + a_{j\ell}M^{(2)}_{ik} + a_{k\ell}M^{(2)}_{ij}) + (a_{ij}a_{k\ell} + a_{ik}a_{j\ell} + a_{i\ell}a_{jk})\right\}. \qquad (2.20)\text{(contd.)}$$

Thus $A^{(0)}(t)$ and $A^{(1)}_i(t)$ are invariant. The first few terms of (2.17) may now be written

$$\Gamma(\underline{x},t) = Q\, n(\underline{\alpha})\left\{1 + \frac{1}{2}(M^{(2)}_{ij} - a_{ij})\, H^{(2)}_{ij}(\underline{x},\underline{\alpha}) + \frac{1}{3!}M^{(3)}_{ijk}\, H^{(3)}_{ijk}(\underline{x},\underline{\alpha}) + \ldots\right\} \exp\left[-\frac{1}{2}\alpha_{pq}x_p x_q\right]. \qquad (2.21)$$

In (2.20) and (2.21), the dependency of $M^{(n)}_{ij\ldots k}(t)$, $\alpha_{ij}(t)$ and $a_{ij}(t)$ on t has been omitted for simplicity. The same will be done in subsequent equations wherever practicable.

2.4.2 The Representation for $C(\underline{x},t)$

Following the same procedure as in Section 2.4.1 for the representation for $C(\underline{x},t)$, (2.12), let $b_{ij}(t)$ denote the inverse of $\beta_{ij}(t)$, i.e.

$$b_{ij}\beta_{jk} = \delta_{ik} \qquad (2.22)$$

and let $N^{(n)}_{ij\ldots k}(t)$ denote the nth order moment of $C(\underline{x},t)$, i.e.

$$N^{(n)}_{ij\ldots k}(t) = \overline{M^{(n)}_{ij\ldots k}(t)} = Q^{-1}\int x_i x_j \ldots x_k\, C(\underline{x},t)\, dV(\underline{x}) \qquad (2.23)$$

where $M^{(n)}_{ij\ldots k}(t)$ is given by (2.18). Thus, using (2.19)

$$N^{(0)}(t) = 1; \qquad N^{(1)}_i(t) = 0. \tag{2.24}$$

From (A10)-(A13) (with $C^{(n)}_{ij\ldots k}$, $S^{(n)}_{ij\ldots k}$ and Ψ_{ij} replaced by $B^{(n)}_{ij\ldots k}(t)$, $N^{(n)}_{ij\ldots k}(t)$ and $b_{ij}(t)$ respectively)

$$B^{(0)}(t) = \overline{A^{(0)}(t)} = A^{(0)}(t) = 1$$

$$B^{(1)}_i(t) = \overline{A^{(1)}_i(t)} = A^{(1)}_i(t) = 0$$

$$B^{(2)}_{ij}(t) = \frac{1}{2}\,(N^{(2)}_{ij} - b_{ij})$$

$$B^{(3)}_{ijk}(t) = \frac{1}{3!}\,N^{(3)}_{ijk} \tag{2.25}$$

$$B^{(4)}_{ijk\ell}(t) = \frac{1}{4!}\left\{N^{(4)}_{ijk\ell} - (b_{ij}N^{(2)}_{k\ell} + b_{ik}N^{(2)}_{j\ell} + b_{i\ell}N^{(2)}_{jk} + b_{jk}N^{(2)}_{i\ell} + b_{j\ell}N^{(2)}_{ik} + b_{k\ell}N^{(2)}_{ij}) + (b_{ij}b_{k\ell} + b_{ik}b_{j\ell} + b_{i\ell}b_{jk})\right\}$$

so that $B^{(0)}(t)$ and $B^{(1)}_i(t)$ are invariant. The first few terms of (2.12) may now be written

$$C(\underline{x},t) = Q\,n(\underline{\beta})\left\{1 + \frac{1}{2}\,(N^{(2)}_{ij} - b_{ij})\,H^{(2)}_{ij}(\underline{x},\underline{\beta}) + \frac{1}{3!}\,N^{(3)}_{ijk}\,H^{(3)}_{ijk}(\underline{x},\underline{\beta}) + \ldots\right\}\exp\left[-\frac{1}{2}\,\beta_{pq}x_p x_q\right]. \tag{2.26}$$

Note that since the initial distribution of material is the same in each realisation, using (2.23)

$$N^{(n)}_{ij\ldots k}(0) = M^{(n)}_{ij\ldots k}(0) \qquad \text{for all } n \geq 0 \tag{2.27}$$

Therefore for each $n \geq 0$, $B^{(n)}_{ij\ldots k}(0)$ can be expressed in terms of the $M^{(r)}_{ij\ldots k}(0)$, $r \leq n$, and $b_{ij}(0)$ and therefore in terms of the $A^{(r)}_{ij\ldots k}(0)$, $r \leq n$, $b_{ij}(0)$ and $a_{ij}(0)$, ($a_{ij}(0)$ must be chosen non-random). For example

$$B^{(2)}_{ij}(0) = \tfrac{1}{2}\,(M^{(2)}_{ij}(0) - b_{ij}(0)) = A^{(2)}_{ij}(0) + \tfrac{1}{2}\,(a_{ij}(0) - b_{ij}(0)).$$

For general t, each $B^{(n)}_{ij\ldots k}(t)$ can be expressed in terms of the $\overline{M^{(r)}_{ij\ldots k}(t)}$, $r \leq n$, and $b_{ij}(t)$ and therefore in terms of the $\overline{A^{(r)}_{ij\ldots k}(t)}$, $r \leq n$, $b_{ij}(t)$ and $\overline{a_{ij}(t)}$. For example

$$\begin{aligned} B^{(2)}_{ij}(t) &= \tfrac{1}{2}\,(\overline{M^{(2)}_{ij}(t)} - b_{ij}(t)) \\ &= \overline{A^{(2)}_{ij}(t)} + \tfrac{1}{2}\,(\overline{a_{ij}(t)} - b_{ij}(t)) \end{aligned} \tag{2.28}$$

$$\begin{aligned} B^{(3)}_{ijk}(t) &= \frac{1}{3!}\,\overline{M^{(3)}_{ijk}(t)} \\ &= \overline{A^{(3)}_{ijk}(t)}. \end{aligned}$$

2.4.3 The Representation for $\overline{c^2}(\underline{x},t)$

Let $d_{ij}(t)$ denote the inverse of $\rho_{ij}(t)$ in (2.13), i.e.

$$d_{ij}\,\rho_{jk} = \delta_{ik}$$

and let $Q^{(n)}_{ij\ldots k}(t)$ denote the nth order moment of $\overline{c^2}(\underline{x},t)$, i.e.

$$Q^{(n)}_{ij\ldots k}(t) = Q^{-2} \int x_i x_j \ldots x_k \, \overline{c^2}(\underline{x},t)\, dV(\underline{x}). \tag{2.29}$$

Using (A10)-(A13) (with $C^{(n)}_{ij\ldots k}$, $S^{(n)}_{ij\ldots k}$ and Ψ_{ij} replaced by $D^{(n)}_{ij\ldots k}(t)$, $Q^{(n)}_{ij\ldots k}(t)$ and $d_{ij}(t)$ respectively)

$$D^{(0)}(t) = Q^{(0)}$$

$$D^{(1)}_i(t) = Q^{(1)}_i$$

$$D^{(2)}_{ij}(t) = \tfrac{1}{2}\,(Q^{(2)}_{ij} - d_{ij})$$

$$D^{(3)}_{ijk}(t) = \frac{1}{3!}\left\{Q^{(3)}_{ijk} - (d_{ij}Q^{(1)}_k + d_{ik}Q^{(1)}_j + d_{jk}Q^{(1)}_i)\right\} \tag{2.30}$$

$$D^{(4)}_{ijk\ell}(t) = \frac{1}{4!}\left\{Q^{(4)}_{ijk\ell} - (d_{ij}Q^{(2)}_{k\ell} + d_{ik}Q^{(2)}_{j\ell} + d_{i\ell}Q^{(2)}_{jk} + d_{jk}Q^{(2)}_{i\ell} + d_{j\ell}Q^{(2)}_{ik} + d_{k\ell}Q^{(2)}_{ij}) + (d_{ij}d_{k\ell} + d_{ik}d_{j\ell} + d_{i\ell}d_{jk})\right\}.$$

Unlike $A^{(0)}(t)$, $A_i^{(1)}(t)$, $B^{(0)}(t)$ and $B_i^{(1)}(t)$, $D^{(0)}(t)$ and $D_i^{(1)}(t)$ are not invariant. The first few terms of (2.13) may be written

$$\overline{c^2}(\underline{x},t) = Q^2\, n(\underline{\rho}) \left\{Q^{(0)} + Q_i^{(1)}\, H_i^{(1)}(\underline{x},\underline{\rho}) + \frac{1}{2}\,(Q_{ij}^{(2)} - d_{ij})\, H_{ij}^{(2)}(\underline{x},\underline{\rho}) + \frac{1}{3!}\left[Q_{ijk}^{(3)} - (d_{ij}Q_k^{(1)} + d_{ik}Q_j^{(1)} + d_{jk}Q_i^{(1)})\right] H_{ijk}^{(3)}(\underline{x},\underline{\rho}) + \ldots\right\} \exp\left[-\frac{1}{2}\,\rho_{pq}x_p x_q\right]. \tag{2.31}$$

Using (1.11b)

$$\overline{c^2}(\underline{x},0) = 0$$

so that

$$Q_{ij\ldots k}^{(n)}(0) = D_{ij\ldots k}^{(n)}(0) = 0 \qquad \text{for all } n>0.$$

In addition, since (Chatwin and Sullivan 1979a)

$$\int \overline{c^2}(\underline{x},t)\, dV(\underline{x}) \to 0 \quad \text{as} \quad t \to \infty$$

it follows that

$$D^{(0)}(t) \to 0 \quad \text{as} \quad t \to \infty.$$

2.4.4. The Representation for $p(\underline{y},t)$

The first few terms of the representation for $p(\underline{y},t)$, (2.14), like that for $C(\underline{x},t)$, can be simplified somewhat. Let $e_{ij}(t)$ denote the inverse of $\eta_{ij}(t)$ so that

$$e_{ij}\,\eta_{jk} = \delta_{ik}.$$

Denote the nth order moment of $p(\underline{y},t)$ by $P^{(n)}_{ij\ldots k}(t)$, i.e.

$$P^{(n)}_{ij\ldots k}(t) = \int y_i y_j \ldots y_k\, p(\underline{y},t)\, dV(\underline{y})$$

$$= Q^{-2} \iint y_i y_j \ldots y_k\, \overline{\Gamma(\underline{x},t)\,\Gamma(\underline{x}+\underline{y},\,t)}\, dV(\underline{x})\, dV(\underline{y}). \tag{2.32}$$

Clearly, from (1.21), $p(\underline{y},t)$ is even in $\underline{y}$ so that

$$p(\underline{y},t) = p(-\underline{y},\,t).$$

It follows that (Chatwin and Sullivan 1980a)

$$P^{(2n+1)}_{ij\ldots k}(t) = 0 \qquad \text{for all } n>0. \tag{2.33}$$

In addition (Batchelor 1952)

$$P^{(0)}(t) = \int p(\underline{y},t)\, dV(\underline{y}) = 1. \tag{2.34}$$

Using (A10)-(A13) (with $C^{(n)}_{ij\ldots k}$, $S^{(n)}_{ij\ldots k}$ and Ψ_{ij} replaced by $E^{(n)}_{ij\ldots k}(t)$, $P^{(n)}_{ij\ldots k}(t)$ and $e_{ij}(t)$ respectively), (2.33) and (2.34)

$$E^{(0)}(t) = 1$$

$$E^{(2n+1)}_{ij\ldots k}(t) = 0 \qquad \text{for all } n \geq 0$$

(2.35)

$$E^{(2)}_{ij}(t) = \frac{1}{2}\left(P^{(2)}_{ij} - e_{ij}\right)$$

$$E^{(4)}_{ijk\ell}(t) = \frac{1}{4!}\left\{P^{(4)}_{ijk\ell} - \left(e_{ij}P^{(2)}_{k\ell} + e_{ik}P^{(2)}_{j\ell} + e_{i\ell}P^{(2)}_{jk} + e_{jk}P^{(2)}_{i\ell} + e_{j\ell}P^{(2)}_{ik} + e_{k\ell}P^{(2)}_{ij}\right) + \left(e_{ij}e_{k\ell} + e_{ik}e_{j\ell} + e_{i\ell}e_{jk}\right)\right\}$$

so that $E^{(0)}(t)$ and $E^{(2n+1)}_{ij\ldots k}(t)$ are invariant. Equation (2.14) may now be written

$$p(\underline{y},t) = n(\underline{\eta})\left\{1 + \sum_{m=1}^{\infty} E^{(2m)}_{ij\ldots k}(t)\, H^{(2m)}_{ij\ldots k}(\underline{y},\underline{\eta})\right\} \exp\left[-\frac{1}{2}\eta_{pq}y_p y_q\right]$$

$$p(\underline{y},t) = n(\underline{\eta})\left\{1 + \frac{1}{2}\left(P^{(2)}_{ij} - e_{ij}\right) H^{(2)}_{ij}(\underline{y},\underline{\eta}) + \frac{1}{4!}\left[P^{(4)}_{ijk\ell} - \left(P^{(2)}_{ij}e_{k\ell} + 5 \text{ similar terms}\right) + \left(e_{ij}e_{k\ell} + 2 \text{ similar terms}\right)\right] H^{(4)}_{ijk\ell}(\underline{y},\underline{\eta}) + \ldots\right\} \exp\left[-\frac{1}{2}\eta_{pq}y_p y_q\right]. \qquad (2.36)$$

Looking at the relationships between the $E^{(2n)}_{ij\ldots k}(t)$ $n \geq 1$ and the coefficients of the representations for $\Gamma(\underline{x},t)$ and $C(\underline{x},t)$,

$A^{(m)}_{ij\ldots k}(t)$ and $B^{(m)}_{ij\ldots k}(t)$ respectively, since (Batchelor 1952)

$$P^{(2)}_{ij}(t) = 2N^{(2)}_{ij}(t) \tag{2.37}$$

where $N^{(2)}_{ij}(t)$ is defined by (2.23), then using (2.35c), (2.37), (2.25c) and (2.28a)

$$\begin{aligned} E^{(2)}_{ij}(t) &= \frac{1}{2}\,(2N^{(2)}_{ij} - e_{ij}) \\ &= 2B^{(2)}_{ij} + \frac{1}{2}\,(2b_{ij} - e_{ij}) \\ &= 2\overline{A^{(2)}_{ij}} + \frac{1}{2}\,(2\overline{a_{ij}} - e_{ij}). \end{aligned} \tag{2.38}$$

More generally, letting the nth moment of $r(\underline{y},t)$ be denoted by $R^{(n)}_{ij\ldots k}(t)$, i.e.

$$R^{(n)}_{ij\ldots k}(t) = \int y_i y_j \ldots y_k \; r(\underline{y},t)\; dV(\underline{y}) \tag{2.39}$$

for each $n \geq 2$

$$\left\{P^{(2n)}_{ij\ldots k}(t) - R^{(2n)}_{ij\ldots k}(t)\right\}$$

is a function of the $N^{(m)}_{ij\ldots k}(t)$, $m < 2n$ (Chatwin and Sullivan 1980a). Hence for general t, relationships between the $E^{(2n)}_{ij\ldots k}(t)$, $n \geq 2$, and the coefficients of the representations for $C(\underline{x},t)$ and $r(\underline{y},t)$ (and therefore $\Gamma(\underline{x},t)$ and $r(\underline{y},t)$) can be derived. This is done in Section 2.4.5, after developing the representation for $r(\underline{y},t)$.

However using (1.22) and (1.11b), for $t=0$ we have

$$r(\underline{y},0) = 0$$

so that

$$R^{(n)}_{ij\ldots k}(0) = 0 \qquad \text{for all } n\geq 0 \tag{2.40}$$

Hence, for each $n\geq 1$, $P^{(2n)}_{ij\ldots k}(0)$ is a function only of the $N^{(2m)}_{ij\ldots k}(0)$, $m\leq 2n$, and therefore, using (2.26), of the $M^{(2m)}_{ij\ldots k}(0)$, $m\leq 2n$. It follows that for each $n\geq 1$, $E^{(2n)}_{ij..k}(0)$ can be expressed in terms of the $A^{(m)}_{ij\ldots k}(0)$, $m\leq 2n$, $a_{ij}(0)$ and $e_{ij}(0)$. As a simple example, from (2.38) it follows that

$$E^{(2)}_{ij}(0) = 2A^{(2)}_{ij}(0) + \frac{1}{2}\,(2a_{ij}(0) - e_{ij}(0))$$

2.4.5 The Representation for $r(\underline{y},t)$

Finally, consider the representation for $r(\underline{y},t)$, (2.15). Let $l_{ij}(t)$ denote the inverse of $\lambda_{ij}(t)$ so that

$$l_{ij}\,\lambda_{jk} = \delta_{ik}.$$

As demonstrated by Chatwin and Sullivan (1980a) there are several invariants of $r(\underline{y},t)$. First, from (1.10), (1.22) and (2.39) it follows that

$$r(\underline{y},t) = r(-\underline{y}, t)$$

$$R^{(0)}(t) = 0. \tag{2.41}$$

From (1.10), (1.20), (1.22) and (2.39)

$$R^{(2)}_{ij}(t) = 0. \tag{2.42}$$

Finally, from (2.41a) and (2.39)

$$R^{(2n+1)}_{ij\ldots k}(t) = 0 \qquad \text{for all } n>0 \tag{2.43}$$

Note that (2.41) and (2.43) are true for relative and absolute diffusion whilst (2.42) only holds for relative diffusion. Using (2.41)-(2.43) the representation for $r(\underline{y},t)$ can be simplified to

$$r(\underline{y},t) = n(\underline{\lambda}) \sum_{m=2}^{\infty} L^{(2m)}_{ij\ldots k}(t) H^{(2m)}_{ij\ldots k}(\underline{y},\underline{\lambda}) \exp\left[-\frac{1}{2}\lambda_{pq}y_p y_q\right]. \tag{2.44}$$

As explained in Section 2.4.4., for general t, relationships between the coefficients of the representations for $r(\underline{y},t)$, $p(\underline{y},t)$ and $C(\underline{x},t)$ (i.e. $L^{(n)}_{ij\ldots k}$, $E^{(n)}_{ij\ldots k}$ and $B^{(n)}_{ij\ldots k}$ respectively) can be derived. As an example consider

$$\left\{P^{(4)}_{ijk\ell}(t) - R^{(4)}_{ijk\ell}(t)\right\}$$

where $P^{(n)}_{ij\ldots k}(t)$ and $R^{(n)}_{ij\ldots k}(t)$ are given by (2.32) and (2.39)

respectively. Now (Chatwin and Sullivan 1980a)

$$P^{(4)}_{ijk\ell}(t) - R^{(4)}_{ijk\ell}(t) = 2(N^{(4)}_{ijk\ell} + N^{(2)}_{ij}N^{(2)}_{k\ell} + N^{(2)}_{ik}N^{(2)}_{j\ell} + N^{(2)}_{i\ell}N^{(2)}_{jk}) \tag{2.45}$$

From (2.35d) and (2.37)

$$P^{(4)}_{ijk\ell}(t) = 4!E^{(4)}_{ijk\ell} + 2(e_{ij}N^{(2)}_{k\ell} + e_{ik}N^{(2)}_{j\ell} + e_{i\ell}N^{(2)}_{jk} + e_{jk}N^{(2)}_{i\ell} + e_{j\ell}N^{(2)}_{ik} + e_{k\ell}N^{(2)}_{ij}) - (e_{ij}e_{k\ell} + e_{ik}e_{j\ell} + e_{i\ell}e_{jk}) \tag{2.46}$$

Using the equation for $L^{(4)}_{ijk\ell}$ analogous to (2.35d), and (2.42) gives

$$R^{(4)}_{ijk\ell}(t) = 4!\, L^{(4)}_{ijk\ell} - (1_{ij}1_{k\ell} + 1_{ik}1_{j\ell} + 1_{i\ell}1_{jk}) \tag{2.47}$$

Substituting (2.46) and (2.47) into (2.45), using (2.25c and e) to express $N^{(4)}_{ijk\ell}(t)$ and $N^{(2)}_{ij}(t)$ in terms of the $B^{(m)}_{ij\ldots k}$, $m\leq 4$, and rearranging leads to the following relationship between the fourth order coefficients of the series for $r(\underline{y},t)$, $p(\underline{y},t)$ and $C(\underline{x},t)$

$$4!(E^{(4)}_{ijk\ell} - L^{(4)}_{ijk\ell}) - \{(e_{ij}e_{k\ell} - 1_{ij}1_{k\ell}) + (e_{ik}e_{j\ell} - 1_{ik}1_{j\ell}) + (e_{i\ell}e_{jk} - 1_{i\ell}1_{jk})\}$$

$$= 2.4!\, B^{(4)}_{ijk\ell} + 8(B^{(2)}_{ij}B^{(2)}_{k\ell} + B^{(2)}_{ik}B^{(2)}_{j\ell} + B^{(2)}_{i\ell}B^{(2)}_{jk})$$

(contd.)

$$+ 8(b_{ij}B^{(2)}_{k\ell} + b_{ik}B^{(2)}_{j\ell} + b_{i\ell}B^{(2)}_{jk} + b_{jk}B^{(2)}_{i\ell} + b_{j\ell}B^{(2)}_{ik} + b_{k\ell}B^{(2)}_{ij})$$

$$- 2\{e_{ij}(2B^{(2)}_{k\ell} + b_{k\ell}) + e_{ik}(2B^{(2)}_{j\ell} + b_{j\ell}) + e_{i\ell}(2B^{(2)}_{jk} + b_{jk})$$

$$+ e_{jk}(2B^{(2)}_{i\ell} + b_{i\ell}) + e_{j\ell}(2B_{ik} + b_{ik}) + e_{k\ell}(2B^{(2)}_{ij} + b_{ij})\}$$

$$+ 4(b_{ij}b_{k\ell} + b_{ik}b_{j\ell} + b_{i\ell}b_{jk}). \qquad (2.48)$$

(* see footnote on page 48)

The series (2.44) was first suggested by Chatwin and Sullivan (1980a). They applied the corresponding one dimensional series to the analogue of $r(\underline{y},t)$ in a plume dispersing on the surface of a lake, $r(y,x)$. Here, x denotes the distance from the source along the instantaneous centre line of the plume and y denotes the perpendicular distance in the surface of the lake from the centre of the plume. Figure 1 of their paper is reproduced in Fig. 2.2. It compares the approximation obtained from the first term of the one dimensional series, after suitably choosing the analogue of $l_{ij}(t)$, with the corresponding curve for $r(y,x)$ derived from the plume measurements. As discussed by Chatwin and Sullivan, the level of agreement between the curves is very good considering the experimental errors involved and certainly appears to suggest that the three dimensional series (2.44) will be of practical value.

2.5 The Way Forward

Sections 2.2-2.4 have shown how a series of generalised three dimensional Hermite polynomials can be used to represent $\Gamma(\underline{x},t)$ and many of its ensemble mean properties. An investigation of the

use of these representations needs to address a number of important questions. These questions divide naturally into those relating, on the one hand, to the potential practical uses of the representations, and, on the other, to their potential theoretical uses. Initially, the former will be identified by considering the representation for $C(\underline{x},t)$, (2.12).

Consider a problem in which the behaviour of several of the lower order moments of $C(\underline{x},t)$ is known but that of $C(\underline{x},t)$ itself is not. Without loss of generality we may assume that the behaviour of the moments of order <4 is known, a reasonable assumption given the errors typically associated with moments of order >4 calculated from measurements (Kendall and Stuart 1969). Then (2.12) will be of practical value if there exists a choice for $\beta_{ij}(t)$, and thereby a choice for $b_{ij}(t)$, which

(1) ensures that a satisfactory approximation to $C(\underline{x},t)$ is obtained from, at most, the first five terms of (2.12) (the option of approximating $C(\underline{x},t)$ by a rearrangement of the terms of the representation is discussed below)

(2) can be determined from measurement and/or theory

and (3) is such that the accuracy of the approximation can be quantified in terms of the parameters of the flow and/or the variables $\underline{x}$ and t.

Any $b_{ij}(t)$ satisfying (1)-(3) will be called '<u>suitable</u>'.

Experience of the use of a Hermite series representation, or more precisely of the one dimensional analogue of (2.12), suggests we should not expect to find a suitable choice for $b_{ij}(t)$ for each flow, rather that there may exist choices for $b_{ij}(t)$ which are suitable for certain classes of flow. For example, given the observed Gaussianity of the one dimensional analogue of $C(\underline{x},t)$ in a plume (Csanady 1973; Sullivan 1971) one choice for $b_{ij}(t)$ of particular interest is

$$b_{ij}(t) = N_{ij}^{(2)}(t) \tag{2.49}$$

where $N_{ij}^{(2)}(t)$ is given by (2.23). As discussed in Section 2.3, with this choice for $b_{ij}(t)$, (2.12) is the Gram-Charlier series for $C(\underline{x},t)$ (see (2.11)). Then, one needs to ask

(1) for which flows is (2.49) of practical use?

(2) Given the previous uses of the Edgeworth series (Chatwin 1970, 1980; Kendall and Stuart 1969; Smith 1978, 1982b) are there flows which require the rearrangement of (2.12) for it to be of optimum practical use?

(3) Are there flows for which a choice other than (2.49) is suitable?

These questions typify those that could be asked of the Hermite series representations for $\overline{c^2}(\underline{x},t)$, $p(\underline{y},t)$ and $r(\underline{y},t)$,

(2.13)-(2.15). Consequently, it is important to examine if governing equations like (1.17) and (1.18) can be used to express the coefficients of (2.12)-(2.15) in terms of the statistical properties of the velocity field $\underline{\Upsilon}(\underline{x},t)$. If this is possible, the existence of any practically useful criteria for choosing the arbitrary tensors of the representations, $b_{ij}(t)$, $d_{ij}(t)$, $e_{ij}(t)$ and $l_{ij}(t)$, can be investigated. Unfortunately, since the hierachy of governing equations for the ensemble mean properties is not closed (Section 1.3.1), substitution of, for example, (2.12) and (2.13) into (1.17) and (1.18) obviously leads to a complex system of non-closed governing equations for the coefficients.

There appear to be two particularly interesting ways of making progress. The first is to choose a particular $\underline{\Upsilon}(\underline{x},t)$ random in some specified way and thereby investigate the use of the representations (2.12)-(2.15) and (2.17), especially the choices of the arbitrary tensors of the representations. In this way the analysis can be kept exact and the practically important questions simplified somewhat. The second is to use a particular closed model equation for one (or more) of the ensemble mean properties of $\Gamma(\underline{x},t)$ and investigate the resulting form of the coefficients of the representation(s). In this case the analysis cannot be exact. The former option is tackled in the next chapter, Chapter 3. The latter is addressed in Chapter 4.

* If we assume that $C(\underline{x},t)$ and $p(\underline{y},t)$ are Gaussian (Sullivan 1975), and choose $b_{ij}(t)$ and $e_{ij}(t)$ such that each is represented by the first term of their respective Gram-Charlier series, using (2.37), (2.48) may be simplified to give

$$L^{(4)}_{ijk\ell}(t) = \frac{1}{4!}(\ell_{ij}\ell_{k\ell} + \ell_{ik}\ell_{j\ell} + \ell_{i\ell}\ell_{jk})$$

Hence, from (2.47), the fourth order moment of $r(\underline{y},t)$, $R^{(4)}_{ijk\ell}(t)$, is identically zero. This result follows directly from equation (3.21) of Chatwin and Sullivan (1980a).

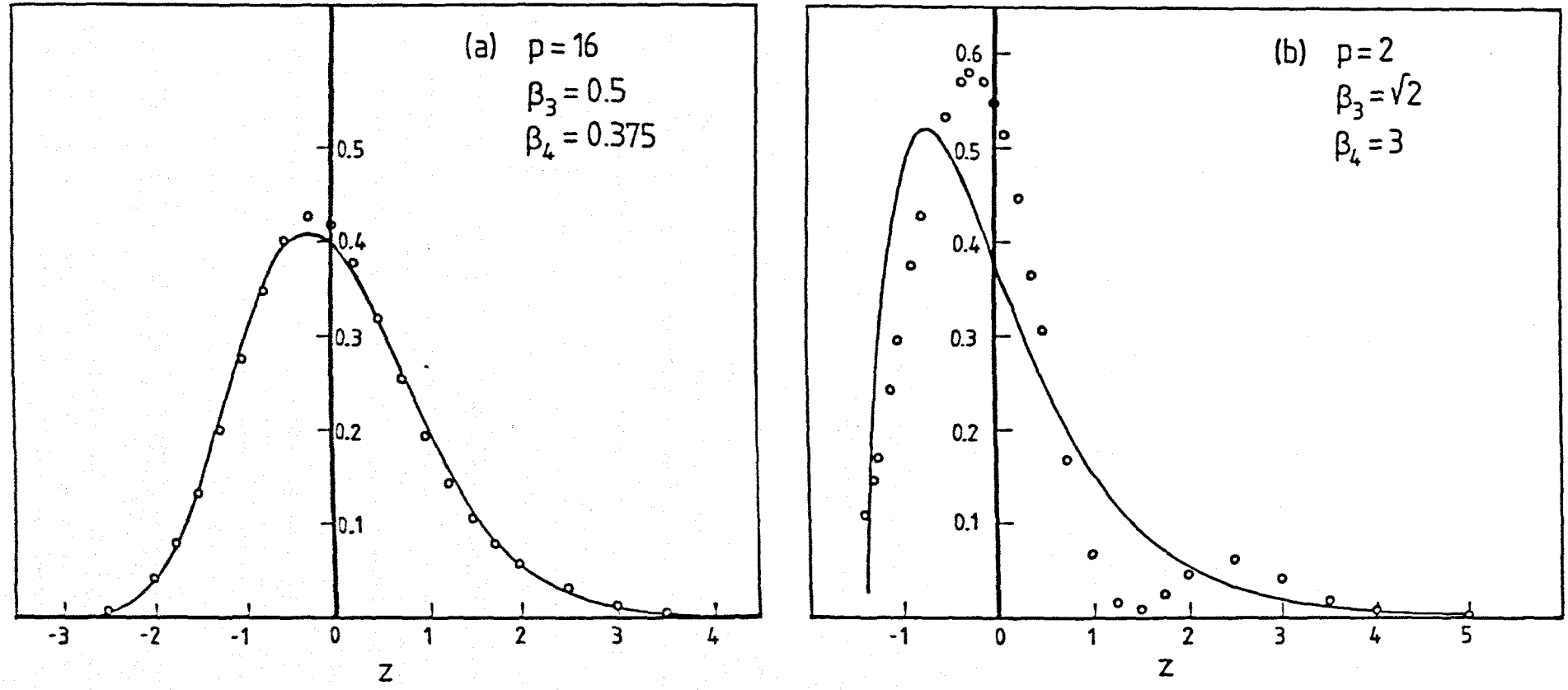

Fig.2.1(a) and (b) The Standardised Gamma Function ('——', Equation 2.6) and Gram-Charlier Series Approximation ('∘', Equation 2.5)

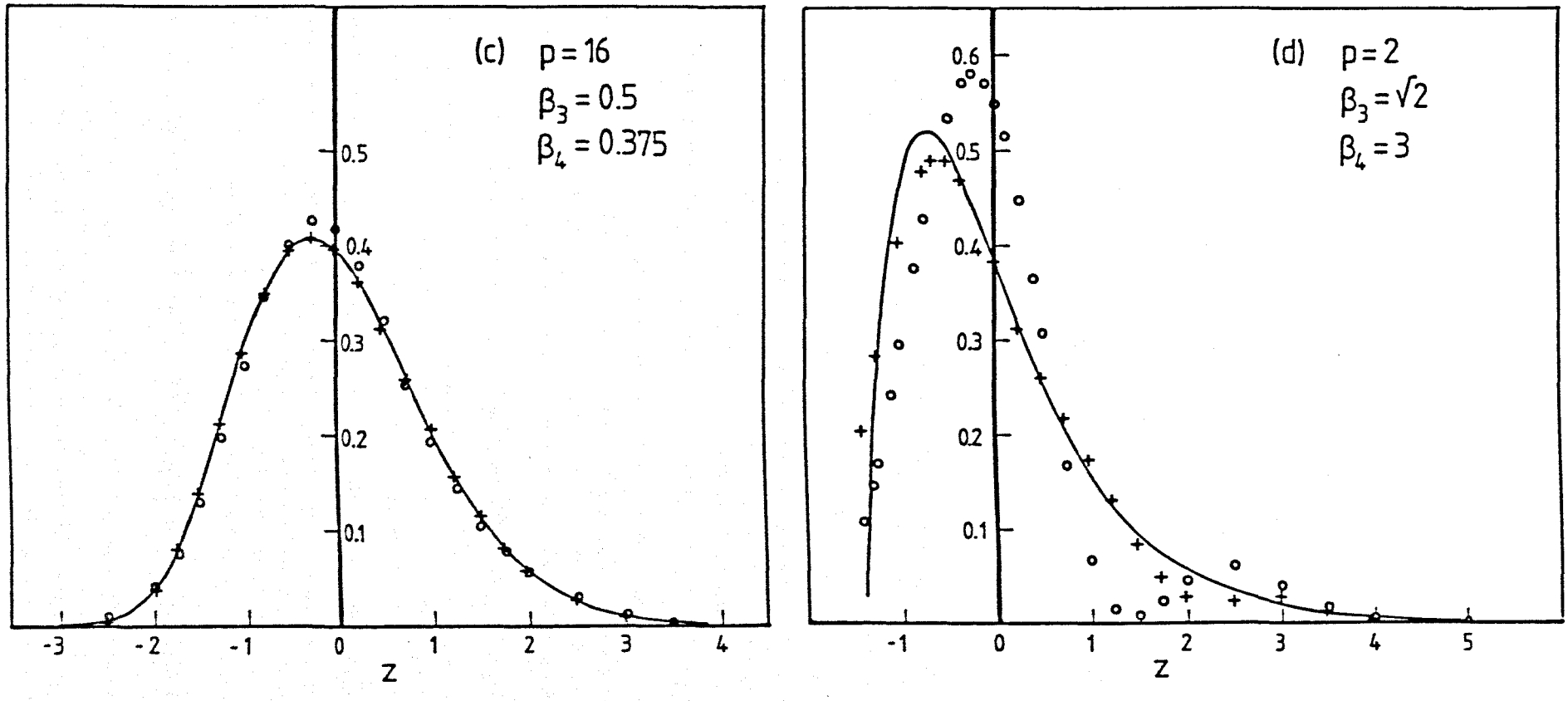

Fig.2.1(c) and (d) The Standardised Gamma Function ('——', Equation 2.6), Gram-Charlier Series ('∘', Equation 2.5) and Edgeworth Series ('+', Equation 2.7) Approximations

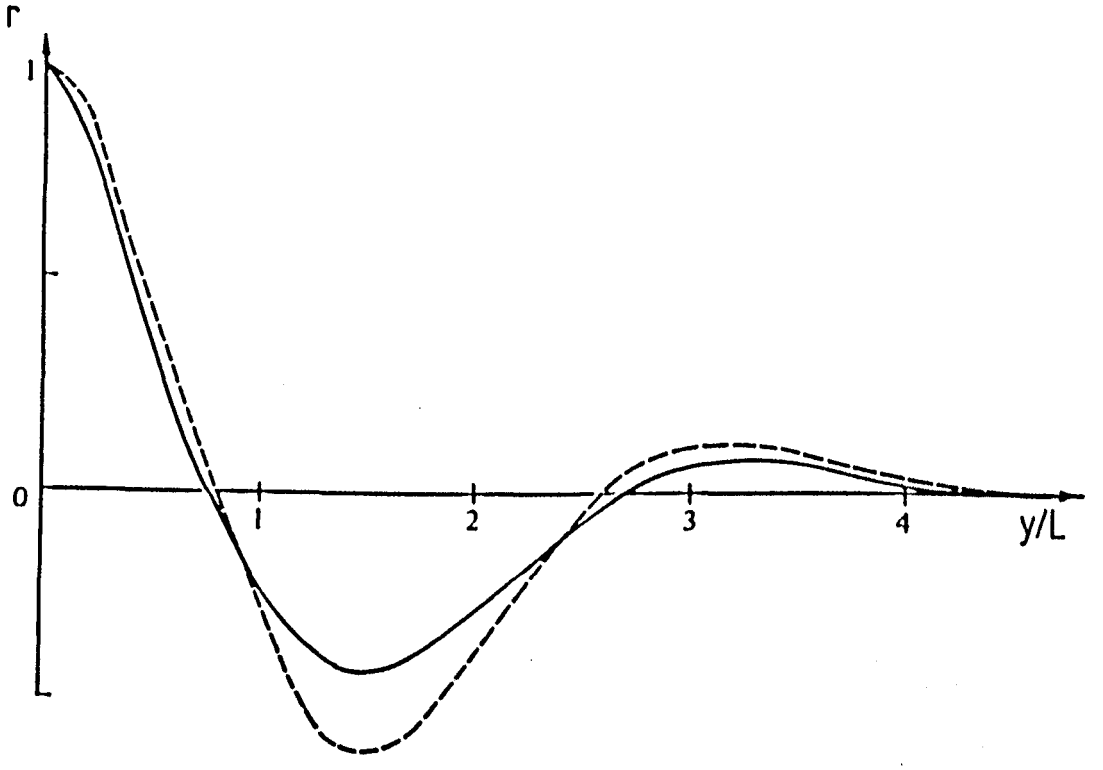

Key: ——— derived from measurements

----- Hermite series approximation

L(x) is a measured mean plume width

Fig.2.2 Hermite Series Approximation to the Analogue of r(y,t) in a Two Dimensional Plume, r(y,x). Reproduced from Chatwin and Sullivan (1980a)

CHAPTER THREE

Dispersion in a Linear Strain Velocity Field

3.1 Introduction

In this chapter the use of a Hermite series representation for $\Gamma(\underline{x},t)$ and $C(\underline{x},t)$ is investigated for a particular choice of velocity field, $\underline{\Upsilon}(\underline{x},t)$. The aim is to explore the nature of the influence on the first few terms of each representation of:

(1) the velocity field

(2) the molecular diffusivity, K

(3) the initial distribution, $\Gamma(\underline{x},0)$

and (4) particular choices for the arbitrary tensor in the exponential of each representation.

Sections 3.2 and 3.3 introduce the chosen velocity field and develop and solve the governing equations for the coefficients, $A^{(n)}_{ij\ldots k}(t)$, of the Hermite series for $\Gamma(\underline{x},t)$, (2.17), with respect to arbitrary and particular axes, respectively. Section 3.4 illustrates the way in which equations for the small or large time behaviour of the coefficients can be derived for arbitrary $\alpha_{ij}(t)$ of (2.17). The small and large time behaviour of the coefficients of the Gram-Charlier series for $\Gamma(\underline{x},t)$, that is for a particular choice of $\alpha_{ij}(t)$, is examined in Section 3.5. The influence of the initial distribution, $\Gamma(\underline{x},0)$, is addressed in Section 3.6.

Sections 3.7 and 3.8 discuss and show how the Hermite series for $\Gamma(\underline{x},t)$ can be used to derive a Hermite series for $C(\underline{x},t)$.

The series for $C(\underline{x},t)$ is developed for an arbitrary initial distribution (Section 3.7) and for a spherically symmetric initial distribution (Section 3.8). The summary of and conclusions from the chapter are given in Section 3.9.

3.2 The Velocity Field and Hermite Series Representation for $\Gamma(\underline{x},t)$ With Respect to Arbitrary Axes

This section introduces the chosen velocity field and derives the resulting general governing equations for the coefficients, $A^{(n)}_{ij\ldots k}(t)$, of the Hermite series for $\Gamma(\underline{x},t)$.

3.2.1 The Velocity Field

The velocity field chosen is the pure straining motion (Batchelor 1970, p.79; Monin and Yaglom 1975, p.421)

$$\tau_i = \tau_{ij} x_j$$

where (3.1)

$$\frac{\partial \tau_i}{\partial x_j} = \frac{\partial \tau_j}{\partial x_i} = \tau_{ij}.$$

τ_{ij} is the rate of strain tensor and is assumed symmetrical. The axes with respect to which τ_{ij} is diagonal are the principal strain axes. By incompressibility, (1.2),

$$\tau_{ii} = 0. \qquad (3.2)$$

We will assume τ_{ij} is constant in time and does not vary from realisation to realisation. In addition, the orientation of the principal strain axes will be fixed throughout each realisation. Then $\Gamma(\underline{x},t)$ is a random function of $\underline{x}$ and t solely because the orientation of these axes varies from realisation to realisation. The ensemble mean properties of $\Gamma(\underline{x},t)$ then follow from averaging $\Gamma(\underline{x},t)$ over all possible orientations of the axes.

The velocity field (3.1) is an idealised flow which has been applied widely in the literature (Batchelor 1959; Chatwin and Sullivan 1979a, 1979c, 1980b; Kowe 1982; Kowe and Chatwin 1983, 1985; Saffman 1963; Townsend 1951). A summary of how it is conventionally justified as a suitable, though idealised, flow will illustrate why it has been so widely used.

On release into a turbulent flow, a small, finite quantity of material is spread by both turbulent and molecular diffusion. Because of incompressibility, (1.2), the material is stretched in at least one direction and compressed in another (Chatwin and Sullivan 1980b; Corrsin 1959; Kowe 1982; Monin and Yaglom 1971, p.592).

Schematic of the effect of turbulent diffusion on a finite quantity of material

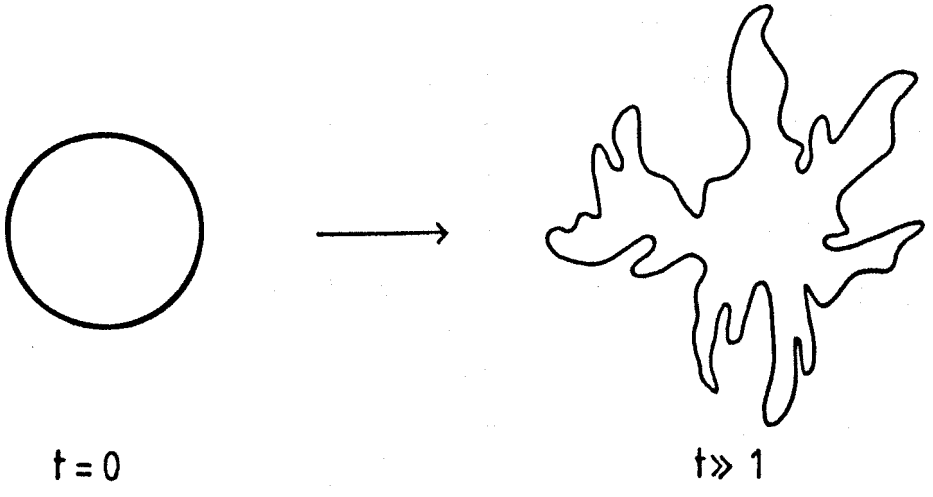

Eventually, the large scale eddies of the flow cause the material to form distended threads or filaments. These filaments, in turn, are spread out by molecular diffusion which smoothes out the large gradients in concentration caused by the filaments and increases the volume occupied by the material. In most flows the turbulent diffusivity is many orders of magnitude greater than the molecular diffusivity. For example, in the atmospheric surface layer, the turbulent diffusivity, which ranges from $\sim 1\text{-}10^2$ $m^2 s^{-1}$, is approximately $10^5\text{-}10^6$ times greater than the molecular diffusivity (Monin and Yaglom 1971).

Let the velocity at a point $\underline{x}+\underline{r}$ in the vicinity of a point $\underline{x}$ be denoted by $\underline{\tau}+\underline{\delta\tau}$. Then

$$\delta\tau_i = \frac{\partial \tau_i}{\partial x_j} r_j + O(|\underline{r}|^2) \ .$$

Now $\partial\tau_i/\partial x_j$ may be written as the sum of symmetrical and anti-symmetrical tensors τ_{ij} and T_{ij} respectively, i.e.

$$\frac{\partial \tau_i}{\partial x_j} = \tau_{ij} + T_{ij}$$

where

$$\tau_{ij} = \frac{1}{2}\left[\frac{\partial \tau_i}{\partial x_j} + \frac{\partial \tau_j}{\partial x_i}\right]$$

$$T_{ij} = \frac{1}{2}\left[\frac{\partial \tau_i}{\partial x_j} - \frac{\partial \tau_j}{\partial x_i}\right]$$

so that

$$\delta T_i \sim \tau_{ij} r_j + T_{ij} r_j .$$

The two contributions to δT_i, $\tau_{ij} r_j$ and $T_{ij} r_j$, are distinct in character (for a detailed discussion see Batchelor 1970). First, we may write

$$T_{ij} r_j = \frac{1}{2} (\underline{\omega} \times \underline{r})_i$$

where $\underline{\omega} = \nabla \times \underline{T}$ is the local vorticity of the fluid. The contribution $T_{ij} r_j$ therefore represents a rigid body rotation about $\underline{x}$ with angular velocity $\frac{1}{2} \underline{\omega}$.

The other contribution to δT_i, $\tau_{ij} r_j$, represents a pure straining motion. In reality, the principal axes of strain - with respect to which τ_{ij} is diagonal and which may always be chosen since τ_{ij} is symmetrical - will rotate (as a consequence of $\underline{\omega}$) and the components of τ_{ij} will change with time (Batchelor 1959). However, we may use the two parameters which characterise the small-scale structure of the flow, namely the kinematic viscosity, ν, and the mean energy dissipation rate, ε, to construct time and length scales over which the velocity field (3.1) is valid. Then we find that the orientation of the principal strain axes and the constancy of τ_{ij} persist for times of the order of $\lambda_t = (\nu/\varepsilon)^{1/2}$. Similarly, because of the assumed linearity in $\underline{r}$, (3.1) is only valid over distances of the order of the viscous cut-off length, or Kolmogorov microscale, $\lambda_x = (\nu^3/\varepsilon)^{1/4}$. In the planetary boundary layer, λ_x is of the order of 10^{-3}m (Pasquill and Smith 1983, p.61). Using a value for ν of 0.14×10^{-4} $m^2 s^{-1}$ (Batchelor 1970) for air at

10^{o}C leads to an estimate of ~0.1s for λ_t. In contrast, Kowe (1982) found values of 0.5×10^{-3}m and 3s, respectively, for λ_x and λ_t in a freon jet, and refers to similar values found by other authors. The validity of λ_x and λ_t as measures of the applicability of (3.1) has been confirmed by work of several authors. Fuller references to and discussion of the relevant results are given in the works already referenced. Suffice it to say here that the velocity field (3.1) has proved to be a useful, simple field with which to examine several aspects of the small-scale structure of the statistical properties of turbulent motion.

In the remainder of this section and Sections 3.3-3.6, with the velocity field given by (3.1), the Hermite series for $\Gamma(\underline{x},t)$ is developed. Sections 3.2.2 and 3.3-3.5 illustrate how the governing equations for the coefficients, $A^{(n)}_{ij\ldots k}(t)$, can be derived for general t, and develop the expressions for small and large times. Ultimately (Section 3.6), it will be shown that for the most natural choice for $\alpha_{ij}(t)$ of the Hermite series, (2.17), namely $\alpha_{ij}(t)$ such that (2.17) is the Gram-Charlier series for $\Gamma(\underline{x},t)$, and with respect to the principal strain axes, for any initial distribution and large enough times the series reduces to its simplest form in which only the first term is non-zero.

3.2.2 The General Governing Equations for the Coefficients $A^{(n)}_{ij\ldots k}(t)$, of the Hermite Series for $\Gamma(\underline{x},t)$

With $\underline{\Upsilon}(\underline{x},t)$ given by (3.1), the governing equation for $\Gamma(\underline{x},t)$ is

$$\frac{\partial \Gamma}{\partial t} + \tau_{pq} x_q \frac{\partial \Gamma}{\partial x_p} = K \frac{\partial^2}{\partial x_p \partial x_p} \Gamma \ . \tag{3.3}$$

Substitution of the Hermite series for $\Gamma(\underline{x},t)$, (2.17), gives

$$\begin{aligned} &\frac{\partial}{\partial t}\left\{n(\underline{\underline{\alpha}}) \sum_{m=0}^{\infty} A^{(m)}_{st\ldots v} H^{(m)}_{st\ldots v} \exp\left[-\tfrac{1}{2}\alpha_{ab} x_a x_b\right]\right\} \\ &\quad + n(\underline{\underline{\alpha}})\, \tau_{pq} x_q \sum_{m=0}^{\infty} A^{(m)}_{st\ldots v} \frac{\partial}{\partial x_p}\left\{H^{(m)}_{st\ldots v} \exp\left[-\tfrac{1}{2}\alpha_{ab} x_a x_b\right]\right\} \\ &\quad = Kn(\underline{\underline{\alpha}}) \sum_{m=0}^{\infty} A^{(m)}_{st\ldots v} \frac{\partial^2}{\partial x_p \partial x_p}\left\{H^{(m)}_{st\ldots v} \exp\left[-\tfrac{1}{2}\alpha_{ab} x_a x_b\right]\right\} \end{aligned} \tag{3.4}$$

In (3.4), the dependency of $H^{(m)}_{st\ldots v}(\underline{x},\underline{\underline{\alpha}})$ on $\underline{x}$ and $\underline{\underline{\alpha}}$ and of $A^{(m)}_{st\ldots v}(t)$ and $\alpha_{ij}(t)$ on t has been omitted for simplicity. Multiplying by $G^{(n)}_{ij\ldots \ell}(\underline{x},\underline{\underline{\alpha}})$ and integrating over $\underline{x}$ leads (after some algebra) to the governing equation for $A^{(n)}_{ij\ldots \ell}(t)$

$$\begin{aligned} &n(n-1)\left\{\frac{\partial A^{(n)}_{ij\ldots \ell}}{\partial t} - \left[\tau_{iq} A^{(n)}_{qj\ldots \ell} + \ldots + \tau_{\ell q} A^{(n)}_{qi\ldots k}\right]\right\} \\ &+ \left[\left\{\frac{\partial a}{\partial t}_{ij} - a_{iq}\tau_{jq} - a_{jq}\tau_{iq}\right\} A^{(n-2)}_{k\ldots \ell} + \ldots + \left\{\frac{\partial a_{k\ell}}{\partial t} - a_{kq}\tau_{\ell q} - a_{\ell q}\tau_{kq}\right\} A^{(n-2)}_{i\ldots j}\right] \\ &= 2K\left[\delta_{ij} A^{(n-2)}_{k\ldots \ell} + \ldots + \delta_{k\ell} A^{(n-2)}_{i\ldots j}\right] \end{aligned} \tag{3.5}$$

where there are n terms in the first set of square brackets, $[\ldots]$, on the left side of this equation and $1/2n(n-1)$ terms inside each of

the remaining square brackets. In (3.5), $a_{ij}(t)$ is given as in Section 2.4.1 and $A^{(0)}(t)$ and $A_i^{(1)}(t)$ are given by (2.20a) and (2.20b) viz.

$$a_{ij}\alpha_{jk} = \delta_{ik}$$
$$A^{(0)}(t) = 1$$
$$A_i^{(1)}(t) = 0 .$$

Whilst for n=2, 3 and 4, (3.5) gives

$$\frac{\partial A_{ij}^{(2)}}{\partial t} - \left[\tau_{iq}A_{qj}^{(2)} + \tau_{jq}A_{qi}^{(2)}\right] + \frac{1}{2}\left[\frac{\partial a_{ij}}{\partial t} - a_{iq}\tau_{jq} - a_{jq}\tau_{iq}\right] = K\delta_{ij} \qquad (3.6)$$

$$\frac{\partial A_{ijk}^{(3)}}{\partial t} - \left[\tau_{iq}A_{qjk}^{(3)} + \tau_{jq}A_{qik}^{(3)} + \tau_{kq}A_{qij}^{(3)}\right] = 0 \qquad (3.7)$$

$$\frac{\partial A_{ijk\ell}^{(4)}}{\partial t} - \left[\tau_{iq}A_{qjk\ell}^{(4)} + \tau_{jq}A_{qik\ell}^{(4)} + \tau_{kq}A_{qij\ell}^{(4)} + \tau_{\ell q}A_{qijk}^{(4)}\right]$$
$$+ \frac{1}{12}\left[\left[\frac{\partial a_{ij}}{\partial t} - a_{iq}\tau_{jq} - a_{jq}\tau_{iq}\right]A_{k\ell}^{(2)} + \left[\frac{\partial a_{ik}}{\partial t} - a_{iq}\tau_{kq} - a_{kq}\tau_{iq}\right]A_{j\ell}^{(2)}\right.$$
$$+ \left[\frac{\partial a_{i\ell}}{\partial t} - a_{iq}\tau_{\ell q} - a_{\ell q}\tau_{iq}\right]A_{jk}^{(2)} + \left[\frac{\partial a_{jk}}{\partial t} - a_{jq}\tau_{kq} - a_{kq}\tau_{jq}\right]A_{i\ell}^{(2)}$$
$$\left.+ \left[\frac{\partial a_{j\ell}}{\partial t} - a_{jq}\tau_{\ell q} - a_{\ell q}\tau_{jq}\right]A_{ik}^{(2)} + \left[\frac{\partial a_{k\ell}}{\partial t} - a_{kq}\tau_{\ell q} - a_{\ell q}\tau_{kq}\right]A_{ij}^{(2)}\right]$$
$$= \frac{K}{6}\left[\delta_{ij}A_{k\ell}^{(2)} + \delta_{ik}A_{j\ell}^{(2)} + \delta_{i\ell}A_{jk}^{(2)} + \delta_{jk}A_{i\ell}^{(2)} + \delta_{j\ell}A_{ik}^{(2)} + \delta_{k\ell}A_{ij}^{(2)}\right] \qquad (3.8)$$

In general, the odd order coefficents, $A^{(2n+1)}_{ij\ldots k}(t)$, n=0,1,...., do not depend on K.

3.3 The Velocity Field and Hermite Series Representation for $\Gamma(\underline{x},t)$ With Respect to the Principal Strain Axes

To simplify the algebra, the behaviour of the coefficients with respect to the principal axes of rate of strain will be examined. As will be seen, these axes represent the most convenient to use for discussion of the choice of the arbitrary tensor $\alpha_{ij}(t)$, and hence $a_{ij}(t)$, of the series for $\Gamma(\underline{x},t)$, (2.17). Choosing axes such that τ_{ij} has components

$$\begin{bmatrix} \tau_1 & 0 & 0 \\ 0 & \tau_2 & 0 \\ 0 & 0 & \tau_3 \end{bmatrix} \tag{3.9}$$

(3.5) may now be written

$$\begin{aligned} n(n-1)\left\{\frac{\partial A^{(n)}_{ij\ldots\ell}}{\partial t} - [\tau_i+\tau_j+\ldots+\tau_\ell]A^{(n)}_{ij\ldots\ell}\right\} \\ + \left[\left\{\frac{\partial a_{ij}}{\partial t} - a_{ij}(\tau_i+\tau_j)\right\}A^{(n-2)}_{k\ldots\ell} + \ldots + \left\{\frac{\partial a_{k\ell}}{\partial t} - a_{k\ell}(\tau_k+\tau_\ell)\right\}A^{(n-2)}_{i\ldots j}\right] \\ = 2K\left[\delta_{ij}A^{(n-2)}_{k\ldots\ell} + \ldots + \delta_{k\ell}A^{(n-2)}_{i\ldots j}\right] \end{aligned} \tag{3.10}$$

where now there is no summation over repeated subscripts. Using the same notation, (3.6)-(3.8) simplify to give

$$\frac{\partial A^{(2)}_{ij}}{\partial t} - (\tau_i+\tau_j)A^{(2)}_{ij} + \frac{1}{2}\left[\frac{\partial a_{ij}}{\partial t} - a_{ij}(\tau_i+\tau_j)\right] = K\delta_{ij} \qquad (3.11)$$

$$\frac{\partial A^{(3)}_{ijk}}{\partial t} - (\tau_i+\tau_j+\tau_k)A^{(3)}_{ijk} = 0 \qquad (3.12)$$

$$\frac{\partial A^{(4)}_{ijk\ell}}{\partial t} - (\tau_i+\tau_j+\tau_k+\tau_\ell)A^{(4)}_{ijk\ell}$$

$$+ \frac{1}{12}\left[\left[\frac{\partial a_{ij}}{\partial t} - a_{ij}(\tau_i+\tau_j)\right]A^{(2)}_{k\ell} + 5 \text{ similar terms}\right]$$

$$= \frac{K}{6}\left[\delta_{ij}A^{(2)}_{k\ell} + 5 \text{ similar terms}\right] . \qquad (3.13)$$

For example, for $i=j=1$, (3.11) gives

$$\left[\frac{\partial}{\partial t} - 2\tau_1\right]\left[A^{(2)}_{11} + \frac{1}{2}a_{11}\right] = K$$

so that

$$A^{(2)}_{11}(t) = \left[A^{(2)}_{11} + \frac{1}{2}a_{11}\right](0)\exp(2\tau_1 t) + \frac{K}{2\tau_1}\left[\exp(2\tau_1 t) - 1\right] - \frac{1}{2}a_{11}. \qquad (3.14a)$$

Similar equations for $A^{(2)}_{22}(t)$ and $A^{(2)}_{33}(t)$ can obviously be derived. For $i=1$, $j=2$, (3.11) gives

$$A^{(2)}_{12}(t) = \left[A^{(2)}_{12} + \frac{1}{2}a_{12}\right](0)\exp([\tau_1+\tau_2]t) - \frac{1}{2}a_{12} \qquad (3.14b)$$

and similarly for $A^{(2)}_{13}(t)$ and $A^{(2)}_{23}(t)$. Following a similar

procedure for the third and fourth order coefficients, using (3.12) and (3.13) we obtain

$$A^{(3)}_{111}(t) = A^{(3)}_{111}(0)\exp(3\tau_1 t) \tag{3.15a}$$

(similarly for $A^{(3)}_{222}(t)$ and $A^{(3)}_{333}(t)$)

$$A^{(3)}_{112}(t) = A^{(3)}_{112}(0)\exp([2\tau_1+\tau_2]t) \tag{3.15b}$$

(similarly for $A^{(3)}_{113}(t)$, $A^{(3)}_{221}(t)$, $A^{(3)}_{223}(t)$, $A^{(3)}_{331}(t)$ and $A^{(3)}_{332}(t)$)

$$\begin{aligned} A^{(3)}_{123}(t) &= A^{(3)}_{123}(0)\exp([\tau_1+\tau_2+\tau_3]t) \\ &= A^{(3)}_{123}(0) \qquad \text{(using (3.2))} \end{aligned} \tag{3.15c}$$

and

$$A^{(4)}_{1111}(t) = A^{(4)}_{1111}(0)\exp(4\tau_1 t) + f^{(4)}_{1111}(0)\exp(4\tau_1 t) - f^{(4)}_{1111}(t) \tag{3.16a}$$

where

$$f^{(4)}_{1111}(t) = \frac{K}{2\tau_1}\left[A^{(2)}_{11} + \frac{1}{2}a_{11} + \frac{K}{4\tau_1}\right] + \frac{1}{8}a_{11}\left[4A^{(2)}_{11} + a_{11}\right]$$

(similarly for $A^{(4)}_{2222}(t)$ and $A^{(4)}_{3333}(t)$)

$$A^{(4)}_{1112}(t) = A^{(4)}_{1112}(0)\exp([3\tau_1+\tau_2]t) + f^{(4)}_{1112}(0)\exp([3\tau_1+\tau_2]t) - f^{(4)}_{1112}(t) \tag{3.16b}$$

where

$$f^{(4)}_{1112}(t) = \frac{K}{4\tau_1}\left[A^{(2)}_{12} + \frac{1}{2}a_{12}\right] + \frac{1}{4}\left[a_{11}A^{(2)}_{12} + a_{12}A^{(2)}_{11} + \frac{1}{2}a_{11}a_{12}\right]$$

(similarly for $A^{(4)}_{1113}(t)$, $A^{(4)}_{2221}(t)$, $A^{(4)}_{2223}(t)$, $A^{(4)}_{3331}(t)$ and $A^{(4)}_{3332}(t)$)

$$A^{(4)}_{1122}(t) = A^{(4)}_{1122}(0)\exp(2[\tau_1+\tau_2]t) + f^{(4)}_{1122}(0)\exp(2[\tau_1+\tau_2]t) - f^{(4)}_{1122}(t) \tag{3.16c}$$

where

$$f^{(4)}_{1122}(t) = \frac{K}{12\tau_1}\left[A^{(2)}_{22} + \frac{1}{2}a_{22} + \frac{K}{4\tau_2}\right] + \frac{K}{12\tau_2}\left[A^{(2)}_{11} + \frac{1}{2}a_{11} + \frac{K}{4\tau_1}\right]$$
$$+ \frac{1}{24}\left[2\left[a_{11}A^{(2)}_{22} + a_{22}A^{(2)}_{11}\right] + 8a_{12}A^{(2)}_{12} + \left[a_{11}a_{22} + 2a^2_{12}\right]\right]$$

(similarly for $A^{(4)}_{1133}(t)$ and $A^{(4)}_{2233}(t)$)

$$A^{(4)}_{1123}(t) = A^{(4)}_{1123}(0)\exp(\tau_1 t) + f^{(4)}_{1123}(0)\exp(\tau_1 t) - f^{(4)}_{1123}(t) \tag{3.16d}$$

where

$$f^{(4)}_{1123}(t) = \frac{K}{12\tau_1}\left[A^{(2)}_{23} + \frac{1}{2}a_{23}\right] + \frac{1}{12}\left[a_{11}A^{(2)}_{23} + a_{23}A^{(2)}_{11}\right.$$

$$+ 2\left[a_{12}A_{13}^{(2)} + a_{13}A_{12}^{(2)}\right] + \frac{1}{2}\left[a_{11}a_{23} + 2a_{12}a_{13}\right]\Big]$$

(similarly for $A_{2213}^{(4)}(t)$ and $A_{3312}^{(4)}(t)$)

Since each $A_{ij\ldots k}^{(n)}(t)$ is a sum of functions of the moments of $\Gamma(\underline{x},t)$, $M_{ij\ldots k}^{(m)}(t)$, $m<n$, (Section 2.4.1), the right hand side of each of (3.14)-(3.16) can be expressed in the form of a sum of one or more of the following:

(1) terms depending on τ_1, τ_2, τ_3, t and, through $M_{ij\ldots k}^{(n)}(0)$, the initial distribution, $\Gamma(\underline{x},0)$, only

(2) terms depending on τ_1, τ_2, τ_3, t, $\Gamma(\underline{x},0)$ and K

(3) terms depending on τ_1, τ_2, τ_3, t and K

and (4) other terms.

For example, from (3.14) and (2.20c)

$$A_{11}^{(2)}(t) = \frac{1}{2}\left\{M_{11}^{(2)}(0)\exp(2\tau_1 t) + \frac{K}{\tau_1}\left[\exp(2\tau_1 t) - 1\right] - a_{11}\right\}$$

$$A_{12}^{(2)}(t) = \frac{1}{2}\left\{M_{12}^{(2)}(0)\exp([\tau_1+\tau_2]t) - a_{12}\right\}. \qquad (3.17)$$

Following the same procedure for the third and fourth order coefficients, from (3.15) and (3.16) we obtain

$$A_{111}^{(3)}(t) = \frac{1}{6}M_{111}^{(3)}(0)\exp(3\tau_1 t) \qquad (3.18a)$$

$$A^{(3)}_{112}(t) = \frac{1}{6} M^{(3)}_{112}(0)\exp([2\tau_1+\tau_2]t) \tag{3.18b}$$

$$A^{(3)}_{123}(t) = \frac{1}{6} M^{(3)}_{123}(0) \tag{3.18c}$$

$$\begin{aligned} A^{(4)}_{1111}(t) = \frac{1}{24} \Big\{ & M^{(4)}_{1111}(0)\exp(4\tau_1 t) - 6M^{(2)}_{11}(0)a_{11}\exp(2\tau_1 t) \\ & + 6 \frac{K}{\tau_1} M^{(2)}_{11}(0)\exp(2\tau_1 t)[\exp(2\tau_1 t) - 1] \\ & + 3 \frac{K}{\tau_1} [\exp(2\tau_1 t) - 1]\Big[\frac{K}{\tau_1} [\exp(2\tau_1 t) - 1] - 2a_{11}\Big] + 3a^2_{11}\Big\} \end{aligned} \tag{3.19a}$$

$$\begin{aligned} A^{(4)}_{1112}(t) = \frac{1}{24} \Big\{ & M^{(4)}_{1112}(0)\exp([3\tau_1+\tau_2]t) - 3\exp(\tau_1 t)\Big[M^{(2)}_{12}(0)a_{11}\exp(\tau_2 t) \\ & + M^{(2)}_{11}(0)a_{12}\exp(\tau_1 t)\Big] \\ & + 3 \frac{K}{\tau_1} M^{(2)}_{12}(0)\exp([\tau_1+\tau_2]t)[\exp(2\tau_1 t) - 1] \\ & - 3 \frac{K}{\tau_1} a_{12} [\exp(2\tau_1 t) - 1] + 3a_{11}a_{12}\Big\} \end{aligned} \tag{3.19b}$$

$$\begin{aligned} A^{(4)}_{1122}(t) = \frac{1}{24} \Big\{ & M^{(4)}_{1122}(0)\exp(2[\tau_1+\tau_2]t) \\ & - \Big[M^{(2)}_{11}(0)a_{22}\exp(2\tau_1 t) + M^{(2)}_{22}(0)a_{11}\exp(2\tau_2 t) \\ & + 4M^{(2)}_{12}(0)a_{12}\exp([\tau_1+\tau_2]t)\Big] \\ & + K \Big[\frac{1}{\tau_2} M^{(2)}_{11}(0)\exp(2\tau_1 t)[\exp(2\tau_2 t) - 1] \\ & + \frac{1}{\tau_1} M^{(2)}_{22}(0)\exp(2\tau_2 t)[\exp(2\tau_1 t) - 1]\Big] \end{aligned}$$

(contd.)

$$+ \frac{K^2}{\tau_1\tau_2}[1 - \exp(2\tau_1 t)][1 - \exp(2\tau_2 t)]$$

$$- K\left[\frac{1}{\tau_1} a_{22}[\exp(2\tau_1 t) - 1] + \frac{1}{\tau_2} a_{11}[\exp(2\tau_2 t) - 1]\right]$$

$$+ (a_{11}a_{22} + 2a_{12}^2)\Big\} . \qquad (3.19c)(\text{contd.})$$

$$A^{(4)}_{1123}(t) = \frac{1}{24}\Big\{M^{(4)}_{1123}(0)\exp(\tau_1 t) - \Big[M^{(2)}_{23}(0)a_{11}\exp([\tau_2+\tau_3]t)$$

$$+ M^{(2)}_{11}(0)a_{23}\exp(2\tau_1 t)$$

$$+ 2M^{(2)}_{12}(0)a_{13}\exp([\tau_1+\tau_2]t) + 2M^{(2)}_{13}(0)a_{12}\exp([\tau_1+\tau_3]t)\Big]$$

$$+ \frac{K}{\tau_1} M^{(2)}_{23}(0)\exp([\tau_2+\tau_3]t)[\exp(2\tau_1 t) - 1]$$

$$- \frac{K}{\tau_1} a_{23}[\exp(2\tau_1 t) - 1] + (a_{11}a_{23} + 2a_{12}a_{13})\Big\} . \qquad (3.19d)$$

From (3.17) and (3.18) (or (3.11) and (3.12) we see that $A^{(2)}_{ij}(t)$, $i\neq j$, does not depend on K; $A^{(3)}_{ijk}(t)$ does not depend on K or $a_{ij}(t)$ and, in particular, $A^{(3)}_{123}(t)$ is independent of K, $a_{ij}(t)$ and $\underline{\Upsilon}$, and so is constant for all t. On expressing the left side of each of (3.17)-(3.19) in terms of the moments of $\Gamma(\underline{x},t)$, $M^{(n)}_{ij\ldots k}(t)$ we obtain the governing equations for $M^{(n)}_{ij\ldots k}(t)$, $n\leq 4$, with respect to the principal axes of strain. For example, from (3.19a and c)

$$M^{(4)}_{1111}(t) = M^{(4)}_{1111}(0)\exp(4\tau_1 t) + 6\frac{K}{\tau_1} M^{(2)}_{11}(0)\exp(2\tau_1 t)[\exp(2\tau_1 t) - 1]$$

$$+ 3\frac{K^2}{\tau_1^2}[\exp(2\tau_1 t) - 1]^2$$

(contd.)

$$M^{(4)}_{1122}(t) = M^{(4)}_{1122}(0)\exp(2[\tau_1+\tau_2]t) + \frac{K}{\tau_2} M^{(2)}_{11}(0)\exp(2\tau_1 t)[\exp(2\tau_2 t) - 1]$$

$$+ \frac{K}{\tau_1} M^{(2)}_{22}(0)\exp(2\tau_2 t)[\exp(2\tau_1 t) - 1]$$

$$+ \frac{K^2}{\tau_1\tau_2} [\exp(2\tau_1 t)-1][\exp(2\tau_2 t) - 1] \; . \qquad (3.20)(\text{contd.})$$

These expressions, and the corresponding expressions which can be derived from (3.17), (3.18) and (3.19b and d) for other $M^{(n)}_{ij\ldots k}(t)$, $n\leq 4$, could obviously be derived more directly by multiplying (3.3) by $x_1^a x_2^b x_3^c$ for appropriate integers a,b and c and integrating over $\underline{x}$.

Having developed the general equations for $A^{(n)}_{ij\ldots k}(t)$, $n\leq 4$, with respect to the principal axes of strain, it is of interest to examine the behaviour of these coefficients for both small and large t:

(a) for arbitrary $\alpha_{ij}(t)$

(b) for particular choices of $\alpha_{ij}(t)$.

Initially, no assumptions about the initial distribution of material, $\Gamma(\underline{x},0)$, and therefore about $M^{(n)}_{ij\ldots k}(0)$, will be made.

3.4 Behaviour of the Coefficients, $A^{(n)}_{ij\ldots k}(t)$, for Arbitrary $\alpha_{ij}(t)$ and Small Times With Respect to the Principal Strain Axes

For arbitrary $\alpha_{ij}(t)$ - and hence $a_{ij}(t)$ - and initial distribution, $\Gamma(\underline{x},0)$, using the governing equations derived in Section 3.3, it is obviously possible to examine the behaviour of the coefficients of the Hermite series, $A^{(n)}_{ij\ldots k}(t)$, for both small and large times (that is with respect to the principal strain axes).

For example, from (3.17a), (3.18a) and (3.19a), for small t

$$A_{11}^{(2)}(t) = \frac{1}{2}\left\{M_{11}^{(2)}(0) + 2\tau_1\left[M_{11}^{(2)}(0) + \frac{K}{\tau_1}\right]\left[t + \tau_1 t^2 + \frac{2}{3}\tau_1^2 t^3 + \ldots\right] - a_{11}\right\} \tag{3.21}$$

$$A_{111}^{(3)}(t) = \frac{1}{6} M_{111}^{(3)}(0)\left[1 + 3\tau_1 t + \frac{9}{2}\tau_1^2 t^2 + \frac{9}{2}\tau_1^3 t^3 + \ldots\right] \tag{3.22}$$

$$\begin{aligned} A_{1111}^{(4)}(t) = \frac{1}{24}\Bigg\{ & \left[M_{1111}^{(4)}(0) - 6M_{11}^{(2)}(0)a_{11} + 3a_{11}^2\right] \\ & + \left[M_{1111}^{(4)}(0) - 3M_{11}^{(2)}(0)a_{11} + 3\frac{K}{\tau_1}\left[M_{11}^{(2)}(0) - a_{11}\right]\right]4\tau_1 t \\ & + \left[2M_{1111}^{(4)}(0) - 3M_{11}^{(2)}(0)a_{11} + 3\frac{K}{\tau_1}\left[\frac{K}{\tau_1} + 3M_{11}^{(2)}(0) - a_{11}\right]\right]4\tau_1^2 t^2 \\ & + \left[4M_{1111}^{(4)}(0) - 3M_{11}^{(2)}(0)a_{11} + 3\frac{K}{\tau_1}\left[3\frac{K}{\tau_1} + 7M_{11}^{(2)}(0) - a_{11}\right]\right]\frac{8}{3}\tau_1^3 t^3 \\ & + \ldots\Bigg\} \end{aligned} \tag{3.23}$$

The corresponding equations for other $A_{ij\ldots k}^{(n)}(t)$ can be readily derived. In general they show that, as expected, to $O(1)$, the coefficients depend on the initial distribution, $\Gamma(\underline{x},0)$, only. To $O(t)$ they depend on $\Gamma(\underline{x},0)$ and advection (via the τ_i, $i=1(1)3$) and diffusion separately. Interaction between advection and diffusion only becomes evident to $O(t^2)$. The results for the second order coefficients $(A_{ij}^{(2)}(t))$ can be shown to be consistent with the analysis by Saffman (1960) of the effect of the interaction between molecular diffusion and turbulent advection on the small

time dispersion. With the summation convention, using

$$L^2(t) = \int x_i x_i \Gamma(\underline{x},t)dV(\underline{x})$$

as a measure of the spread of the instantaneous cloud about its centre of mass, from (2.18) and (2.20c) we have

$$L^2(t) = 2\left[A_{ii}^{(2)} + \frac{1}{2} a_{ii}\right](t) .$$

Using (3.21), the corresponding equations for $A_{22}^{(2)}(t)$ and $A_{33}^{(2)}(t)$, and (3.2), for small t

$$\begin{aligned} L^2(t) = {} & \left[M_{11}^{(2)}+M_{22}^{(2)}+M_{33}^{(2)}\right](0) + 2\left[\tau_1 M_{11}^{(2)}(0)+\tau_2 M_{22}^{(2)}(0)+\tau_3 M_{33}^{(2)}(0)\right]t + 6Kt \\ & + 2\left[\tau_1^2 M_{11}^{(2)}(0)+\tau_2^2 M_{22}^{(2)}(0)+\tau_3^2 M_{33}^{(2)}(0)\right]t^2 \\ & + \frac{4}{3}\left[\tau_1^3 M_{11}^{(2)}(0)+\tau_2^3 M_{22}^{(2)}(0)+\tau_3^3 M_{33}^{(2)}(0)\right]t^3 \\ & + \frac{4}{3} K \left[\tau_1^2 + \tau_2^2 + \tau_3^2\right]t^3 . \end{aligned}$$

So that the accelerating effect (Saffman 1960) on $L^2(t)$ of the interaction between molecular diffusion and advection becomes evident at $O(t^3)$.

The above equations have simply served to illustrate the way in which the small, and by analogy the large, time behaviour of the coefficients for an arbitrary initial distribution, $\Gamma(\underline{x},0)$, and $\alpha_{ij}(t)$ can be investigated. However, it is more illuminating to examine this behaviour for particular initial distributions and

choices of the arbitrary tensor $\alpha_{ij}(t)$. This is done in Sections 3.5 and 3.6.

3.5 Behaviour of the Coefficients, $A^{(n)}_{ij\ldots k}(t)$, of the Gram-Charlier Series for $\Gamma(\underline{x},t)$ With Respect to the Principal Strain Axes

As discussed in chapter two, there is one choice for $a_{ij}(t)$, and therefore $\alpha_{ij}(t)$, of obvious interest, namely $a_{ij}(t)$ such that $A^{(2)}_{ij}(t)=0$. With this choice for $a_{ij}(t)$, (2.17) corresponds to the Gram-Charlier series for $\Gamma(\underline{x},t)$ (Section 2.2.2). Initially, the general equation for $A^{(n)}_{ij\ldots k}(t)$ for this choice of $a_{ij}(t)$ will be developed.

3.5.1 General Equation for the Coefficents

Choosing

$$a_{ij}(t) = M^{(2)}_{ij}(t) = Q^{-1} \int x_i x_j \Gamma(\underline{x},t) dV(\underline{x}). \tag{3.24}$$

Then

$$A^{(2)}_{ij}(t) = 0 \ . \tag{3.25}$$

From (3.5) and (3.6) the general equation for $A^{(n)}_{ij\ldots\ell}(t)$ for arbitrary τ_{ij} simplifies to

$$\frac{\partial A^{(n)}_{ij\ldots\ell}}{\partial t} - \left[\tau_{iq}A^{(n)}_{qj\ldots\ell} + \ldots. + \tau_{\ell q}A^{(n)}_{qi\ldots j}\right] = 0$$

where the summation convention has been used. Hence we see that with respect to arbitrary axes, and unlike the case for arbitrary $a_{ij}(t)$ (Section 3.2.2), for this particular choice of $a_{ij}(t)$ each $A^{(n)}_{ij\ldots k}(t)$ is independent of $a_{ij}(t)$ and molecular diffusion, and depends only on the advection, via τ_{ij}, and the initial distribution, $\Gamma(\underline{x},0)$, via $A^{(n)}_{ij\ldots k}(0)$. With respect to the principal strain axes, using (3.9), the equation for $A^{(n)}_{ij\ldots k}(t)$ simplifies to

$$\frac{\partial A^{(n)}_{ij\ldots\ell}}{\partial t} - (\tau_i + \tau_j + \ldots + \tau_\ell)A^{(n)}_{ij\ldots\ell} = 0$$

where there is no summation over repeated subscripts. Hence

$$A^{(n)}_{ij\ldots\ell}(t) = A^{(n)}_{ij\ldots\ell}(0)\ \exp([\tau_i+\tau_j+\ \ldots\ +\tau_\ell]t). \tag{3.26}$$

Thus with $a_{ij}(t)$ given by (3.24) and using the summation convention, the series for $\Gamma(\underline{x},t)$ becomes

$$\Gamma(\underline{x},t) = Qn(\underline{\gamma})\left\{1 + \sum_{m=3}^{\infty} A^{(m)}_{ij\ldots k}(t)H^{(m)}_{ij\ldots k}(\underline{x},\underline{\gamma})\right\}\exp\left[-\tfrac{1}{2}\gamma_{pq}x_p x_q\right] \tag{3.27a}$$

where $A^{(m)}_{ij\ldots k}(t)$ is given by (3.26) and

$$\gamma_{ij}(t)M^{(2)}_{jk}(t) = \delta_{ik}. \tag{3.27b}$$

Using (3.11) and (2.20c)

$$M_{ij}^{(2)}(t) = M_{ij}^{(2)}(0)\exp([\tau_i+\tau_j]t) + \frac{2K}{(\tau_i+\tau_j)}\left[\exp([\tau_i+\tau_j]t) - 1\right]\delta_{ij}. \tag{3.28}$$

Equation (3.27) is the Gram-Charlier series for $\Gamma(\underline{x},t)$. On the right of (3.27a), the dependence of $\Gamma(\underline{x},t)$ on molecular diffusion is now reflected in the exponential $\exp\left[-\frac{1}{2}\gamma_{pq}x_p x_q\right]$ - via the dependence of $M_{ij}^{(2)}(t)$ and hence $\gamma_{ij}(t)$ on K.

3.5.2 Small Time Behaviour of the Coefficients

With $a_{ij}(t)$ given by (3.24) and (3.28), the small time behaviour of the coefficients follows directly from (3.26). For small t and general τ_i, i=1(1)3, we have

$$A_{ij\ldots\ell}^{(n)}(t) = A_{ij\ldots\ell}^{(n)}(0)\left\{1 + (\tau_i+\tau_j+\ldots+\tau_\ell)t + \frac{1}{2}(\tau_i+\tau_j+\ldots+\tau_\ell)t^2 + \ldots\right\}. \tag{3.29}$$

Hence to O(1), as expected the coefficients only depend on the initial distribution, $\Gamma(\underline{x},0)$, whilst to higher order in t, they depend on both $\Gamma(\underline{x},0)$ and advection. In particular, using (2.20c), (2.20d) and (3.24)

$$A_{ijk}^{(3)}(0) = \frac{1}{6}M_{ijk}^{(3)}(0)$$

and

$$A^{(4)}_{ijk\ell}(0) = \frac{1}{24}\left\{M^{(4)}_{ijk\ell}(0) - \left[M^{(2)}_{ij}M^{(2)}_{k\ell} + M^{(2)}_{ik}M^{(2)}_{j\ell} + M^{(2)}_{i\ell}M^{(2)}_{jk}\right](0)\right\} .$$

So that, substituting into (3.29), letting $S_3 = \tau_i+\tau_j+\tau_k$ and $S_4 = S_3+\tau_\ell$

$$A^{(3)}_{ijk}(t) = \frac{1}{6} M^{(3)}_{ijk}(0)\left[1 + S_3 t + \frac{1}{2} S_3^2 t^2 + \ldots\right]$$

and

$$A^{(4)}_{ijk\ell}(t) = \frac{1}{24}\left\{M^{(4)}_{ijk\ell}(0)-\left[M^{(2)}_{ij}M^{(2)}_{k\ell}+2 \text{ similar terms}\right](0)\right\}\left[1+S_4 t+ \frac{1}{2} S_4^2 t^2+..\right]$$

The difference between these equations and the corresponding equations for general $a_{ij}(t)$ (Section 3.4) is their lack of dependence on $a_{ij}(t)$ and K. Obviously this is a direct consequence of the independence of the coefficients for all times from $a_{ij}(t)$ and K, (3.26).

3.5.3 Large Time Behaviour of the Coefficients

To examine the large time behaviour of the coefficients (i.e. as $t \to \infty$), consider two particular choices for τ_i:

$$\text{(a)} \quad \tau_1 < 0,\ \tau_2 = \tau_3 > 0 \quad (\text{i.e. } \tau_1 = -2\tau_3 < 0)$$

$$\text{(b)} \quad \tau_1 = \tau_2 < 0,\ \tau_3 > 0 \quad (\text{i.e. } \tau_1 = -\tfrac{1}{2}\tau_3 < 0) . \qquad (3.30)$$

These two cases provide simple illustrative examples with which to examine the time development of the coefficients of the Hermite series for $\Gamma(\underline{x},t)$. They have been used by other authors to discuss various aspects of dispersion in a linear strain velocity field (Chatwin and Sullivan 1979a, 1980b; Kowe 1982; Kowe and Chatwin 1983, 1985). In order to compare the two cases, consider what happens in each case, and in the absence of molecular diffusion, to a blob of contaminant on release into the flow. In the first case, the blob is compressed in the direction of one of the principal strain axes and stretched in the directions of the other two axes. Hence, adopting the terminology of Chatwin and Sullivan (1980b), the blob is transformed into a 'discus'. In the other case, (b) above, the blob is compressed in the directions of two of the principal strain axes and stretched in the direction of the other, and so is transformed into a 'cigar' shape.

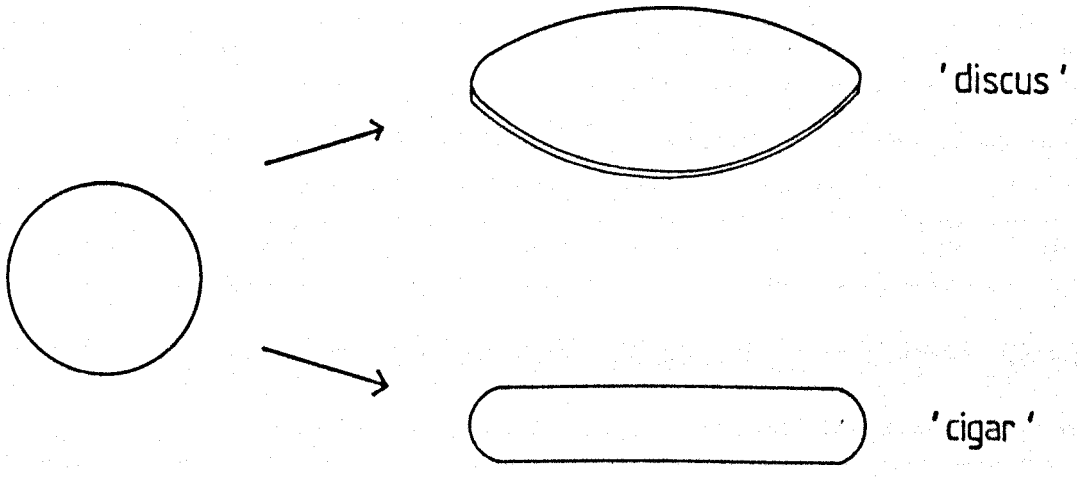

(a) $\tau_1 < 0, \tau_2 = \tau_3 > 0$

The behaviour of $A^{(n)}_{ij\ldots k}(t)$, n=3,4 as $t \to \infty$ follows from (3.26) and (3.30a):

$A^{(3)}_{111}(t)$ $\propto \exp(-6\tau_3 t)$

$A^{(3)}_{112}(t)$, $A^{(3)}_{113}(t)$ $\propto \exp(-3\tau_3 t)$

$\Big\}\ \to 0$ as $t \to \infty$ (3.31a)

$A^{(3)}_{133}(t)$, $A^{(3)}_{122}(t)$, $A^{(3)}_{123}(t)$ are constant for all t (3.31b)

$A^{(3)}_{222}(t)$, $A^{(3)}_{333}(t)$, $A^{(3)}_{233}(t)$, $A^{(3)}_{322}(t)$ increase like $\exp(3\tau_3 t)$ as $t \to \infty$ (3.31c)

$$A^{(4)}_{1111}(t) \qquad \propto \exp(-8\tau_3 t)$$

$$A^{(4)}_{1112}(t), \quad A^{(4)}_{1113}(t) \qquad \propto \exp(-5\tau_3 t)$$

$$A^{(4)}_{1122}(t), \quad A^{(4)}_{1133}(t), \quad A^{(4)}_{1123}(t) \qquad \propto \exp(-2\tau_3 t)$$

$$\Big\} \to 0 \quad \text{as} \quad t \to \infty \qquad (3.32a)$$

$$A^{(4)}_{2222}(t), \quad A^{(4)}_{3333}(t), \quad A^{(4)}_{2233}(t), \quad A^{(4)}_{3332}(t), \quad A^{(4)}_{2223}(t)$$

$$\text{increase like} \quad \exp(4\tau_3 t) \quad \text{as} \quad t \to \infty \qquad (3.32b)$$

$A^{(4)}_{1333}(t)$, $A^{(4)}_{1222}(t)$, $A^{(4)}_{1233}(t)$, $A^{(4)}_{1322}(t)$ } increase like $\exp(\tau_3 t)$ as $t \to \infty$ (3.32c)

(b) $\tau_1 = \tau_2 < 0$, $\tau_3 > 0$

$A^{(3)}_{111}(t)$, $A^{(3)}_{112}(t)$, $A^{(3)}_{122}(t)$, $A^{(3)}_{222}(t)$ } $\propto \exp\left[-\frac{3}{2}\tau_3 t\right] \to 0$ as $t \to \infty$ (3.33a)

$A^{(3)}_{123}(t)$, $A^{(3)}_{223}(t)$, $A^{(3)}_{113}(t)$ } are constant for all t (3.33b)

$A^{(3)}_{333}(t)$ increases like $\exp(3\tau_3 t)$ as $t \to \infty$ (3.33c)

$A^{(3)}_{133}(t)$, $A^{(3)}_{233}(t)$ increase like $\exp\left[\frac{3}{2}\tau_3 t\right]$ as $t \to \infty$ (3.33d)

$A^{(4)}_{1111}(t) \propto \exp(-2\tau_3 t)$

$A^{(4)}_{1113}(t)$, $A^{(4)}_{2223}(t)$, $A^{(4)}_{1223}(t)$, $A^{(4)}_{1123}(t) \propto \exp\left[-\frac{1}{2}\tau_3 t\right]$

$\to 0$ as $t \to \infty$ (3.34a)

$A^{(4)}_{3333}(t)$ increases like $\exp(4\tau_3 t)$ as $t \to \infty$ (3.34b)

$A^{(4)}_{1333}(t)$, $A^{(4)}_{2333}(t)$ increase like $\exp\left[\frac{5}{2}\tau_3 t\right]$ as $t \to \infty$ (3.34c)

$$\left.\begin{array}{l} A^{(4)}_{1133}(t) \\ \\ A^{(4)}_{2233}(t) \\ \\ A^{(4)}_{1233}(t) \end{array}\right\} \quad \text{increase like} \quad \exp(\tau_3 t) \quad \text{as} \quad t \to \infty \qquad (3.34d)$$

Although it is possible to use these results to examine the behaviour of the first few (three say) terms of (3.27) for large times, the resulting expressions are rather complex. As will be shown in the next section (Section 3.6), because of the nature of the chosen velocity field, for large enough times, any initial distribution, and $a_{ij}(t)$ given by (3.24), the Hermite series for $\Gamma(\underline{x},t)$ can be simplified.

3.6 Behaviour of the Coefficients, $A^{(n)}_{ij\ldots k}(t)$, for a Spherically Symmetric Initial Distribution

By choosing a particular velocity field, the previous sections have illustrated how the governing equations and properties of the coefficients of the series for $\Gamma(\underline{x},t)$ can be developed. So far the analysis has been in terms of an arbitrary initial distribution, $\Gamma(\underline{x},0)$, and both arbitrary and particular choices for the tensor $\alpha_{ij}(t)$ of the series for $\Gamma(\underline{x},t)$. This section demonstrates how, when referred to the principal strain axes, the Hermite series for $\Gamma(\underline{x},t)$ simplifies for:

(a) any spherically symmetric initial distribution

and (b) a particular spherically symmetric initial distribution.

3.6.1 A General Spherically Symmetric Initial Distribution

The general solution of (3.3) with τ_{ij} given by (3.9) is (Saffman 1963)

$$\Gamma(\underline{x},t) = \frac{Q}{\sqrt{(2\pi)^3}\, \ell_1\ell_2\ell_3} \int \exp\left\{ - \sum_{i=1}^{3} \frac{(x_i - y_i \exp[\tau_i t])^2}{2\ell_i^2} \right\} \Gamma(\underline{y},0)\, dV(\underline{y}) \tag{3.35a}$$

where

$$\ell_i^2 = \frac{K}{\tau_i} (\exp(2\tau_i t) - 1) \tag{3.35b}$$

Particular solutions of (3.35), corresponding to particular choices for $\Gamma(\underline{y},0)$, have been used by other authors (Batchelor 1959; Chatwin and Sullivan 1979a, 1979c, 1980b; Kowe 1982; Kowe and Chatwin 1983, 1985; Saffman 1963). For example

$$\Gamma(\underline{y},0) = A_1 \exp(-A_2 r^2) \qquad r = |\underline{y}| \tag{3.36a}$$

and

$$\Gamma(\underline{y},0) = \begin{cases} B_1 & \text{for } |\underline{y}| < B_2 \\ 0 & \text{otherwise} \end{cases} \tag{3.36b}$$

where A_1, A_2, B_1 and B_2 are constants satisfying (1.1). Initially, a more general choice for $\Gamma(\underline{y},0)$ will be of value for this work. We shall assume that $\Gamma(\underline{y},0)$ is spherically symmetric. With this choice it is obvious that, with respect to the principal strain axes, $\Gamma(\underline{x},t)$ is a function of x_i^2, τ_i^2 i=1(1)3, K and t. Thus, for any integer n, the moments, $M^{(n)}_{ij\ldots k}(t)$, of $\Gamma(\underline{x},t)$, given by (2.18), satisfy

$$M^{(2n+1)}_{ij\ldots\ell}(t) = 0 \tag{3.37}$$

$$M^{(2n)}_{ij\ldots\ell}(t) = M^{(2n)}(i,j,\ldots,\ell,t)(\delta_{ij}\ldots\delta_{k\ell} + \delta_{ik}\ldots\delta_{j\ell} + \ldots + \delta_{i\ell}\ldots\delta_{jk})$$

where the number of terms on the right of (3.37b) is equal to the number of unique combinations of pairs of subscripts i,j,...,ℓ, i.e.

$$\frac{(2n!)}{2^n(n!)}\,. \tag{3.38}$$

For example

$$M^{(4)}_{ijk\ell}(t) = M^{(4)}(i,j,k,\ell,t)(\delta_{ij}\delta_{k\ell} + \delta_{ik}\delta_{j\ell} + \delta_{i\ell}\delta_{jk})$$

so that

$$M^{(4)}(1,1,1,1,t) = \frac{1}{3} M^{(4)}_{1111}(t).$$

Since $M^{(2n)}_{ij\ldots\ell}(t)$ is symmetric in its subscripts then

$M^{(2n)}(i,j,\ldots,\ell,t)$ is symmetric in $i,j,\ldots,\ell$.

With $\Gamma(\underline{x},0)$ spherically symmetric, for consistency $\alpha_{ij}(t)$, and hence $a_{ij}(t)$, of (2.17), when referred to the principal strain axes, must be chosen diagonal i.e.

$$\alpha_{ij}(t) = \begin{bmatrix} \alpha_{11}(t) & 0 & 0 \\ 0 & \alpha_{22}(t) & 0 \\ 0 & 0 & \alpha_{33}(t) \end{bmatrix} . \tag{3.39}$$

It then follows that the coefficients of the Hermite series representation for $\Gamma(\underline{x},t)$, (2.17), are of the form

$$A^{(2n+1)}_{ij\ldots\ell}(t) = 0$$

$$A^{(2n)}_{ij\ldots\ell}(t) = A^{(2n)}(i,j,\ldots,\ell,t)(\delta_{ij}\ldots\delta_{k\ell} + \delta_{ik}\ldots\delta_{j\ell} + \ldots + \delta_{i\ell}\ldots\delta_{jk}) \tag{3.40}$$

for any integer n. Similarly to (3.37), the number of terms on the right of (3.40b) is given by (3.38). For example

$$A^{(4)}_{ijk\ell}(t) = A^{(4)}(i,j,k,\ell,t)(\delta_{ij}\delta_{k\ell} + \delta_{ik}\delta_{j\ell} + \delta_{i\ell}\delta_{jk})$$

so that

$$A^{(4)}(1,1,1,1,t) = \frac{1}{3} A^{(4)}_{1111}(t) .$$

Since $A^{(2n)}_{ij\ldots\ell}(t)$ is symmetric in its subscripts, like

$M^{(2n)}(i,j,\ldots,\ell,t)$, $A^{(2n)}(i,j,\ldots,\ell,t)$ is symmetric in $i,j,\ldots,\ell$. Substitution of (3.39) and (3.40) into the Hermite series for $\Gamma(\underline{x},t)$, (2.17), leads to

$$\Gamma(\underline{x},t) = Qn(\underline{\underline{\alpha}})\left\{1 + \sum_{m=1}^{\infty} A^{(2m)}(i,j,\ldots,\ell,t)\left[\delta_{ij}\ldots\delta_{k\ell} + \ldots + \delta_{i\ell}\ldots\delta_{jk}\right] H^{(2m)}_{ij\ldots\ell}(\underline{x},\underline{\underline{\alpha}})\right\} \exp\left[-\frac{1}{2}\left[\alpha_{11}x_1^2 + \alpha_{22}x_2^2 + \alpha_{33}x_3^2\right]\right] .$$

Since the Hermite polynomials are symmetric in their subscripts, using (3.38), this equation may be written

$$\Gamma(\underline{x},t) = Qn(\underline{\underline{\alpha}})\left\{1 + \sum_{m=1}^{\infty} \frac{(2m)!}{2^m(m!)} A^{(2m)}(i,j,\ldots,\ell,t)\delta_{ij}\ldots\delta_{k\ell}\, H^{(2m)}_{ij\ldots\ell}(\underline{x},\underline{\underline{\alpha}})\right\} \exp\left[-\frac{1}{2}\left[\alpha_{11}x_1^2 + \alpha_{22}x_2^2 + \alpha_{33}x_3^2\right]\right] . \tag{3.41}$$

Hence for any spherically symmetric initial distribution, when referred to the principal strain axes, the Hermite series for $\Gamma(\underline{x},t)$ can be simplified considerably.

3.6.2 A Particular Spherically Symmetric Initial Distribution

Writing the particular initial distribution (3.36a) in the form

$$\Gamma(\underline{y},0) = \frac{Q}{\sqrt{(2\pi)^3 L_0^3}} \exp\left[-\frac{1}{2}\frac{r^2}{L_0^2}\right] \tag{3.42}$$

the solution to the governing equation for $\Gamma(\underline{x},t)$, (3.3), referred to the principal strain axes is (Saffman 1963)

$$\Gamma(\underline{x},t) = \frac{Q}{\sqrt{(2\pi)^3 L_1 L_2 L_3}} \exp\left\{-\frac{1}{2}\left[\frac{x_1^2}{L_1^2} + \frac{x_2^2}{L_3^2} + \frac{x_3^2}{L_3^2}\right]\right\} \tag{3.43}$$

where

$$L_i^2(t) = Q^{-1} \int x_i^2 \, \Gamma(\underline{x},t) \, dV(\underline{x}) \tag{3.44}$$

and is given by

$$L_i^2(t) = \left[L_0^2 + \frac{K}{\tau_i}\right] \exp(2\tau_i t) - \frac{K}{\tau_i} \, . \tag{3.45}$$

Indeed, for any initial distribution and large enough times (i.e. after the effect of the initial distribution has become negligible), (3.43) is the solution for $\Gamma(\underline{x},t)$ (Saffman 1963). Equation (3.43) represents a family of ellipsoids centred on the centre of mass of the cloud, with principal axes aligned along the principal strain axes. At any fixed t, the instantaneous concentration is constant on each ellipsoid and the maximum concentration is located at the centre of mass of the cloud, which represents the smallest ellipsoid of the family. $L_i(t)$, (3.44), is a measure of the spread of the cloud along the ith principal strain axis. It is readily seen from

(3.43) and (3.44) that the general solution for $\Gamma(\underline{x},t)$ is in fact the first and therefore, in this particular case, the only non-zero term of the Gram-Charlier series for $\Gamma(\underline{x},t)$. So that, when referred to the principal strain axes, and choosing $\alpha_{ij}(t)$ such that the Hermite series, (2.17), represents the Gram-Charlier series for $\Gamma(\underline{x},t)$, the only non-zero term of the series is the first term.

Having examined and developed various aspects of the Hermite series representation for $\Gamma(\underline{x},t)$ for the particular velocity field (3.1), the remainder of this chapter focusses on the Hermite series representation for the ensemble mean concentration $C(\underline{x},t)$, (2.12), for the same velocity field.

3.7 A Representation for $C(\underline{x},t)$

The next two sections of this chapter examine methods of deriving a representation for $C(\underline{x},t)$ when the velocity field is given by (3.1). For the reasons explained below, the focus throughout is on a representation for $C(\underline{x},t)$ for an isotropic flow.

Section 3.7.1 looks at some of the methods of using the results for $\Gamma(\underline{x},t)$ (Sections 3.2-3.6), to derive a representation for $C(\underline{x},t)$. Section 3.7.2 applies one of these methods to derive a Hermite series representation for $C(\underline{x},t)$ for an arbitrary initial distribution, $\Gamma(\underline{x},0)$. In Section 3.8 the representation for $C(\underline{x},t)$ for both a general and particular spherically symmetric initial distribution is investigated.

3.7.1 Deriving a Hermite Series Representation for $C(\underline{x},t)$ for an Isotropic Flow

Clearly, to develop a representation for $C(\underline{x},t)$, we need to specify the nature of the variable orientation of the principal strain axes. Given that most turbulent flows possess local isotropy (Monin and Yaglom 1975, p.337), in this initial exploration of the representation for $C(\underline{x},t)$, it is sensible to consider the relatively simple case when all directions of the axes are equiprobable.

Other authors have investigated the behaviour of $C(\underline{x},t)$ for $\underline{\Upsilon}$ given by (3.1) and for *particular* initial distributions, $\Gamma(\underline{x},0)$. The case of isotropic flow was considered by, for example, Batchelor (1959), Chatwin and Sullivan (1979a, 1979c), Saffman (1963) and Townsend (1951), while Kowe (1982), has considered cases of non-isotropic flow. As was found in the case of the series for $\Gamma(\underline{x},t)$ (Sections 3.2-3.6), one advantage of using the Hermite series representation for $C(\underline{x},t)$, (2.12), is that, in order to derive the series, no assumptions need be made about the initial distribution of material. The task then is to examine the behaviour of the series, in particular the first few terms of the series, for particular initial distributions and for particular choices of the arbitrary tensor, $\beta_{ij}(t)$, of (2.12).

The method adopted to derive a series for $C(\underline{x},t)$ makes use of some of the results of Section 3.3. Before describing the method in detail, it is worth looking at some other ways in which the Hermite series for $\Gamma(\underline{x},t)$ can be used to derive an expression for $C(\underline{x},t)$, in particular at the links between these ways and the one adopted.

If our aim was to derive an expression for $C(\underline{x},t)$, not necessarily a Hermite series like (2.12), we could attempt to derive one directly, as follows, from the Hermite series for $\Gamma(\underline{x},t)$, (2.17), referred to axes whose orientation is fixed in space and does not vary from realisation to realisation. For convenience, from now on we shall call any such set of axes a 'fixed' set of axes and use unprimed vectors, tensors and components thereof, such as x_i and α_{ij} to denote quantities referred to such axes. Conversely primes, as in x_i' and α_{ij}', will be used to denote quantities referred to any set of axes whose orientation does vary from realisation to realisation, such as the principal strain axes. Then, in general $\alpha_{ij}(t)$ of (2.17) may be chosen random so that we may write

$$C(\underline{x},t) = \overline{\Gamma(\underline{x},t)} = Qn(\underline{\underline{\alpha}}) \sum_{m=0}^{\infty} \overline{A^{(m)}_{ij\ldots k}(t)\, H^{(m)}_{ij\ldots k}(\underline{x},\underline{\underline{\alpha}}) \exp(-\tfrac{1}{2}\alpha_{pq}x_p x_q)} \tag{3.46}$$

(Note that in (3.46) $n(\underline{\underline{\alpha}})$, being dependent on the determinant of α_{ij} (see Appendix A, Equation (A5)), has been taken outside the averaging procedure since any determinant is invariant under any orthogonal transformation.) The problem is now to average

$$A^{(m)}_{ij\ldots k}(t)\, H^{(m)}_{ij\ldots k}(\underline{x},\underline{\underline{\alpha}}) \exp(-\tfrac{1}{2}\alpha_{pq}x_p x_q)$$

for each m over all possible directions of the principal axes of strain, with $A^{(m)}_{ij\ldots k}(t)$ in general given by (3.5). Assuming we could solve (3.5), unless we specified the precise functional form of $\alpha_{ij}(t)$ no further progress could be made. However, assuming that

the functional form of $\alpha_{ij}(t)$ was specified, we could then use Euler angles (θ,ϕ,ψ) to define the orientation of the principal strain axes with respect to any fixed set of axes, and integrate over θ, ϕ and ψ. Indeed, with the additional assumption that all possible directions of the principal strain axes are equiprobable, we could even choose to use spherical polars, r, θ_r, and ϕ_r say, to define the orientation of the axes. Depending on the form chosen for $\alpha_{ij}(t)$, we may or may not be able to derive analytic expressions for the integrals involved and, in general, the resulting expression for $C(\underline{x},t)$ will not be an infinite Hermite series. Obviously this method is equivalent to deriving an expression for $C(\underline{x},t)$ from a Hermite series for $\Gamma(\underline{x},t)$ for a particular choice of random $\alpha_{ij}(t)$.

We could simplify things and choose $\alpha_{ij}(t)$ non-random. Then since $(-\frac{1}{2}\alpha_{ij}x_ix_j)$ is non-random (3.46) may be written

$$C(\underline{x},t) = \overline{\Gamma(\underline{x},t)} = Qn(\underline{\underline{\alpha}}) \sum_{m=0}^{\infty} \overline{A^{(m)}_{ij\ldots k}(t)\, H^{(m)}_{ij\ldots k}(\underline{x},\underline{\underline{\alpha}})} \exp(-\tfrac{1}{2}\alpha_{pq}x_px_q). \tag{3.47}$$

Indeed this equation may be simplified further because, having assumed that $\alpha_{ij}(t)$ is non-random, the Hermite polynomials are also non-random. In other words

$$C(\underline{x},t) = \overline{\Gamma(\underline{x},t)} = Qn(\underline{\underline{\alpha}}) \sum_{m=0}^{\infty} \overline{A^{(m)}_{ij\ldots k}(t)}\, H^{(m)}_{ij\ldots k}(\underline{x},\underline{\underline{\alpha}}) \exp(-\tfrac{1}{2}\alpha_{pq}x_px_q). \tag{3.48}$$

Using the orthogonality property of the polynomials (A4)

$$\overline{A^{(n)}_{ij\ldots k}(t)} = Q^{-1} \int G^{(n)}_{ij\ldots k}(\underline{x},\underline{\underline{\alpha}})\ \overline{\Gamma(\underline{x},t)}\ dV(\underline{x})$$

$$= Q^{-1} \int G^{(n)}_{ij\ldots k}(\underline{x},\underline{\underline{\alpha}})\ C(\underline{x},t)\ dV(\underline{x}). \qquad (3.49)$$

Without loss of generality we may let

$$\alpha_{ij}(t) = \beta_{ij}(t) \quad \text{of} \quad (2.12)$$

so that

$$\underline{\underline{\alpha}}(t) = \underline{\underline{\beta}}(t)$$

Hence from (3.49) and Section 2.4.2

$$\overline{A^{(n)}_{ij\ldots k}(t)} = B^{(n)}_{ij\ldots k}(t)$$

and (3.48) may be written

$$C(\underline{x},t) = Qn(\underline{\underline{\beta}}) \sum_{m=0}^{\infty} B^{(m)}_{ij\ldots k}(t)\ H^{(m)}_{ij\ldots k}(\underline{x},\underline{\underline{\beta}}) \exp(-\tfrac{1}{2}\beta_{pq}x_p x_q) \qquad (3.50)$$

which is exactly the same as (2.12). In other words, using the Hermite series for $\Gamma(\underline{x},t)$, (2.17), to derive $C(\underline{x},t)$ assuming that $\alpha_{ij}(t)$ is chosen non-random is equivalent to using a Hermite series representation for $C(\underline{x},t)$ directly.

In this work, the possibility of deriving an expression for $C(\underline{x},t)$ from (3.46) for particular choices of random $\alpha_{ij}(t)$ is not pursued. Rather, attention is focussed on the use of (2.12) for particular choices of $\beta_{ij}(t)$. It will be show that the expressions derived for the coefficients of the series for $\Gamma(\underline{x}',t)$, $A^{(n)'}_{ij\ldots k}(t)$, in Section 3.3 can be used to simplify the derivation of $B^{(n)}_{ij\ldots k}(t)$.

3.7.2 Behaviour of the Coefficients, $B^{(n)}_{ij\ldots k}(t)$, for an Arbitrary Initial Distribution, $\Gamma(\underline{x},0)$

In this section, the expressions for the coefficients of the Hermite series for $\Gamma(\underline{x}',t)$ referred to the principal strain axes, and derived in Section 3.3, are used to derive the first few terms of the Hermite series for $C(\underline{x},t)$.

The method as described below is, in theory, identical to that outlined in Section 3.7.1 and expressed by equations (3.48)-(3.50). The differences in practice arise because the starting point of the discussion of Section 3.7.1 was a series for $\Gamma(\underline{x},t)$ referred to a fixed set of axes. To be able to apply the method of Section 3.7.1, initially we need to generate a series for $\Gamma(\underline{x},t)$ in terms of tensor components referred to a fixed set of axes. This can be done by using the expressions for the coefficients of the series for $\Gamma(\underline{x}',t)$ referred to the principal strain axes derived in Section 3.3.

In order to describe the procedure, consider the second order term of the series for $\Gamma(\underline{x}',t)$ referred to the principal strain axes, i.e.

$$A_{ij}^{(2)'}(t)H_{ij}^{(2)'}(\underline{x}',\underline{\underline{\alpha}}')\exp(-\tfrac{1}{2}\alpha'_{pq}x'_p x'_q) \qquad (3.51)$$

where, as explained in Section 3.7.1, a prime is now being used to denote tensors (etc.) referred to the principal strain axes. From (3.14a and b) we see that (3.51) includes terms like

$$A_{11}^{(2)'}(t)H_{11}^{(2)'}(\underline{x}',\underline{\underline{\alpha}}')\exp(-\tfrac{1}{2}\alpha'_{pq}x'_p x'_q)$$

$$= \left\{(A_{11}^{(2)'} + \tfrac{1}{2}a'_{11})(0)\exp(2\tau_1 t) + \frac{K}{2\tau_1}(\exp(2\tau_1 t) - 1) - \tfrac{1}{2}a'_{11}(t)\right\}$$

$$H_{11}^{(2)'}(\underline{x}',\underline{\underline{\alpha}}')\exp(-\tfrac{1}{2}\alpha'_{pq}x'_p x'_q) \qquad (3.52)$$

$$A_{12}^{(2)'}(t)H_{12}^{(2)'}(\underline{x}',\underline{\underline{\alpha}}')\exp(-\tfrac{1}{2}\alpha'_{pq}x'_p x'_q)$$

$$= \left\{(A_{12}^{(2)'} + \tfrac{1}{2}a'_{12})(0)\exp([\tau_1+\tau_2]t) - \tfrac{1}{2}a'_{12}(t)\right\}$$

$$H_{12}^{(2)'}(\underline{x}',\underline{\underline{\alpha}}')\exp(-\tfrac{1}{2}\alpha'_{pq}x'_p x'_q) \ .$$

The primed quantities, when expressed in terms of components referred to a fixed set of axes, vary from realisation to realisation depending on the orientation of the principal strain axes. Let θ_{ij} denote the direction cosine of the ith principal strain axis to the jth axis of the fixed set so that, using the summation convention,

$$\theta_{ij}\theta_{jk} = \delta_{jk}. \qquad (3.53)$$

Then, for example, x'_i and α'_{ij} transform like

$$x'_i = \theta_{ip}x_p \qquad (3.54a)$$

and

$$\alpha'_{ij} = \theta_{ip}\theta_{jq}\alpha_{pq} \tag{3.54b}$$

respectively, where x_p and α_{pq} are referred to a fixed set of axes, and, as explained in Section 3.7.1, we will assume that α_{pq} is chosen non-random. Applying (3.53), (3.54), and similar transformations to, for example, (3.52b) we obtain

$$\begin{aligned} &A_{12}^{(2)'}(t)H_{12}^{(2)'}(\underline{x}',\underline{\underline{\alpha}}')\exp(-\tfrac{1}{2}\alpha'_{pq}x'_p x'_q) \\ &= \theta_{1i}\theta_{2j}\theta_{1k}\theta_{2\ell}\left\{(A_{ij}^{(2)} + \tfrac{1}{2}a_{ij})(0)\exp([\tau_1+\tau_2]t - \tfrac{1}{2}a_{ij}(t)\right\} \\ &\qquad H_{k\ell}^{(2)}(\underline{x},\underline{\underline{\alpha}})\exp(-\tfrac{1}{2}\alpha_{pq}x_p x_q). \end{aligned} \tag{3.55}$$

By similarly treating the other terms of the series for $\Gamma(\underline{x}',t)$ derived in Section 3.3, we obtain the first few terms of the generalised Hermite series for $\Gamma(\underline{x},t)$ referred to the fixed set of axes. We are now at the starting point of the discussion leading to equation (3.48). Following that method, without loss of generality for the series for $C(\underline{x},t)$, let

$$\alpha_{ij}(t) = \beta_{ij}(t) \tag{3.56}$$

where $\beta_{ij}(t)$ is given by (2.22). Then the first few terms of the general Hermite series for $C(\underline{x},t)$ are obtained by averaging the corresponding terms of the series for $\Gamma(\underline{x},t)$ over all possible orientations of the principal strain axes.

We may define the direction cosines in terms of the Euler angles, (θ,ϕ,ψ), as follows

$$(\theta_{ij}) = \begin{bmatrix} \cos\phi\cos\psi - \cos\theta\sin\phi\sin\psi & -\cos\phi\sin\psi - \cos\theta\sin\phi\cos\psi & \sin\theta\sin\phi \\ \sin\phi\cos\psi + \cos\theta\cos\phi\sin\psi & -\sin\phi\sin\psi + \cos\theta\cos\phi\cos\psi & -\sin\theta\cos\phi \\ \sin\theta\sin\psi & \sin\theta\cos\psi & \cos\theta \end{bmatrix} \tag{3.57}$$

where $0<\theta<\pi$, $0<\phi,\psi<2\pi$. Continuing with the example of (3.55) above, using (3.56), the contribution to $C(\underline{x},t)$ from averaging $A_{12}^{(2)'}(t)H_{12}^{(2)'}(\underline{x}',\underline{\underline{\alpha}}')$ over all possible directions of the principal strain axes is

$$\frac{1}{8\pi^2}\left\{(A_{ij}^{(2)} + \frac{1}{2}b_{ij})(0)\exp([\tau_1+\tau_2]t - \frac{1}{2}b_{ij}(t)\right\}$$

$$H_{k\ell}^{(2)}(\underline{x},\underline{\underline{\beta}})\exp(-\frac{1}{2}\beta_{pq}x_px_q)\int_0^{2\pi}\int_0^{2\pi}\int_0^{\pi}(\sin\theta)\,\theta_{1i}\theta_{2j}\theta_{1k}\theta_{2\ell}\;d\theta d\phi d\psi\,. \tag{3.58}$$

The work required to calculate the integrals in (3.58) and those associated with the other contributions to $C(\underline{x},t)$ can be minimised by making use of equalities like

$$\begin{aligned}\int_0^{2\pi}\int_0^{2\pi}\int_0^{\pi}(\sin\theta)\,\theta_{pi}\theta_{qj}\theta_{rk}\theta_{s\ell}\,d\theta d\phi d\psi \\ = I_1[\delta_{pq}\delta_{rs}(\delta_{ik}\delta_{j\ell}+\delta_{i\ell}\delta_{jk}) + \delta_{pr}\delta_{qs}(\delta_{ij}\delta_{k\ell}+\delta_{i\ell}\delta_{jk}) \\ + \delta_{ps}\delta_{qr}(\delta_{ij}\delta_{k\ell}+\delta_{ik}\delta_{j\ell})] \\ + I_2(\delta_{pq}\delta_{rs}\delta_{ij}\delta_{k\ell} + \delta_{pr}\delta_{qs}\delta_{ik}\delta_{j\ell} + \delta_{ps}\delta_{qr}\delta_{i\ell}\delta_{jk})\end{aligned} \tag{3.59}$$

where I_1 and I_2 are constants. For example, letting $p=q=1$,

r=s=i=k=2 and j=ℓ=3 in (3.59), and using (3.57) gives

$$I_1 = \int_0^{2\pi}\int_0^{2\pi}\int_0^{\pi} (\sin\theta)\ \theta_{12}\theta_{13}\theta_{22}\theta_{23}\ d\theta d\phi d\psi = -\frac{4\pi^2}{15}\ . \tag{3.60}$$

Similarly, letting p=q=1, r=s=i=j=2 and k=ℓ=3 in (3.59), we obtain

$$I_2 = \int_0^{2\pi}\int_0^{2\pi}\int_0^{\pi} (\sin\theta)\ \theta_{12}\theta_{12}\theta_{23}\theta_{23}\ d\theta d\phi d\psi = \frac{16\pi^2}{15}\ . \tag{3.61}$$

Letting p=r=1 and q=s=2 in (3.59) gives

$$\int_0^{2\pi}\int_0^{2\pi}\int_0^{\pi} (\sin\theta)\ \theta_{1i}\theta_{2j}\theta_{1k}\theta_{2\ell}\ d\theta d\phi d\psi = I_1(\delta_{ij}\delta_{k\ell} + \delta_{i\ell}\delta_{jk}) + I_2\delta_{ik}\delta_{j\ell}. \tag{3.62}$$

Substituting (3.62) into (3.58), using (2.20c), (2.25c), (2.27), (3.60), (3.61) and the fact that the polynomials are symmetric in their subscripts (Appendix A), gives the following contribution to $C(\underline{x},t)$ from averaging $A_{12}^{(2)'}(t)H_{12}^{(2)'}(\underline{x}',\underline{\underline{\alpha}}')$ over all possible directions of the principal strain axes

$$-\frac{1}{30}\left\{(B_{ii}^{(2)} + \frac{1}{2}\,b_{ii})(0)\ \exp([\tau_1+\tau_2]t) - \frac{1}{2}\,b_{ii}(t)\right\} H_{jj}^{(2)}(\underline{x},\underline{\underline{\beta}})$$

$$+\frac{1}{10}\left\{(B_{ij}^{(2)} + \frac{1}{2}\,b_{ij})(0)\ \exp([\tau_1+\tau_2]t) - \frac{1}{2}\,b_{ij}(t)\right\} H_{ij}^{(2)}(\underline{x},\underline{\underline{\beta}}) \tag{3.63}$$

where $B_{ij}^{(2)}(t)$ is given by (2.25c). Following a similar procedure for the contributions from the other terms of second order or less in the series for $\Gamma(\underline{x},t)$, we obtain the following expression for the first three terms of the series for $C(\underline{x},t)$ (i.e. up to and including $B_{ij}^{(2)}(t)H_{ij}^{(2)}(\underline{x},\underline{\beta})$)

$$C(\underline{x},t) = Qn(\underline{\beta})\Big\{1 + \frac{1}{15}(B_{ij}^{(2)} + \frac{1}{2}b_{ij})(0)(2E_1 + 3E_2)\,H_{ij}^{(2)}(\underline{x},\underline{\beta}) + \frac{1}{15}(B_{ii}^{(2)} + \frac{1}{2}b_{ii})(0)(E_1 - E_2)\,H_{jj}^{(2)}(\underline{x},\underline{\beta}) + \frac{1}{6}K\,E_3 H_{jj}^{(2)}(\underline{x},\underline{\beta}) - \frac{1}{2}b_{ij}(t)\,H_{ij}^{(2)}(\underline{x},\underline{\beta})\Big\}\exp(-\frac{1}{2}\beta_{pq}x_p x_q) \tag{3.64}$$

where

$$E_1(t) = \exp(2\tau_1 t) + \exp(2\tau_2 t) + \exp(2\tau_3 t)$$

$$E_2(t) = \exp(-\tau_1 t) + \exp(-\tau_2 t) + \exp(-\tau_3 t) \tag{3.65}$$

$$E_3(t) = \frac{1}{\tau_1}[\exp(2\tau_1 t) - 1] + \frac{1}{\tau_2}[\exp(2\tau_2 t) - 1] + \frac{1}{\tau_3}[\exp(2\tau_3 t) - 1]$$

and from (2.25c), (2.27) and (2.18)

$$(B_{ij}^{(2)} + \frac{1}{2}b_{ij})(0) = \frac{1}{2}N_{ij}^{(2)}(0) = \frac{1}{2}\int x_i x_j\,\Gamma(\underline{x},0)\,dV(\underline{x}). \tag{3.66}$$

3.8 Behaviour of the Coefficients, $B_{ij\ldots k}^{(n)}(t)$, for a Spherically Symmetric Initial Distribution

In this section the expressions for the coefficients, $B_{ij\ldots k}^{(n)}(t)$, of the series for $C(\underline{x},t)$ are derived with the

assumption that the initial distribution of material is spherically symmetric (Section 3.8.1). The case of a particular spherically symmetric distribution is considered in Section 3.8.2. Under these conditions, and continuing to assume that the flow is isotropic, the rotation of the principal strain axes which has been neglected in this work (Section 3.2.1) has no effect on the ensemble mean properties of $\Gamma(\underline{x},t)$. Therefore, in considering the ensemble mean properties of $\Gamma(\underline{x},t)$ for $\underline{\tau}$ a pure straining motion, it is sensible initially to consider the case of a spherically symmetric initial distribution.

3.8.1 A General Spherically Symmetric Initial Distribution

With the assumptions given above, $C(\underline{x},t)$ is a function of $r=|\underline{x}|$, t, K and functions like τ_{ii} and $\tau_{ij}\tau_{ji}$, that is scalar functions of τ_{ij}. Therefore, for consistency the arbitrary tensor, $\beta_{ij}(t)$, of the series for $C(\underline{x},t)$, (2.12), must be proportional to δ_{ij}, that is, using $\beta(t)$ to denote a scalar function to t,

$$\beta_{ij}(t) = \beta(t)\delta_{ij} \tag{3.67}$$

so that (2.12) may be written

$$C(r,t) = Qn(\underline{\beta}) \sum_{m=0}^{\infty} B^{(m)}_{ij\ldots k}(t) H^{(m)}_{ij\ldots k}(\underline{x},\underline{\beta}) \exp(-\tfrac{1}{2}\beta r^2) \tag{3.68}$$

where

$$r^2 = x_i x_i .$$

As described in Section 2.4.2, $B^{(m)}_{ij\ldots k}(t)$ is a sum of functions of the moments of $C(r,t)$, $N^{(n)}_{ij\ldots k}(t)$, $n \leq m$ where $N^{(n)}_{ij\ldots k}(t)$ is given by (2.23). Since $C(r,t)$ is spherically symmetric, for any integer n, we may write $N^{(n)}_{ij\ldots k}(t)$, in the form (compare (3.37))

$$N^{(2n+1)}_{ij\ldots \ell}(t) = 0$$

$$N^{(2n)}_{ij\ldots \ell}(t) = N^{(2n)}(t)(\delta_{ij}\ldots\delta_{k\ell} + \delta_{ik}\ldots\delta_{j\ell} + \ldots + \delta_{i\ell}\ldots\delta_{jk}) \tag{3.69}$$

where the number of terms on the right of (3.69b) equals the number of unique combinations of pairs of subscripts $i,j,\ldots,\ell$, i.e.

$$\frac{(2n!)}{2^n(n!)} . \tag{3.70}$$

For example, letting n=0,1 and 2 respectively in (3.69b)

$$N^{(0)}(t) = 1 \qquad \text{(as in (2.24a))}$$

$$N^{(2)}_{ij}(t) = N^{(2)}(t)\delta_{ij}$$

$$N^{(4)}_{ijk\ell}(t) = N^{(4)}(t)(\delta_{ij}\delta_{k\ell} + \delta_{ik}\delta_{j\ell} + \delta_{i\ell}\delta_{jk}). \tag{3.71}$$

Letting $i=j$, $k=\ell$ and using (2.23)

$$N^{(2)}_{ii}(t) = 3N^{(2)}(t) = Q^{-1} \int r^2 \, C(r,t) \, dV(\underline{x})$$

$$N^{(4)}_{iijj}(t) = 15N^{(4)}(t) = Q^{-1} \int r^4 \, C(r,t) \, dV(\underline{x}). \tag{3.72}$$

Since $\beta_{ij}(t)$ satisfies (3.67), in a way similar to that used for $N^{(n)}_{ij\ldots k}(t)$ above, for any integer n we may write $B^{(n)}_{ij\ldots k}(t)$ in the form

$$B^{(2n+1)}_{ij\ldots \ell}(t) = 0$$

$$B^{(2n)}_{ij\ldots \ell}(t) = B^{(2n)}(t)(\delta_{ij}\ldots\delta_{k\ell} + \delta_{ik}\ldots\delta_{j\ell} + \ldots + \delta_{i\ell}\ldots\delta_{jk}). \tag{3.73}$$

Substituting (3.73) into the series (3.68), using (3.70) and the fact that the polynomials are symmetric in their subscripts, leads to

$$C(r,t) = Qn(\underline{\beta}) \sum_{m=0}^{\infty} \frac{(2m!)}{2^m(m!)} B^{(2m)}(t) H^{(2m)}_{iijj\ldots kk}(\underline{x},\underline{\beta}) \exp(-\tfrac{1}{2}\beta r^2). \tag{3.74}$$

Looking at the first few $B^{(n)}_{ij\ldots k}(t)$, from (2.25) and (3.71) we get

$$B^{(0)}(t) = 1 \qquad \text{(as in 2.25a)}$$

$$B^{(2)}_{ij}(t) = B^{(2)}(t)\delta_{ij} = \tfrac{1}{2}(N^{(2)} - b)\delta_{ij}$$

(contd.)

$$B^{(4)}_{ijk\ell}(t) = B^{(4)}(t)(\delta_{ij}\delta_{k\ell} + \delta_{ik}\delta_{j\ell} + \delta_{i\ell}\delta_{jk})$$

$$= \frac{1}{4!}(N^{(4)} - 2bN^{(2)} + b^2)(\delta_{ij}\delta_{k\ell} + \delta_{ik}\delta_{j\ell} + \delta_{i\ell}\delta_{jk})$$

(3.75)(contd.)

where

$$b(t) = \beta^{-1}(t) \tag{3.76}$$

and the dependency of $N^{(2n)}(t)$ and $b(t)$ on t has been omitted for simplicity. From (3.75)

$$B^{(2)}_{ii}(t) = 3B^{(2)}(t) = \frac{3}{2}(N^{(2)} - b)$$

$$B^{(4)}_{iijj}(t) = 15B^{(4)}(t) = \frac{15}{4!}(N^{(4)} - 2bN^{(2)} + b^2). \tag{3.77}$$

Thus in order to obtain $B^{(2n)}(t)$, $n=1,2,\ldots,$ we need to calculate

$$N^{(2m)}_{iijj\ldots kk}(t) = Q^{-1}\int r^{2m}\, C(r,t)\, dV(\underline{x}), \quad m=1,2,\ldots n. \tag{3.78}$$

Since the flow is isotropic and the initial distribution is symmetric

$$\int r^{2n}\, C(r,t)\, dV(\underline{x}) = \int r^{2n}\, \Gamma(\underline{x},t)\, dV(\underline{x}), \quad n=1,2,\ldots . \tag{3.79}$$

Therefore

$$N^{(2n)}_{iijj\ldots kk}(t) = M^{(2n)}_{iijj\ldots kk}(t), \quad n=1,2,\ldots \tag{3.80}$$

where $M^{(n)}_{ij\ldots k}(t)$ is the nth order moment of $\Gamma(\underline{x},t)$, (2.18). Hence, the results for the moments of $\Gamma(\underline{x}',t)$ (Section 3.3) which followed from the derivation of the coefficients of the series for $\Gamma(\underline{x}',t)$, can be used to derive $B^{(2n)}(t)$. Before proceeding to do this, it is important to point out that the consequences for $C(\underline{x},t)$ and its Hermite series of choosing an isotropic flow and/or a symmetric initial distribution, as given by (3.68)-(3.80), are applicable to <u>any</u> isotropic flow and not just the particular flow (3.1).

Using (3.77a), (3.72a), (3.80), (3.28) and the fact that the initial distribution of material is symmetric

$$\begin{aligned} B^{(2)}(t) &= \frac{1}{6}\left(M^{(2)}_{ii}(t) - 3b(t)\right) \\ &= \frac{1}{18}\Big\{M^{(2)}_{ii}(0)\left(\exp(2\tau_1 t) + \exp(2\tau_2 t) + \exp(2\tau_3 t)\right) \\ &\quad + 3K\left[\frac{1}{\tau_1}\left(\exp(2\tau_1 t) - 1\right) + \frac{1}{\tau_2}\left(\exp(2\tau_2 t) - 1\right)\right. \\ &\quad\qquad \left. + \frac{1}{\tau_3}\left(\exp(2\tau_3 t) - 1\right)\right] \\ &\quad - 9b(t)\Big\}. \end{aligned} \tag{3.81}$$

Following a similar procedure for $B^{(4)}(t)$ we obtain

$$B^{(4)}(t) = \frac{1}{15.4!}\left(M^{(4)}_{iijj}(t) - 10b(t)M^{(2)}_{ii}(t) + 15b^2(t)\right) \tag{3.82}$$

where

$$M^{(4)}_{iijj}(t) = \frac{1}{15} M^{(4)}_{iijj}(0) \left\{3 \left(\exp(4\tau_1 t) + \exp(4\tau_2 t) + \exp(4\tau_3 t)\right)\right.$$

$$\left. + 2 \left(\exp(2[\tau_1+\tau_2]t) + \exp(2[\tau_1+\tau_3]t) + \exp(2[\tau_2+\tau_3]t)\right)\right\}$$

$$+ \frac{2}{3} KM^{(2)}_{ii}(0) \left\{\frac{3}{\tau_1}\exp(2\tau_1 t)(\exp(2\tau_1 t) - 1) + \frac{3}{\tau_2}\exp(2\tau_2 t)(\exp(2\tau_2 t) - 1)\right.$$

$$+ \frac{3}{\tau_3} \exp(2\tau_3 t)(\exp(2\tau_3 t) - 1)$$

$$+ \exp(2\tau_1 t)\left[\frac{1}{\tau_2} (\exp(2\tau_2 t) - 1) + \frac{1}{\tau_3} (\exp(2\tau_3 t) - 1)\right]$$

$$+ \exp(2\tau_2 t)\left[\frac{1}{\tau_1} (\exp(2\tau_1 t) - 1) + \frac{1}{\tau_3} (\exp(2\tau_3 t) - 1)\right]$$

$$\left. + \exp(2\tau_3 t)\left[\frac{1}{\tau_1} (\exp(2\tau_1 t) - 1) + \frac{1}{\tau_2} (\exp(2\tau_2 t) - 1)\right]\right\}$$

$$+ K^2 \left\{\frac{3}{\tau_1^2} (\exp(2\tau_1 t) - 1)^2 + \frac{3}{\tau_2^2} (\exp(2\tau_2 t) - 1)^2 + \frac{3}{\tau_3^2} (\exp(2\tau_3 t) - 1)^2\right.$$

$$+ \frac{2}{\tau_1\tau_2} (\exp(2\tau_1 t) - 1)(\exp(2\tau_2 t) - 1)$$

$$+ \frac{2}{\tau_1\tau_3} (\exp(2\tau_1 t) - 1)(\exp(2\tau_3 t) - 1)$$

$$\left. + \frac{2}{\tau_2\tau_3} (\exp(2\tau_2 t) - 1)(\exp(2\tau_3 t) - 1)\right\}$$

(3.83)

and

$$M^{(2)}_{ii}(t) = \frac{1}{3} M^{(2)}_{ii}(0) \left(\exp(2\tau_1 t) + \exp(2\tau_2 t) + \exp(2\tau_3 t)\right)$$

$$+ K \left\{\frac{1}{\tau_1} (\exp(2\tau_1 t) - 1) + \frac{1}{\tau_2} (\exp(2\tau_2 t) - 1) + \frac{1}{\tau_3} (\exp(2\tau_3 t) - 1)\right\}.$$

(3.84)

3.8.2 A Particular Spherically Symmetric Initial Distribution

For the particular spherically symmetric initial distribution (3.42), the first few coefficients of the series for $C(r,t)$ may be derived as follows. Substituting for $M_{ii}^{(2)}(0)$ and $M_{iijj}^{(4)}(0)$ in (3.81), (3.83), (3.84), and hence (3.82), using (3.42), leads to

$$B^{(2)}(t) = \frac{1}{6}(L_1^2 + L_2^2 + L_3^2 - 3b)$$

$$B^{(4)}(t) = \frac{1}{15.4!}(3(L_1^4 + L_2^4 + L_3^4) + 2(L_1^2L_2^2 + L_1^2L_3^2 + L_2^2L_3^2) - 10b(L_1^2 + L_2^2 + L_3^2) + 15b^2) \qquad (3.85)$$

where $L_i(t)$, $i=1(1)3$ is given by (3.45). Hence the series for $C(r,t)$, (3.74), may be written

$$C(r,t) = Qn(\underline{\beta})\left\{1 + \frac{1}{6}(L_1^2 + L_2^2 + L_3^2 - 3b)H_{ii}^{(2)}(\underline{x},\underline{\beta}) + \frac{1}{5.4!}(3(L_1^4 + L_2^4 + L_3^4) + 2(L_1^2L_2^2 + L_1^2L_3^2 + L_2^2L_3^2) - 10b(L_1^2 + L_2^2 + L_3^2) + 15b^2)H_{iijj}^{(4)}(\underline{x},\underline{\beta}) + \ldots\right\} \exp(-\tfrac{1}{2}\beta r^2). \qquad (3.86)$$

Choosing $b(t)$, and therefore $\beta(t)$, such that $B^{(2)}(t)=0$ leads to the Gram-Charlier series for $C(r,t)$

$$C(r,t) = \frac{Q}{\left[\frac{2\pi}{3}\right]^{3/2} L^3} \left\{1 + \frac{3}{10} L^{-4}((L_1^4 + L_2^4 + L_3^4) - (L_1^2L_2^2 + L_1^2L_3^2 + L_2^2L_3^2)) \right.$$

$$\left. (3\left[\frac{r}{L}\right]^4 - 10\left[\frac{r}{L}\right]^2 + 5) \right.$$

$$\left. + \ldots \right\} \exp\left[-\frac{3}{2}\frac{r^2}{L^2}\right] \qquad (3.87)$$

where

$$b(t) = \beta^{-1}(t) = \frac{1}{3}\int r^2\, \Gamma(\underline{x},t)\, dV(\underline{x})$$

$$= \frac{1}{3}(L_1^2 + L_2^2 + L_3^2)$$

$$= \frac{1}{3} L^2(t). \qquad (3.88)$$

Equation (3.87) gives us an expression for the first few terms of $C(r,t)$ in terms of the three measures of spread of the cloud $L_i(t)$, $i=1(1)3$. Exact solutions for $C(r,t)$ are available for $\Gamma(\underline{x},0)$ given by (3.42) and for particular representative choices for τ_i, $i=1(1)3$, such as those considered in Section 3.5.3. For example $\tau_2=\tau_3>0$, $\tau_1=-2\tau_3<0$ (Chatwin and Sullivan 1979a). Having developed the series for $C(r,t)$ for general τ_i, $i=1(1)3$, it would be of interest to extend the work to an examination of the practical use of the Gram-Charlier series for $C(r,t)$ for such representative choices for τ_i, $i=1(1)3$. This could be done by analysing the accuracy of the approximation given by, for example, (3.87) for various choices of the ratio L_1/L. Other choices for $b(t)$ and the effect of the inclusion of additional terms in the series should also be examined.

3.9 Summary and Conclusions

This chapter has developed the Hermite series representations for $\Gamma(\underline{x},t)$ and $C(\underline{x},t)$ for a linear strain velocity field. The nature and quantity of theoretical results presented has been selected to illustrate, for a given velocity field, various ways of investigating the Hermite series representation for $\Gamma(\underline{x},t)$ or one of its ensemble mean properties. For each representation, the governing equations of the coefficients and the form of the first few terms have been established. The effect of the molecular diffusivity, and of particular choices for the initial distribution, $\Gamma(\underline{x},0)$, and the arbitrary tensor of each representation has been examined. The analysis presented for $C(\underline{x},t)$ has been based on the assumption that the flow is isotropic which, given the nature of the chosen velocity field, is a reasonable initial assumption (Section 3.8.1). However, the work could be extended to anisotropic flows.

Although no practical applications have been presented, the work has provided guidance on how, for the chosen velocity field, the series can be simplified for particular choices of axes, initial distribution of material or arbitrary tensor of the representations. Indeed, some of the simplifications pertain to general flows (Section 3.8.1). The next obvious step is to develop the practical application of the series, in particular for $C(r,t)$ (Section 3.8.2). For the same velocity field, it would also be of interest to extend this work to an examination of the use of Hermite series representations for other ensemble mean properties, such as $\overline{c^2}(\underline{x},t)$, for which exact solutions are also available (Chatwin and Sullivan 1979a).

CHAPTER FOUR

Dispersion in the Atmospheric Surface Layer

4.1 Introduction

In Chapters 2 and 3 attention was focussed on the use of a Hermite series representation for the concentration distribution of a cloud of contaminant and its associated ensemble mean properties evaluated in a framework of relative diffusion. Only brief references were made (Chapter 1, Section 1.4 and Chapter 2, Section 2.3) to the possibility of using a Hermite series representation for a concentration field evaluated in frameworks of absolute diffusion. However, for the reasons discussed in Chapter 1 (Section 1.2.2) many problems of turbulent dispersion are conventionally analysed in a framework of absolute diffusion, a case in point being dispersion in the atmospheric surface layer. Because of the practical importance of this particular problem, and because of the wealth of relevant qualitative and quantitative results, it was of interest to examine the application of a Hermite series representation to this problem.

The application involves the use of a one dimensional Hermite series to represent the longitudinal distribution of the ensemble mean concentration of a cloud released in the atmospheric surface layer. In Section 4.2 the dispersion model and Hermite series representation for the mean concentration are introduced. The detailed aims of the application are also discussed. In Section 4.3 the lower order coefficients of the representation are calculated and an explanation is given of the numerical scheme used to calculate

higher order coefficients. Section 4.4 presents and discusses the results of the application. Section 4.5 summarises the main results of the chapter and suggests some areas for future work.

4.2 The Model

4.2.1 The Surface Layer Dispersion Model

The model to be used concerns the release and subsequent dispersion of contaminant in the so-called constant stress region of the atmospheric surface layer (Panofsky and Dutton 1984; Pasquill and Smith 1983). Broadly speaking, the concept of a constant stress region is valid for the lowest 10% of the mixing depth, its height depends on atmospheric conditions and typically varies from ~10m on a clear night, to ~100m during the day time with strong winds (Panofsky and Dutton 1984, p.113; Pasquill and Smith 1983, p.40). Under the assumption of neutral stability, the mean wind, $U(z)$, is given by the logarithmic profile

$$U(z) = \frac{u_*}{k} \log_e\left[\frac{z}{z_0}\right], \quad \frac{z}{z_0} >> 1 \qquad (4.1)$$

where z denotes the height above the ground, u_* is the friction velocity (assumed constant), z_0 is the roughness length and k is von Karman's constant. u_* represents the magnitude of the velocity fluctuations and typically ranges from 0.1-1.0m s^{-1}. z_0 formally denotes the height at which $U(z) \to 0$ although, as indicated in (4.1), the logarithmic profile is only applicable for heights much greater than z_0. Typical values for z_0 range from ~0.01m for cut grass,

to ~1m for towns and forests (Panofsky and Dutton 1984, p.123; Pasquill and Smith 1983, p.317). The value of k is assumed to be 0.4, a discussion of the uncertainty in its value is given by, for example, Pasquill and Smith 1983 (p.42).

Taking coordinate axes, x,y,z fixed relative to the earth with origin at the earth's surface, the surface is assumed infinite in extent in the x-y plane with the mean wind, $U(z)$, parallel to the x axis. A finite quantity of passive contaminant is released instantaneously at time $t=0$ from a point source located at $(0,0,h)$. Let $C(x,y,z,t)$ denote the normalised ensemble mean concentration of the cloud. Then, assuming the quantity of material is conserved throughout the dispersion

$$\iiint_{\text{all space}} C(x,y,z,t)\, dx\, dy\, dz = 1. \qquad (4.2)$$

If the effects of molecular diffusion are neglected, the governing equation for $C(x,y,z,t)$ is

$$\frac{\partial C}{\partial t} + \frac{u_*}{k} \log_e\left[\frac{z}{z_0}\right] \frac{\partial C}{\partial x} = -\left\{\frac{\partial}{\partial x}(\overline{uc}) + \frac{\partial}{dy}(\overline{vc}) + \frac{\partial}{\partial z}(\overline{wc})\right\} \qquad (4.3)$$

where u,v,w and c denote the fluctuations of the x,y,z components of the velocity and of the concentration about their respective means. It will be assumed that the longitudinal turbulent flux of material is negligible compared to longitudinal advection so that

$$\left| \frac{\partial}{\partial x}(\overline{uc}) \right| << \frac{u_*}{k} \log_e\left[\frac{z}{z_0}\right] \left| \frac{\partial C}{\partial x} \right| \qquad (4.4)$$

and that the vertical turbulent flux, $\overline{wc}$, can be represented by an eddy diffusivity, $K(z)$, such that

$$\overline{wc} = -K(z) \frac{\partial C}{\partial z} \tag{4.5}$$

where

$$K(z) = bu_{*}z, \qquad b \text{ a constant } >0.$$

Gradient-transfer theory (Panofsky and Dutton 1984, p.120, Pasquill and Smith 1983) then leads to

$$b = k$$

so that

$$K(z) = ku_{*}z. \tag{4.6}$$

The assumptions on which (4.4), (4.5) and (4.6) are based have been discussed in detail elsewhere (Monin and Yaglom 1971, section 10.5; Pasquill and Smith 1983; Yaglom 1976).

Integrating (4.3) over y, using (4.4), (4.5) and (4.6), leads to

$$\frac{\partial \chi}{\partial t} + \frac{u_{*}}{k} \log_e\left[\frac{z}{z_0}\right] \frac{\partial \chi}{\partial x} = -\frac{\partial}{\partial z}\left[ku_{*}z \frac{\partial \chi}{\partial z}\right] \tag{4.7}$$

where

$$\chi(x,z,t) = \int_{-\infty}^{\infty} C(x,y,z,t)\, dy. \qquad (4.8)$$

In other words, $\chi(x,z,t)$ represents the crosswind integrated mean concentration from a point source or the mean concentration due to an infinite crosswind line source along the y axis. The initial and boundary conditions on $\chi(x,z,t)$ are

$$\chi(x,z,0) = \delta(x)\,\delta(z-h) \qquad (4.9)$$

$$ku_{*}z\,\frac{\partial \chi}{\partial z} \to 0 \quad \text{as} \quad z \to 0 \qquad (4.10)$$

$$\chi \to 0 \quad \text{as} \quad z \to \infty \qquad (4.11)$$

$$\chi \to 0 \quad \text{as} \quad |x| \to \infty. \qquad (4.12)$$

Equation (4.10) corresponds to no loss of material to the ground, whilst (4.11) and (4.12), respectively, follow from the assumption that there is no limit to the height to which material may disperse or to dispersion in the alongwind direction.

The model defined by Equations (4.7)-(4.12) has been analysed widely in the literature. Reviews of and references to these analyses are given by Monin and Yaglom (1971), Pasquill and Smith (1983) and Panofsky and Dutton (1984), for example. Certain results of these analyses will be referred to and discussed throughout the remainder of this chapter, as appropriate, in order to put the present analysis into context. In particular, in the next sub-section, and as part of the description of the aims of and

motivation for this analysis, the limitations on the range of applicability of the model are summarised.

4.2.2 The Hermite Series Representation for $\chi(x,z,t)$

The main aim of the chapter is to examine the use of the following Hermite series representation for $\chi(x,z,t)$

$$\chi(x,z,t) = \frac{1}{\sqrt{2\pi}} \sum_{n=0}^{\infty} A_n(Z,T) H_n(X) \exp\left[-\frac{1}{2} X^2\right] \qquad (4.13)$$

where (4.7) is the governing equation for $\chi(x,z,t)$ and the dimensionless variables X,Z and T are given by

$$X = \frac{x-m}{\sigma} \; ; \quad Z = \frac{z}{z_0} \; ; \quad T = \frac{k u_* t}{z_0} \qquad (4.14)$$

and, in general, the arbitrary functions $m(z,t)$ and $\sigma(z,t)$ may each be chosen functions of z and t. The one dimensional Hermite polynomials $H_n(X)$ are defined by (Kendall and Stuart 1969; also discussed in Section 2.2.1)

$$H_n(X)\exp\left[-\frac{1}{2} X^2\right] = (-1)^n \frac{d^n}{dX^n} \exp\left[-\frac{1}{2} X^2\right] . \qquad (4.15)$$

Attention is focussed on the practical value of (4.13), in particular on the effect of different choices for m and σ on the approximation to χ obtained from the first few terms of (4.13).

The choice of the dispersion model outlined in the previous

section and of the Hermite series (4.13) was prompted by the work of several authors. The main criteria were to identify a practical problem which was suitable for applying a Hermite series and which offered the opportunity to perform calculations and, in some way, verify the validity of the results.

The use of a three dimensional Gaussian distribution to represent the distribution of the mean concentration of a cloud dispersing in the atmospheric surface layer is well documented (Monin and Yaglom 1971, pp.579-693; Pasquill and Smith 1983). However, starting from Equation (4.3) for $C(x,y,z,t)$ and for medium-range dispersion - that is after the effects of the initial distribution of the cloud have become negligible but before the existance of any lid on the atmosphere affect the distribution - the Gaussian model can only be proved rigorously by assuming a constant mean wind, and by adopting an eddy diffusivity tensor to represent the RHS of (4.3), with principal axes parallel to the x,y and z axes, and with constant components. There are several other methods of deriving a Gaussian distribution for $C(x,y,z,t)$, for example by using a Lagrangian description of particle dispersion (Monin and Yaglom 1971, pp.540-579). However, all of these methods are based on certain simplifying assumptions, in particular they do not account for the effects of the increase of wind speed with height.

The dispersion model, (4.7), is often used as the starting point for a more precise analysis of the effects of the increase of mean wind speed with height. There are three main factors which limit its range of applicability. First, the use of an eddy diffusivity to represent vertical transfer, (4.5), is recognised as being most appropriate for dispersion close to the ground, that is when the scale of the eddies acting on the cloud are much smaller

than the vertical scale of the cloud itself. Second, because of the assumed boundary condition, (4.11), in practice the model will only be valid while the vertical spread of the cloud is much less than the height of any inversion layer, H_I say. Since the vertical spread of the cloud in neutral conditions is typically $\sim x/10$ and $|U(z)| \sim 10u_*$, this implies that $u_* t \ll H_I$. Third, since the model equation, (4.7), is parabolic, the assumed rate of vertical spread is infinitely fast, that is the cloud immediately fills the whole height of the boundary layer (Monin and Yaglom 1971, Sections 10.3 and 10.6). Thus the model will not give an accurate picture of the distribution for $\chi(x,z,t)$ in the upper edges of the cloud or where the concentration is relatively small.

Saffman (1962), using a simplified form of the model used here, has examined the effect on the longitudinal spread of a cloud dispersing in the atmosphere of the interaction between wind shear and vertical diffusion. His analysis highlights the difference between the nature of the spread (a) when there is a limit on the height to which material may disperse, for example when an inversion exists, and (b) when vertical dispersion is unbounded. In order to achieve analytic results without losing the main features of dispersion in the surface layer, Saffman considered a model in which the coordinate axes x,y,z coincided with the principal axes of the eddy diffusivity tensor $K_{ij}(z)$, and in which the mean wind was directed along the x-axis and was proportional to a power of z. One of the conclusions of Saffman's work is that when there is a lid on the atmosphere, the longitudinal distribution of material at any fixed height approaches the Gaussian as $t \to \infty$. This was a natural conclusion of applying the results of earlier work by Taylor (1953, 1954b) and Aris (1956) on dispersion in pipes and channels, to

dispersion in the atmospheric surface layer. On the other hand, when there is no lid on the atmosphere, Saffman shows that the horizontal distribution at any fixed height is not asymptotically Gaussian. For the particular case of a wind profile linear in z and a constant vertical eddy diffusivity, Saffman shows that for dispersion unbounded above, the skewness of the distribution of material at ground-level released from a ground-level source approaches ~1.3 as $t \to \infty$, i.e. is significantly different from the Gaussian value of zero (Kendall and Stuart 1969; also discussed in Section 2.2.1). Saffman concludes that these results will also apply, for sufficiently large times (i.e. $t \gg O(1)$), to the situation where the mean wind, vertical and horizontal eddy diffusivities are represented by more general, but realistic, power law profiles.

From these results, the model (4.7) obviously represented an interesting and important practical problem which appeared to be suitable for applying a Hermite series and for which, as mentioned in Section 4.1, there was an abundance of relevant qualitative and quantitive data. It was of interest to examine the practical value of a Hermite series representation for $\chi(x,z,t)$, in particular the ability of a Hermite series to reflect the expected deviation of the horizontal distribution from the Gaussian. Whilst it might have been simpler to assume a velocity profile proportional to a power of z, the logarithmic profile was retained precisely because most other analyses abandon it in favour of a simpler profile. In addition, some exact results for various relevant measures of quantity, location and spread of the cloud as represented by the adopted model, (4.7)-(4.12), were available (Smith 1957; Chatwin 1968), and provided the opportunity to compare the results of any numerical scheme which

might be developed here, with the 'exact' model. These exact results are introduced in Section 4.3.1.

Turning to the particular form of the chosen Hermite series, (4.13) involves the one dimensional Hermite polynomials $H_n(X)$. Clearly it satisfies the boundary condition, (4.12). The governing equation for $\chi(x,z,t)$, (4.7), and the other boundary/initial conditions, (4.9)-(4.11), will determine the behaviour of the coefficients, $A_n(Z,T)$. There are two other natural choices for the polynomial dependency of any series for χ, (a) a series involving one dimensional polynomials $H_n(Z_0)$, $Z_0=(z-m_0(x,t))/\sigma_0(x,t)$ - defined analogously to $H_n(X)$ in (4.15) above, and (b) a series involving the two dimensional polynomials, $H_{nm}(X_1,Z_1)$, which may be defined by

$$H_{nm}(X_1,Z_1)\exp\left\{-\frac{1}{2}\left[X_1^2 + 2X_1Z_1 + Z_1^2\right]\right\}$$

$$= (-1)^{n+m}\frac{d^{(n+m)}}{dX_1^n\, dZ_1^m}\exp\left\{-\frac{1}{2}\left[X_1^2 + 2X_1Z_1 + Z_1^2\right]\right\} \qquad (4.16)$$

$$X_1 = \frac{x-m_x(t)}{\sigma_x(t)}\ ; \qquad Z_1 = \frac{z-m_z(t)}{\sigma_z(t)}$$

where $m_x(t)$, $m_z(t)$, $\sigma_x(t)$ and $\sigma_z(t)$ are arbitrary functions of time. However, since the domain of χ is restricted to the half-space $z\geq 0$, if we were to adopt a Hermite series involving polynomials dependant on an exponential function of z, such as $H_n(Z_0)$ or $H_{nm}(X_1,Z_1)$, complex expressions for the coefficients of the series would be obtained. For example, let χ be represented by the series

$$\chi(x,z,t) = \frac{1}{\sqrt{2\pi}} \sum_{n=0}^{\infty} B_n(X_0,T) H_n(Z_0) \exp\left[-\frac{1}{2} Z_0^2\right] \qquad (4.17)$$

$$Z_0 = \frac{z-m_0(x,t)}{\sigma_0(x,t)} ; \qquad X_0 = \frac{x}{z_0} .$$

With (4.17) we would like to be able to derive expressions for the coefficients, $B_n(X_0,T)$, in terms of the vertical moments of χ, that is in terms of

$$\int_0^{\infty} z^n \chi(x,z,t)\, dz; \qquad n=0,1,2,\ldots . \qquad (4.18)$$

However, the orthogonality property of the polynomials involves the domain $-\infty<z<\infty$ (Kendall and Stuart 1969; also discussed in Section 2.2.1). Thus, for example, multiplying (4.17) by $H_1(Z_0)$ and integrating between $z=0$ and $z=\infty$ leads to the following complex integral on the RHS of the equation

$$\sum_{n=0}^{\infty} B_n(X_0,T) \int_{\frac{-m_0}{\sigma_0}}^{\infty} H_1(Z_0) H_n(Z_0) \exp\left[-\frac{1}{2} Z_0^2\right] dZ_0$$

Hence a simple expression for $B_1(X_0,T)$, or for any other $B_n(X_0,T)$, in terms of the vertical moments is not necessarily obtainable. The same problem arises if χ is represented by a series involving the two dimensional polynomials defined in (4.16).

Having explained the reasons for choosing the particular Hermite series, (4.13), the remainder of this section looks in

general at (a) the main aims in examining the series and (b) the natural choices for the arbitrary functions of the series, $m(z,t)$ and $\sigma(z,t)$.

4.2.3 Some Natural Choices for $m(z,t)$ and $\sigma(z,t)$

Clearly, in examining the practical value of (4.13), the main aim is to examine the value of the approximation to χ obtained from a finite number of terms of the series. Let χ_p denote the sum of the first $(p+1)$ terms, so that

$$\chi_p(x,z,t) = \frac{1}{\sqrt{2\pi}} \sum_{n=0}^{p} A_n(Z,T) H_n(X) \exp\left[-\frac{1}{2} X^2\right]. \qquad (4.19)$$

Then, interest lies in the effect of different choices for m and σ on χ_p. For any chosen m and σ, having identified criteria to define "acceptable", we would like to ascertain if there exists a p such that χ_p provides an acceptable approximation to χ. In the discussion below, the following measures of location and spread of the cloud will be useful. Let $\bar{Z}(t)$, $\bar{X}(t)$ and $\bar{X}_z(z,t)$ denote the z and x coordinates of the centre of mass of the cloud and the x coordinate of the centre of mass of material at a height z, respectively, so that

$$\bar{Z}(t) = \frac{\int_0^\infty \int_{-\infty}^{\infty} z\,\chi\,dx\,dz}{\int_0^\infty \int_{-\infty}^{\infty} \chi\,dx\,dz} = \int_0^\infty \int_{-\infty}^{\infty} z\,\chi\,dx\,dz \qquad (4.20)$$

$$\bar{X}(t) = \frac{\int_0^{\infty}\int_{-\infty}^{\infty} x \times dx\, dz}{\int_0^{\infty}\int_{-\infty}^{\infty} \times dx\, dz} = \int_0^{\infty}\int_{-\infty}^{\infty} x \times dx\, dz$$

$$\bar{X}_z(z,t) = \frac{\int_{-\infty}^{\infty} x \times dx}{\int_{-\infty}^{\infty} \times dx} . \qquad (4.20)\text{(contd.)}$$

Let $\Sigma_x(t)$, $\sigma_x(z,t)$ and $s_x(z,t)$ denote the standard deviation (s.d.) in the alongwind direction (a) of the cloud about its centre of mass (b) of material at height z about the centre of mass of material at the same height and (c) of material at height z about the centre of mass of the cloud, respectively, so that

$$\Sigma_x^2(t) = \frac{\int_0^{\infty}\int_{-\infty}^{\infty} (x - \bar{X})^2 \times dx\, dz}{\int_0^{\infty}\int_{-\infty}^{\infty} \times dx\, dz} = \int_0^{\infty}\int_{-\infty}^{\infty} (x - \bar{X})^2 \times dx\, dz$$

$$\sigma_x^2(z,t) = \frac{\int_{-\infty}^{\infty} (x - \bar{X}_z)^2 \times dx}{\int_{-\infty}^{\infty} \times dx}$$

$$s_x^2(z,t) = \frac{\int_{-\infty}^{\infty} (x - \bar{X})^2 \times dx}{\int_{-\infty}^{\infty} \times dx} . \qquad (4.21)$$

From (4.20 b,c) and (4.21 b,c) it follows that

$$s_x^2(z,t) = \sigma_x^2 + (\bar{X} - \bar{X}_z)^2. \qquad (4.22)$$

Analytic expressions for some of these measures of location and spread are available or can be derived and are detailed in Appendix B.

Using (4.20a and b), and from the Lagrangian similarity hypothesis (Batchelor 1964), $\chi(x,z,t)$ is of the form

$$\frac{1}{\bar{z}^2} F\left\{\frac{z - \bar{X}}{\bar{z}}, \frac{z}{z_0}, \frac{h}{z_0}, \frac{ku_*t}{z_0}\right\} \qquad (4.23)$$

and $m(z,t)$ and $\sigma(z,t)$ must be proportional to u_*t. The choices for $m(z,t)$ and $\sigma(z,t)$ will strongly influence the shape and spread, respectively, of any approximation to χ, χ_p, in the alongwind direction, but not of course of the cloud itself. Two natural choices for m are $\bar{X}(t)$ and $\bar{X}_z(z,t)$ defined by (4.20b and c), whilst for $\sigma(z,t)$, the three measures of spread of the cloud $\Sigma_x(t)$, $\sigma_x(z,t)$ and $s_x(z,t)$ defined by (4.21) are the obvious natural choices. Specific examples of χ_p for $m=\bar{X}$ or $\bar{X}_z$ and $\sigma=\Sigma_x$, σ_x or s_x are presented in Section 4.3.2, after the equations for the horizontal moments of $\chi(x,z,t)$ have been developed. However, at this stage it is interesting to make some general observations on the effects of these choices for m and σ on χ_p, in particular to indicate the way in which the choices simplify the first few terms of χ_p.

For arbitrary m, σ and fixed (Z,T), $\times_0$ - regarded as a function of X - is the Gaussian distribution with zero mean and unit variance defined by

$$\frac{\int_{-\infty}^{\infty} X \times_0 dX}{\int_{-\infty}^{\infty} \times dX} \quad \text{and} \quad \frac{\int_{-\infty}^{\infty} X^2 \times_0 dX}{\int_{-\infty}^{\infty} \times dX} . \tag{4.24}$$

Multiplying (4.13) by $H_1(X)$ and $H_2(X)$, respectively, integrating over X and using (2.4) and (4.20c) gives

$$A_1(Z,T) = \frac{1}{\sigma} (\bar{X}_z - m) \int_{-\infty}^{\infty} \times dX$$

$$A_2(Z,T) = \frac{1}{2\sigma^2} \int_{-\infty}^{\infty} [(x - m)^2 - \sigma^2] \times dX. \tag{4.25}$$

From (4.25b) and (4.21c) it follows that choosing $m=\bar{X}(t)$ and $\sigma=s_x(z,t)$ ensures A_2 is identically zero for all (Z,T) i.e.

$$\times_p(x,z,t) = \frac{1}{\sqrt{2\pi}} \left\{A_0 + A_1 H_1(X) + \sum_{n=3}^{p} A_n H_n(X)\right\} \exp\left[-\frac{1}{2} X^2\right]$$

where

$$X = \frac{x - \bar{X}}{s_x} . \tag{4.26}$$

From (4.25a), choosing $m=\bar{X}_z(z,t)$ ensures $A_1(Z,T)$ is identically zero for all (Z,T). Therefore, from (4.24a), $\times_0$ has the same mean as $\times$ i.e.

$$\int_{-\infty}^{\infty} X \times dX = \int_{-\infty}^{\infty} X \times_0 dX = 0$$

and

$$\times_1(x,z,t) = \times_0(x,z,t) = \frac{1}{\sqrt{2\pi}} A_0 \exp\left[-\frac{1}{2} X^2\right]$$

where

$$X = \frac{x - \bar{X}_z}{\sigma} . \tag{4.27}$$

For the same choice of m, $\times_2$ is also symmetric about $X=0$ and attains its maximum there. Its variance is σ_x^2/σ^2, where σ_x^2 is given by (4.21b). From (4.25b) and (4.21b), choosing $\sigma=\sigma_x(z,t)$ ensures that $A_2(Z,T)$ is zero for all (Z,T). Then

$$\times_2(x,z,t) = \times_0(x,z,t) \tag{4.28}$$

the Gaussian distribution in X defined by (4.24). In addition, (4.13) reduces to the Gram-Charlier distribution of $\times$ (Section 2,2) i.e.

$$\times_p(x,z,t) = \frac{1}{\sqrt{2\pi}} \left\{A_0 + \sum_{n=3}^{p} A_n H_n(X)\right\} \exp\left[-\frac{1}{2} X^2\right]$$

where

$$X = \frac{x - \bar{X}_z}{\sigma_x} . \tag{4.29}$$

Obviously these choices for m and σ which simplify the leading terms of the representation for χ are of particular interest from the point of view of analysing χ_p.

In order to examine specific examples of χ_p, it is necessary to attempt to derive exact expressions for the coefficients, $A_n(Z,T)$. The next section (Section 4.3) introduces the exact expressions for the $A_n(Z,T)$ that are available from work by other authors or that can be derived. These expressions are then used to illustrate some approximations to χ, χ_p, and to explain the rationale behind the rest of the chapter.

4.3 Calculation of the Coefficients of the Hermite Series, $A_n(Z,T)$

In this section, the exact expressions for the coefficients, $A_n(Z,T)$, $n \leq 2$, of the Hermite series for χ, (4.13), are outlined (Section 4.3.1). In Section 4.3.2, these expressions are used to illustrate approximations to $\chi(x,z,t)$, χ_p, for $p \leq 2$, and thereby explain why a numerical scheme has been applied to calculate higher order coefficients and hence higher order approximations to χ. Section 4.3.3 explains the numerical scheme.

4.3.1 The Governing Equations for the Horizontal Moments of $\chi(x,z,t)$ and Some Exact Expressions for $A_n(Z,T)$

Let $N_n(z,t)$ denote the nth order horizontal moment of $\chi(x,z,t)$ i.e.

$$N_n(z,t) = \int_{-\infty}^{\infty} x^n \chi(x,z,t)\, dx. \tag{4.30}$$

Multiplying (4.13) by $H_m(X)$, integrating over X and using (2.4) leads to

$$A_n(Z,T) = \frac{1}{n!} \int_{-\infty}^{\infty} H_n(X)\, \chi(x,z,t)\, dX \tag{4.31}$$

so that A_n depends on N_m, $m \leq n$. For convenience later, expressions for $A_n(Z,T)$ will be derived by developing the governing equations of $N_n(z,t)$.

Multiplying (4.7) by x^n, integrating over x, using the boundary condition (4.12) and transforming to the dimensionless variables X,Z,T defined in (4.14) leads to

$$\frac{\partial N_0}{\partial T} - \frac{\partial}{\partial Z}\left[Z \frac{\partial N_0}{\partial Z}\right] = 0$$

$$\frac{\partial N_n}{\partial T} - \frac{\partial}{\partial Z}\left[Z \frac{\partial N_n}{\partial Z}\right] = \frac{n z_0}{k^2} N_{n-1} \log_e Z \qquad n=1,2,\ldots . \tag{4.32}$$

Using (4.9)-(4.11), the initial and boundary conditions on N_n may be written

$$N_0(z,0) = \delta(Z-H), \quad H = \frac{h}{z_0}$$

$$Z \frac{\partial N_n}{\partial Z} \to 0 \quad \text{as} \quad Z \to 0 \quad \text{for all} \quad n \tag{4.33}$$

$$N_n \to 0 \quad \text{as} \quad Z \to \infty \quad \text{for all} \quad n.$$

From (4.30), N_0 represents the proportion of material at height z and is given by (Smith 1957; Chatwin 1968)

$$N_0(z,t) = \frac{1}{ku_*t} \exp\left\{-\frac{(z+h)}{ku_*t}\right\} I_0\left\{\frac{2\sqrt{hz}}{ku_*t}\right\} = \frac{1}{ku_*t} \exp\left\{-\frac{(Z+H)}{T}\right\} I_0\left\{\frac{2\sqrt{HZ}}{T}\right\} \tag{4.34}$$

where I_0 is the modified Bessel function of order zero (Abramowitz and Stegun 1965, p.374).

From (4.32b), for $n>1$, N_n depends on N_m, $m<n$. The following exact solutions for $1<n<2$ can be derived from the known expressions, given in Appendix B, for the measures of location and spread of the cloud $\bar{Z}(t)$, $\bar{X}(t)$, $\bar{X}_z(z,t)$, $\Sigma_x(t)$, $\sigma_x(z,t)$ and $s_x(z,t)$ defined by (4.20)-(4.21). For $n=1$, from (4.20c) and (4.30)

$$N_1(z,t) = \bar{X}_z(z,t)\, N_0(z,t). \tag{4.35}$$

Hence from (4.34), (B7) and (B8)

$$N_1^{(G)}(z,t) = \frac{1}{k^2}\left\{E_1\left[\frac{Z}{T}\right] + (\log_e Z - 2)\exp\left[-\frac{Z}{T}\right]\right\}$$

$$N_1^{(E)}(0,t) = \frac{1}{k^2}\left\{E_1\left[\frac{H}{T}\right] + (\log_e H - 2)\exp\left[-\frac{H}{T}\right]\right\} \qquad (4.36)$$

where $E_1(x)$ is the exponential integral function (Appendix B, Equation B3).

In (4.36) the superscripts (G) and (E) have been used, as they will throughout the chapter, to denote ground-level and elevated sources respectively. Note that (4.36b) follows directly from (4.36a) and the reciprocal theorem (Smith 1957) which shows that the distribution of concentration at ground-level from an elevated source, height H_1 say, is the same as the distribution at H_1 from a ground-level source. From (4.21b), (4.30) and (4.35)

$$N_2(z,t) = [\sigma_x^2 + \bar{X}_z^2](z,t)\, N_0(z,t)$$

$$= \left[\sigma_x^2 + \left[\frac{N_1}{N_0}\right]^2\right] N_0. \qquad (4.37)$$

Hence using (B9b), (4.36a) and (4.34)

$$N_2^{(G)}(0,t) = \frac{u_* t}{k^2}\left\{2 - \frac{\pi^2}{6} + \left[2 - \log_e\left[Te^{-\gamma}\right]\right]^2\right\} \qquad (4.38)$$

where γ is Euler's constant and is given by (B4).

We can use (4.34), (4.36) and (4.38) to derive exact expressions for the coefficients $A_0(Z,T)$, $A_1^{(G)}(Z,T)$, $A_1^{(E)}(0,T)$ and $A_2^{(G)}(0,T)$ of (4.13). From (4.30) and (4.31)

$$A_0(Z,T) = \frac{1}{\sigma} N_0$$

$$A_1(Z,T) = \frac{1}{\sigma^2} (N_1 - mN_0) \tag{4.39}$$

$$A_2(Z,T) = \frac{1}{\sigma^3} \left[N_2 - 2mN_1 + \left[m^2 - \sigma^2\right] N_0\right] .$$

Therefore using (4.34), (4.36) and (4.38)

$$A_0(Z,T) = \frac{1}{\sigma k u_* t} \exp\left\{- \frac{(Z+H)}{T}\right\} I_0 \left\{\frac{2\sqrt{HZ}}{T}\right\}$$

$$A_1^{(G)}(Z,T) = \frac{1}{\sigma^2 k^2} \left\{E_1\left[\frac{Z}{T}\right] + (\log_e Z - 2 - \frac{mk}{u_* t}) \exp\left[- \frac{Z}{T}\right]\right\} \tag{4.40}$$

$$A_1^{(E)}(0,T) = \frac{1}{\sigma^2(0,t) k^2} \left\{E_1\left[\frac{H}{T}\right] + (\log_e H - 2 - \frac{mk}{u_* t}) \exp\left[- \frac{H}{T}\right]\right\}$$

$$A_2^{(G)}(0,T) = \frac{1}{\sigma^3(0,t) k^2} \left\{u_* t \left(2 - \frac{\pi^2}{6} + \left[2 - \log_e(Te^{-\gamma})\right]^2\right)\right.$$

$$+ 2m(0,t) \left(2 - \log_e (Te^{-\gamma})\right)$$

$$\left. + \frac{k}{u_* t} (m^2 - \sigma^2)(0,t)\right\} .$$

However, from these expressions, for ground-level and elevated sources respectively, and for arbitrary $m(z,t)$ and $\sigma(z,t)$, we can only obtain at best, that is to the highest order in the $H_n(X)$, the approximations $\chi_2^{(G)}(x,0,t)$ and $\chi_1^{(E)}(x,0,t)$, where, from (4.13)

$$\times_2^{(G)}(x,0,t) = \frac{1}{\sqrt{2\pi}}\left\{A_0^{(G)}(0,T) + A_1^{(G)}(0,T)H_1(X) + A_2^{(G)}(0,T)H_2(X)\right\}\exp\left[-\frac{1}{2}X^2\right] \quad (4.41)$$

$$\times_1^{(E)}(x,0,t) = \frac{1}{\sqrt{2\pi}}\left\{A_0^{(E)}(0,T) + A_1^{(E)}(0,T)H_1(X)\right\}\exp\left[-\frac{1}{2}X^2\right]. \quad (4.42)$$

For the distribution of concentration at elevated Z, and from the reciprocal theorem (Smith 1957) it follows from (4.42) that the highest order approximation achievable is for $\times_1^{(G)}(x,z,t)$ given by

$$\times_1^{(G)}(x,z,t) = \frac{1}{\sqrt{2\pi}}\left\{A_0^{(G)}(Z,T) + A_1^{(G)}(Z,T)H_1(X)\right\}\exp\left[-\frac{1}{2}X^2\right] . \quad (4.43)$$

The limitations on the potential practical usefulness of the approximations (4.41)-(4.43) are obvious. First, $\times_2^{(G)}(x,0,t)$, (4.41), only includes moments up to order 2 so that, for example, the effects of skewness in the distribution of material at any fixed height, discussed in Section 4.2.2, are excluded. More critically, $\times_1^{(E)}(x,0,t)$ and $\times_1^{(G)}(x,z,t)$, (4.42) and (4.43), only include moments up to order 1 so that even the effects of the spread of the distribution of material at any fixed height are excluded. It is also important to note that all of these approximations are based on arbitrary $m(z,t)$ and $\sigma(z,t)$. Normally, we would want to use one or more of the natural choices discussed earlier (Section 4.2.3) for each of these functions, that is $\bar{X}(t)$ or $\bar{X}_z(z,t)$ for $m(z,t)$, and $\Sigma_x(t)$, $\sigma_x(z,t)$ or $s_x(z,t)$ for $\sigma(z,t)$. As shown in Appendix B, expressions for all of these natural choices are only available

for $\chi_2^{(G)}(x,0,t)$ since, in the case of $\chi_1^{(E)}(x,0,t)$, $\sigma_x^{(E)}(0,t)$, for example, is not known and, in the case of $\chi_1^{(G)}(x,z,t)$, $\sigma_x^{(G)}(z,t)$ is not known. Hence only for (4.41) would we be able to investigate fully the effects of using each of the various natural choices for $m(z,t)$ and $\sigma(z,t)$. It is obvious, therefore, that in order to perform a worthwhile investigation of the practical value of the Hermite series, (4.13), it will be necessary to derive numerical solutions for higher order moments of χ (i.e. $N_n(z,t)$, $n\geq 3$) and for the, as yet, unknown natural choices for $m(z,t)$ and $\sigma(z,t)$ (i.e. $N_n(z,t)$, $n=1,2$, for all z,t and for both ground-level and elevated sources). Then it will be possible to carry out a fuller investigation, in particular to examine if the expected asymmetry in the horizontal distribution for $\chi(x,z,t)$ can be adequately replicated by using the first few terms of the series. Section 4.3.3 describes the numerical scheme that has been adopted. However, before proceeding to explain and apply the scheme, it is interesting to illustrate the types of approximations to χ that can be obtained from (4.41)-(4.43). This is done in Section 4.3.2.

4.3.2 Approximations to $\chi(x,z,t)$ Derived from the Exact Expressions for $A_n(Z,T)$, $n\leq 2$

The previous sub-section (Section 4.3.1) introduced the exact expressions that are available for the coefficients of the Hermite series, i.e. for $A_n(Z,T)$, $n\leq 2$. This section uses these expressions to illustrate and discuss approximations to χ, $\chi_p(x,z,t)$, for $p\leq 2$.

The main focus will be on the concentration distribution at the ground from a ground-level source, $\chi_p^{(G)}(x,0,t)$, since it is for this

distribution that the highest order approximation is available, (4.41). The abscissa of each graph is fixed as x/ku_*t, whilst the ordinate is some suitably chosen multiple of $(ku_*t)^2\chi_p$. Throughout the section, the choice $m=\bar{X}_z(0,t)$, $\sigma=\sigma_x(0,t)$, is used as the main tool for comparision with, and analysing, other choices for m and σ. The reason for this is that $m=\bar{X}_z$, $\sigma=\sigma_x$ appears to be the most natural of all the so-called "natural" choices discussed in Section 4.2.3. As discussed there, with this choice, the horizontal distribution at any fixed z, Z_0 say, is then represented by a Hermite series whose first term is the Gaussian distribution with mean $\bar{X}_z(Z_0,t)$ and variance $\sigma_x^2(Z_0,t)$. Consequently $A_2=A_1=0$, so that $\chi_2=\chi_1=\chi_0$, the Gaussian (see Equation 4.29). χ_2 for $m=\bar{X}_z$, $\sigma=\sigma_x$ therefore provides a simple and natural approximation against which to analyse second and lower order approximations to χ based on other choices for m and σ.

Most of the graphs presented are for $\chi_p^{(G)}(x,0,t)$ at $T=250$. The reasons for choosing this particular T are twofold. First, the same T is used predominantly in Section 4.4 when examining higher order approximations to χ. Second, as a consequence of the Lagrangian similarity hypothesis (Batchelor 1964 and Section 4.2.3), the results presented for $\chi_p^{(G)}(x,z,t)$ at any fixed T are important to the understanding of the variation with $\sigma(z,t)$ of certain other horizontal distributions. Using the hypothesis, from (4.23), for fixed z/ku_*t $(=Z/T)$, σ and m, $\chi^{(G)}$ and therefore $\chi_p^{(G)}$ as a function of $(x-\bar{X}(t))/ku_*t$ $(=(x-\bar{X}(t))/Tz_0)$ is self-similar (the same shape) for all T. Thus, for any fixed T, $T_1=ku_*t_1/z_0$ say, the changes effected in $\chi_p^{(G)}(x,0,t_1)$ - regarded as a function of X - by altering σ, completely determine the corresponding changes effected in $\chi_p^{(G)}(x,0,t)$ at any other

(non-zero) T. In addition, if

$$\left[T_1 - \frac{h}{z_0}\right] \frac{z_0}{h} >> 1 \tag{4.44}$$

$\chi^{(G)}(x,0,t_1)$ represents the similarity form attained by the distribution of concentration at the ground from an elevated source, $\chi^{(E)}(x,0,t_2)$, where

$$\frac{ku_* t_2}{z_0} = T_1 - \frac{h}{z_0} \tag{4.45}$$

and, if

$$Z_1 = \frac{z_1}{ku_* t_1} << 1 \tag{4.46}$$

$\chi^{(G)}(x,0,t_1)$ also represents the similarity form attained by the distribution at Z_1 from the ground-level source, $\chi^{(G)}(x,z_1,t_1)$. Therefore, subject to the conditions (4.44) and (4.46), the variation in $\chi_p^{(G)}(x,0,t_1)$ with σ, approximately determines the variation in $\chi_p^{(E)}(x,0,t_2)$ and $\chi_p^{(G)}(x,z_1,t_1)$ with the same σ respectively.

Figures (4.1a-c) compare $\chi_p^{(G)}(x,0,t)$ p$\leftarrow$2, for $m=\bar{X}(t)$, $\sigma=\Sigma_x(t)$ (Fig. 4.1a); $m=\bar{X}(t)$, $\sigma=s_x(0,t)$ (Fig. 4.1b); $m=\bar{X}(t)$, $\sigma=\sigma_x(0,t)$ (Fig. 4.1c), with $\chi_2^{(G)}(x,0,t)$ $(=\chi_0^{(G)})$ for $m=\bar{X}_z(0,t)$, $\sigma=\sigma_x(0,t)$. For $m=\bar{X}(t)$ and $\sigma=s_x(0,t)$ (Fig. 4.1b), $A_2=0$, (4.26), so that only two distributions, χ_1 and the Gaussian χ_0 are shown for this m and σ. Figure 4.1d repeats the highest order approximation to $\chi^{(G)}$ for $m=\bar{X}(t)$ shown in each of Figs. (4.1a-c) and compares them with the Gaussian curve for $m=\bar{X}_z$, $\sigma=\sigma_x$. From

(B6), (B7) and (B9), the corresponding values for $\bar{X}(t)$, $\bar{X}_z(0,t)$, $\Sigma_x(t)$, $s_x(0,t)$ and $\sigma_x(0,t)$ for Figs. (4.1a-d), that is for $\chi^{(G)}$ at Z=0, T=250, expressed as multiples of ku_*t, are

$$\begin{aligned} \bar{X}(t) &= 24.65ku_*t \\ \bar{X}_z(0,t) &= 18.40ku_*t \\ \Sigma_x(t) &= 5.02ku_*t \\ s_x(0,t) &= 7.28ku_*t \\ \sigma_x(0,t) &= 3.72ku_*t. \end{aligned} \tag{4.47}$$

From the orthogonality property of the Hermite polynomials it follows that the mean of each curve in Figs. (4.1a-d) is at $\bar{X}_z(0,t)/ku_*t$.

As expected, the curves illustrate the general behaviour that for $\sigma=\alpha u_*t$, α positive, and Z,T fixed, the spread of χ_p increases with α. Likewise as α and hence the spread increases, the maximum of χ_p decreases. The peak value for the chosen multiple of χ_p ranges from ~2.2 for χ_0, $m=\bar{X}(t)$, $\sigma=s_x(0,t)$ (Fig. 4.1b), to ~7.6 for χ_1, $m=\bar{X}(t)$, $\sigma=\sigma_x(0,t)$ (Fig. 4.1c). Compared to the Gaussian curve for χ_2 ($=\chi_0$), $m=\bar{X}_z(0,t)$, $\sigma=\sigma_x(0,t)$, for which the maximum is at $\bar{X}_z(0,t)/ku_*t$, the location of the maxima of χ_1 and χ_2 for $m=\bar{X}(t)$, $\sigma=\Sigma_x(t)$, $s_x(0,t)$ or $\sigma_x(0,t)$ are greater and lie towards $\bar{X}(t)/ku_*t$. From the Hermite series for $\chi^{(G)}$, for $m=\bar{X}(t)$ and for fixed σ and T, it can be shown that the location of the maximum of $\chi_1^{(G)}(x,z,t)$, X_{max} say, increases from its ground-level position with z - as does $\bar{X}_z(z,t)$ though at a faster rate - so that initially

$$\bar{X}_z(z,t) < X_{max} < \bar{X}(t)$$

until

$$\frac{z}{ku_{*}t} \sim 0.74$$

when

$$\bar{X}_z(z,t) - \bar{X}(t) = A_1(Z,T) = 0$$

so that $\times_2^{(G)}$ is symmetric and

$$\bar{X}_z(z,t) = \bar{X}(t) = X_{max}.$$

For larger Z

$$\bar{X}(t) < X_{max} < \bar{X}_z(z,t).$$

The same should also be true of $\times_1^{(E)}(x,z,t_2)$ subject to

$$\frac{ku_{*}t_2}{h} = \left[T - \frac{h}{z_0}\right] \frac{z_0}{h} >> 1 .$$

An encouraging feature of the curve for $\times_1$ for $\sigma=s_x(0,t)$, (Fig. 4.1b), is the non-zero (though small) positive value at the source (x=0). Although not illustrated, at earlier times the analogous curve displays relatively larger positive values at the source. In other words the curve is reflecting the region of negative mean velocity below $z/z_0=1$.

A major feature of the curves for $\times_1$ and $\times_2$ for $m=\bar{X}(t)$, $\sigma=\Sigma_x(t)$, $s_x(0,t)$ or $\sigma_x(0,t)$, (Figs. 4.1a-d), are the negative values. The occurrence of negative values in Hermite series

approximations is a familiar one (Barton and Dennis 1952; Chatwin 1970, 1980; Kendall and Stuart 1969). It is often suggested that, providing the negative values are relatively insignificant, they can be ignored. From (4.41), for fixed Z and T, and therefore fixed m and σ, it is easy to show that χ_2 and χ_1 have three and two critical points, respectively (i.e. points at which $d\chi/dX=0$). The precise nature of the critical points for any χ_p, and therefore the relative magnitudes of any negative values attained, can obviously be calculated. Given that our main interest lies in higher order approximations to χ, this line of analysis is not pursued, rather it is sufficient to make some general observations about the negative values.

In general, for any fixed T, the dependency of $A_1(Z,T)$ on

$$\frac{\bar{X}_z(z,t) - \bar{X}(t)}{ku_*t} \tag{4.48}$$

ensures that as the magnitude of this decreases, with α fixed, the negative values of χ_1 become more negligible, that is towards the 'centre' layers of the cloud. This is a reflection of the approach of the approximation towards the Gaussian, $\chi_0^{(G)}(x,z,t)$ at such z. This is illustrated in Fig. 4.2 by the plots of $\chi_1^{(G)}(x,z,t)$ and $\chi_0^{(G)}(x,z,t)$ at $Z=375$ and $T=250$, for $m=\bar{X}(t)$, $\sigma=\Sigma_x(t)$. At $Z=375$ and $T=250$, $\bar{X}_z(z,t)=27.35ku_*t$. The negative values of the χ_1 curve are much more negligible than the negative values of the corresponding curve for $\chi_1^{(G)}(x,0,t)$ in Fig. 4.1a. However, this does not imply that the approximation will be "acceptable" for any choice of α at such z. For example, Fig. 4.3 illustrates $\chi_1^{(G)}$ and $\chi_0^{(G)}$ at $Z=375$, $T=250$ for $m=\bar{X}(t)$ and $\sigma=ku_*t$ (i.e. $\alpha=1$

compared to $\alpha=5.02$ for Fig. 4.2, see Equation 4.47c). Figure 4.4a illustrates $\chi_2^{(G)}(x,0,t)$, $\chi_1^{(G)}(x,0,t)$ and $\chi_0^{(G)}(x,0,t)$ for the same choice of α. The behaviour of the second and third terms in the series for $\chi_2^{(G)}(x,0,t)$ (i.e. the $A_1(0,T)H_1(X)$ and $A_2(0,T)H_2(X)$ terms, respectively) are also illustrated seperately in Fig. 4.4a. Figure 4.4b illustrates the same χ_p and contributions to χ_p for the same α but for $m = \bar{X}_z(0,t)$ (for this m, $A_1=0$, see Equation 4.27). Clearly the third term is dominating the behaviour of $\chi_2^{(G)}(x,0,t)$ in Figs. 4.4a and b. Figure 4.5 illustrates the behaviour of the same terms for $m=\bar{X}(t)$, $\sigma=\Sigma_x(t)$ previously considered in Fig. 4.1a.

Without trying at this stage to quantify what constitutes "acceptable" values for χ_p or which m and σ lead to acceptable values for χ_p, $p\leq 2$, it is possible to make the following general observation from Figs. 4.1, 4.3 and 4.4. In the Eulerian framework, for fixed z, each successive term of the series for χ represents a deviation of the horizontal distribution from the Gaussian with mean $m(z,t)$ and variance $\sigma^2(z,t)$. Therefore, although $\chi(x,z,t)$ can be represented by (4.13) for arbitrary m and σ, it is not surprising that unacceptable negative values can be obtained when trying to approximate χ by an m and σ significantly different from the corresponding measured characteristics of the horizontal distribution being considered. For example, Figs. (4.4a,b) illustrate, what subjectively appear to be, the unacceptable negative values that are obtained when trying to approximate χ by a χ_p with $\sigma(z,t)$ much smaller than a length characteristic of the spread of the distribution in the alongwind direction. In Figs. (4.4a,b) $\sigma=ku_*t$ whereas, from (4.47), the actual spread of the distribution is $\sim 5ku_*t$.

Figures 4.6 and 4.7 illustrate the point made in (4.44) and (4.45) concerning the approach of the distribution from an elevated source, $\chi^{(E)}$, to the distribution from a ground-level source, $\chi^{(G)}$. For simplicity, attention is focussed on two combinations for m and σ, namely $m=\bar{X}(t)$, $\sigma=\Sigma_x(t)$ and $m=\bar{X}(t)$, $\sigma=s_x(0,t)$. Analogous observations will apply to other combinations for m and σ. First, Fig. 4.6 compares

$$\chi_1^{(E)}(x,0,t_2); \quad m = \bar{X}^{(G)}(t_1), \quad \sigma = \Sigma_x^{(G)}(t_1)$$

$$\text{and} \quad \chi_1^{(E)}(x,0,t_2); \quad m = \bar{X}^{(G)}(t_1), \quad \sigma = s_x^{(G)}(0,t_1) \tag{4.49}$$

where $$t_1 = 250\,\frac{z_0}{ku_*} \quad (\text{i.e. } T_1 = 250)$$

$$H = \frac{h}{z_0} = 100$$

$$t_2 = 150\,\frac{z_0}{ku_*} \quad (\text{i.e. } T_2 = 150)$$

with

$$\chi_1^{(G)}(x,0,t_1); \quad m = \bar{X}^{(G)}(t_1), \quad \sigma = \Sigma_x^{(G)}(t_1)$$

$$\text{and} \quad \chi_1^{(G)}(x,0,t_1); \quad m = \bar{X}^{(G)}(t_1), \quad \sigma = s_x^{(G)}(0,t_1) \tag{4.50}$$

respectively. (The latter two χ_p have already been considered in Figs. 4.1a and b). Substituting the chosen t_2, t_1 and H into (4.44), we have

$$\left[T_1 - \frac{h}{z_0}\right] \frac{z_0}{h} = \left[\frac{ku_* t_1}{z_0} - H\right] \frac{1}{H} = \frac{150}{100} = 1.5 \ . \qquad (4.51)$$

As expected, the distributions for the elevated source are not close to the corresponding distributions for the ground-level source. Figure 4.7 compares the approximations for an elevated source analogous to those in Fig. 4.6 except that now $H=10$ and $t_2=240z_0/ku_*$. For Fig. 4.7 therefore

$$\left[T_1 - \frac{h}{z_0}\right] \frac{z_0}{h} = \frac{(250-10)}{10} = 24 >> 1 \qquad (4.52)$$

and, as expected, the distributions for the elevated source are virtually identical to the corresponding distributions for the ground-level source.

The examples presented above of the types of approximations to the horizontal distribution of χ that are available from the known exact expressions for the horizontal moments of χ, and based on natural choices for m and σ, have served to illustrate several points:

(1) the choice of m and σ, respectively, has a significant effect on the location of the maximum and on the spread of χ_p, $p \lesssim 2$

(2) choosing m and σ significantly different from lengths characteristic of the corresponding measures for the cloud, can result in significant negative values for χ_p, $p \lesssim 2$

(3) in order to reflect the expected asymmetry of the horizontal distribution (Section 4.2.2), it will be necessary to include higher order terms (i.e. A_nH_n, $n>3$) in the approximation to χ.

Points (1) and (3) were obvious from the structure of the series, (4.13), and have been discussed in earlier sections. Because our interest lies in higher order approximations to χ, no attempt has yet been made to quantify:

(a) what represents an acceptable approximation to χ, for example what constitutes 'significant' negative values in the distribution for χ_p

(b) for what choices of m and σ will an acceptable approximation be obtained.

Clearly it will be important to attempt to quantify these problems.

4.3.3 The Numerical Scheme

Sections 4.2.2, 4.3.1 and 4.3.2 have discussed and illustrated the need to calculate higher order horizontal moments of χ, (4.30) (i.e. N_n for $n>3$), and to calculate values for all the natural choices for the arbitrary functions $m(z,t)$ and $\sigma(z,t)$ of interest (i.e. N_n for $n=1,2$, for all z,t and for ground-level and elevated sources). This sub-section describes the numerical scheme adopted to achieve these needs.

The governing equations for N_n, $n<4$ (4.32), have been solved using the implicit, central difference, Crank-Nicholson scheme described by Richtmyer and Morton (1967), pp198-201. The scheme is unconditionally stable.

For any n, (4.32) may be written in the form

$$\left\{\frac{\partial}{\partial T} - \frac{\partial}{\partial Z}\left[Z\,\frac{\partial}{\partial Z}\right]\right\}\theta(Z,T) = g(Z,T)\,\log_e Z \qquad (4.53)$$

where $\theta(Z,T)$ represents any one of the N_n, $n>0$, non-dimensionalised by multiplying by an appropriate power of z_0, and $g(Z,T)$ is a function of N_{n-1}. For each n, $g(Z,T)$ is known since (4.53) can be used to solve (4.32) sequentially in the n from $n=0$ and, from (4.32a), for $\theta=N_0$, $g(Z,T)$ is identically zero. If the finite difference scheme is developed for (4.53) and applied in the whole of the space domain $Z>0$, problems occur because of the behaviour of $\log_e Z$ as $Z\to 0$. To avoid these problems, a scheme is developed and applied in the domain $Z>1$. The lower boundary condition (4.33a) is changed to

$$Z\,\frac{\partial N_n}{\partial Z} \to 0 \quad \text{as} \quad Z \to 1 \quad \text{for all} \quad n$$

so that

$$\frac{\partial N_n}{\partial Z} \to 0 \quad \text{as} \quad Z \to 1 \quad \text{for all} \quad n \qquad (4.54)$$

The influence on the numerical results of this adjustment to the boundary condition is discussed in Section 4.4 where appropriate.

At $(Z,T)=(1 + j\Delta Z, (n + \frac{1}{2})\Delta T)$ where ΔZ and ΔT are positive increments in Z and T, respectively, $j,n>0$, (4.53) may be represented by the finite difference equation

$$-a_j \theta_{j+1}^{n+1} + b_j\theta_j^{n+1} - c_j\theta_{j-1}^{n+1} = a_j\theta_{j+1}^{n} - (b_j-2)\theta_j^n + c_j\theta_{j-1}^n + \Delta T\, g_j^{n+\frac{1}{2}} \log_e Z_j \qquad (4.55)$$

where

$$\theta_j^n = \theta(1 + j\Delta Z, n\Delta T)$$

$$a_j = \alpha_j Z_{j+\frac{1}{2}}$$

$$b_j = 1 + \alpha_{j+\frac{1}{2}} + \alpha_{j-\frac{1}{2}} \qquad (4.56)$$

$$c_j = \alpha_{j-\frac{1}{2}}$$

$$\alpha_j = \frac{1}{2}\frac{\Delta T}{(\Delta Z)^2} Z_j = \frac{1}{2}\frac{\Delta T}{(\Delta Z)^2}(1 + j\Delta Z)$$

$$g_j^{n+\frac{1}{2}} = g(1 + j\Delta Z, (n+\tfrac{1}{2})\Delta T) = \tfrac{1}{2}(g_j^{n+1} + g_j^n).$$

With the aim of deriving an efficient method for solving (4.55), and through adaptation of the Gauss elimination procedure, we seek a solution of the form

$$\theta_j^n = e_j \theta_{j+1}^n + f_j^n \qquad \text{for all} \quad j \geq 1 \tag{4.57}$$

where e_j and f_j^n are known, and which may be solved sequentially in decreasing j for each n. To this end, denote the RHS of (4.55) by d_j^n so that

$$d_j^n = a_j \theta_{j+1}^n - (b_j - 2)\, \theta_j^n + c_j \theta_{j-1}^n + \frac{\Delta T}{2} \left[g_j^{n+1} + g_j^n \right] \log_e Z_j . \tag{4.58}$$

Using (4.57) to replace θ_{j-1}^{n+1} by $\left[e_{j-1} \theta_j^{n+1} + f_{j-1}^{n+1} \right]$ in (4.55) and rearranging leads to

$$\theta_j^n = \frac{a_j}{(b_j - c_j e_{j-1})}\, \theta_{j+1}^n + \frac{\left[d_j^{n-1} + c_j f_{j-1}^n \right]}{(b_j - c_j e_{j-1})} . \tag{4.59}$$

Comparison with (4.57) gives

$$e_j = \frac{a_j}{(b_j - c_j e_{j-1})} \; ; \quad f_j^n = \frac{(d_j^{n-1} + c_j f_{j-1}^n)}{(b_j - c_j e_{j-1})} \quad \text{for all} \quad j \geq 1 \tag{4.60}$$

e_0 and f_0^n may be calculated, as follows, by applying the lower boundary condition (4.54). Then, for each n, (4.60) may be solved sequentially in the j from $j=0$ (i.e. e_0 and f_0 give e_1 and f_1; e_1 and f_1 give e_2 and f_2, etc). In terms of θ_j^n, (4.54) may be approximated by

$$\frac{1}{2\Delta Z}\left[\theta_1^n - \theta_{-1}^n\right] = 0$$

so that

$$\theta_1^n = \theta_{-1}^n \ . \tag{4.61}$$

Setting $j=0$ in (4.55) and using (4.61) gives

$$\theta_0^n = \frac{(a_0 + c_0)}{b_0}\,\theta_1^n + \frac{d_0^{n-1}}{b_0} \ .$$

Comparing this with (4.57) gives

$$e_0 = \frac{(a_0 + c_0)}{b_0} \ ; \quad f_0^n = \frac{d_0^{n-1}}{b_0} \ . \tag{4.62}$$

Finally, having calculated e_j and f_j^n, $j>0$, (4.57) may be solved sequentially in decreasing j for θ_j^n by applying the upper boundary condition (4.33c) as follows. In terms of θ_j^n, (4.33c) may be written

$$\theta_J^n = 0 \tag{4.63}$$

where J is an integer suitably chosen so that $J\Delta Z$ is the height of the upper boundary. For the results presented in Section 4.4, $J\Delta Z$ was set equal to ~8000-9000m. Obviously this is much larger than necessary and could have been reduced appropriately (i.e. according to the size and number of time steps being considered) by estimating the height required and testing the estimates on the computer. However, it proved simpler to set a very large $J\Delta Z$ and

so be certain that, no matter what (realistic) dispersion time was considered, the upper boundary would not be reached. Hence from (4.57)

$$\theta^n_{J-1} = e_{J-1}\,\theta^n_J + f^n_J$$

which may be solved for θ^n_{J-1}, then reapplied to calculate θ^n_{J-2}, θ^n_{J-3}, θ^n_{J-4} etc. To summarise the method:

(1) equation (4.57) is solved for $\theta=N_0(z,t)$, for all $Z\geq 1$, by

(a) calculating e_0 and f^1_0 from (4.62) by using the initial condition (4.33a) and thus, from (4.60), calculating e_j, f^1_j, $j\geq 1$.

(b) Using (4.63) and sequentially applying (4.57) for $j=J-1, J-2, J-3, \ldots, 0$.

(2) Having calculated $N_0(z,t)$ for $Z\geq 1$ and $T=\Delta T$, $N_0(z,t)$ for $Z\geq 1$ and $T=m\Delta T$, $m>1$ can be calculated by following a similar method to (1) above except that the use of the initial condition in (a) is replaced by use of the results for N_0 at the preceding time step to calculate d^{n-1}_0 of (4.62).

(3) Having calculated $N_0(z,t)$ for $Z>1$, $0<T<T'$ say, $N_1(z,t)$ can be calculated for the same range of times by using a method similar to (2) above and the results for $N_0(z,t)$.

4.4 Results and Discussion

4.4.1 Introduction

This section presents and discusses the results from the numerical scheme described in Section 4.3.3. It is divided into three sub-sections. The first (Section 4.4.2) presents comparisons between the known 'exact' expressions for various measures of quantity, location and spread of the cloud and the corresponding numerical results. Section 4.4.3 applies these numerical results to compare approximations to the concentration distribution, χ, from the first three terms of the Hermite series (i.e. χ_p, $0<p<2$), with coefficients, A_n, derived from the exact and numerical results. Finally, in Section 4.4.4, the numerical results are used to derive higher order approximations to χ (χ_p for $2<p<4$), and thus examines the effects of including higher order terms in the Hermite series for χ on the approximation from the first few terms of the series.

In examining the numerical results, attention is focussed on the distribution of material released from a ground-level source (in the numerical model this implies a release height of $H=h/z_0=1$, see Equation 4.54). The reason for this is twofold. First, as discussed in Section 4.2.2, the assumed dispersion model is thought to be most suitable for examining dispersion when the scale of the

eddies acting on the cloud are much smaller than the vertical scale of the cloud itself, and therefore in particular for examining medium-range dispersion from a ground-level source. Second, from the reciprocal theorem (Smith 1957), the distribution of material at an elevated height, Z_1 say $(Z_1>0)$, and released from a ground-level source, is the same as the distribution at ground-level of material released from a source at height Z_1. Thus the results presented in this section for the distributions at various elevated Z of material released from a ground-level source, may be used to examine the behaviour of the distribution of material at ground-level released from an elevated source. Although it is not demonstrated here, the numerical results do conform to the reciprocal theorem. In other words, the moments calculated for the distribution of material, $N_i(z,t)$, (4.30), at an elevated level, $Z_1>1$, released from a source at $Z=1$, are equal to the moments calculated for the distribution of material at $Z=1$ released from a source at height Z_1.

In the initial stages of verifying and applying the numerical scheme, the calculations were carried out using relatively small space and time mesh steps. Typically, steps of $\Delta Z = \Delta(z/z_0)=0.2$ and $\Delta T=\Delta(ku_*t/z_0)=0.02$, or smaller, were used. However, it soon became apparent that in order to carry out calculations to larger T without consuming large amounts of computer time and memory, it would be necessary to increase ΔZ and ΔT somewhat. Eventually values of 0.5 and 0.125 were used for ΔZ and ΔT respectively. The use of these larger mesh steps did not have any significant effect on the calculated magnitude or shape of the resulting distributions for the moments of the cloud, $N_i(z,t)$. With these mesh sizes, calculations for the distributions with Z of N_i, i=1,2,3,4, for $0<T<250$ have

been performed. Using the analytic expression for the vertical coordinate of the centre of mass of the cloud, $\bar{Z}(t)$, as given by the exact model (Equation B1 with H=0), and using typical values for z_0 of ~0.01-0.1m, an upper limit on T of 250 implies that $\bar{Z}(t)$ reaches a maximum of ~2.5-25m. At this stage the calculations have not been extended to larger T, though this might have been thought desirable. However, as will be demonstrated in Section 4.4.4, as far as the present application is concerned, limiting the analysis to T<250 does not severely restrict the main aim of the chapter, viz. to examine the value of using the first few terms of the Hermite series to approximate χ.

There is one final point regarding the numerical calculations that should be made before presenting the results. The calculations were performed using double precision arithmetic with the mesh sizes given above. Integrals of the (non-dimensionalised) N_i over Z were calculated by applying Simpson's rule and stored for subsequent manipulation for values of T ranging from T=1 to T=250 in steps of 1. The calculated values for the non-dimensionalised N_i were stored for subsequent manipulation for values of T ranging from T=5 to T=250 in steps of 5, to an accuracy of 7 or 8 decimal places (dp) and at each fixed T for values of Z=1,3,5,... etc. In particular, the value of

$$\mu_0(Z,T) = z_0 N_0(z,t) = z_0 \int_{-\infty}^{\infty} \chi(x,z,t)\, dx \qquad (4.64)$$

which represents the proportion of material at (Z,T), (4.30), was stored to 8 dp. Since the quantity of material released was

normalised to 1, (4.2), $\mu_0(Z,T)<1$ for all (Z,T). Consequently, if $\mu_0(Z,T)\sim10^{-5}$-10^{-6}, it was only known relatively inaccurately as far as subsequent calculations were concerned. This has limited the range for which sensible curves can be plotted in the graphs presented below and is noted where appropriate.

4.4.2. Comparison of Analytic and Numerical Results for Some Measures of Quantity, Location and Spread of the Cloud

The comparisons discussed in this section are between various measures of quantity, location and spread for the 'exact' model of dispersion from a point source at ground-level, as represented by (4.7)-(4.12) with $h=0$, and the nearest comparable model considered with the numerical scheme, namely dispersion from a point source at $h=z_0$. The measures considered are $\bar{X}(t)$, $\bar{X}_z(z,t)$, $\Sigma_x(t)$, $\sigma_x(z,t)$ and $N_0(z,t)$ defined in (4.20), (4.21) and (4.34) and discussed in Appendix B. The corresponding numerically derived values for $\bar{X}(t)$, $\bar{X}_z(z,t)$, $\Sigma_x(t)$ and $\sigma_x(z,t)$ follow directly from the numerical results by expressing each in terms of the calculated N_i or integrals thereof, as appropriate. For example (4.35) and (4.37) can be rearranged to give $\bar{X}_z$ and σ_x in terms of the N_i.

The main difference between the exact and numerical models is the absence of a region of negative mean velocity in the numerical model, since it is applied in the region $Z\geq1$. Hence when judging the comparisons it is important to bear in mind that certain differences between the numerical and exact models can be expected. For example, in the numerical model, the downwind coordinate of the centre of mass of material at any fixed height, $\bar{X}_z(z,t)$, (4.20c), should never be less than zero. This is unlike the exact model

which at lower z and for early enough times will display $\bar{X}_z<0$. This and other differences are discussed below where appropriate.

Figure 4.8 compares the proportion of material, $N_0(z,t)$, (4.30), non-dimensionalised by multiplying by ku_*t, at various fixed heights above the ground (i.e. fixed Z) as a function of T as determined from the exact expression, (4.34) with $H=0$, and from the numerical scheme. Given the differences between the physical models represented by the exact and numerical results, the general behaviour of the numerical results compares favourably with the exact results. At 'ground' level ($Z=1$) there is less material in the numerical model than the exact at all times. At elevated Z, the numerical and exact results show more similarity. At these Z, and in the early stages following release, the numerical model has more material than the exact model but, at each Z, there is a time beyond which the numerical model has less material than the exact. This behaviour is illustrated in another way in the series of Figures (4.9a-g) showing the distribution with Z of ku_*tN_0 at various times, as calculated by the numerical and exact models. It is not immediately obvious why the numerical ku_*tN_0, for fixed Z, should approach its asymptotic value more slowly than in the exact model, but it cannot be due to the different velocity regimes experienced by the two models since the governing equation for N_0, (4.32a), is independent of $U(z)$.

Figure 4.10 compares the exact expression (B7) and the numerically calculated values for the downwind coordinate of the centre of mass of material, $\bar{X}_z(z,t)$, non-dimensionalised by dividing by ku_*t, at various fixed Z as a function of T. For the reasons discussed at the end of Section 4.4.1, the range of T for which each numerically derived curve is plotted varies, depending

on the amount of material at the corresponding Z and T. Broadly speaking, each curve is only plotted when $\mu_0 \geq 10^{-4}$ and $T \geq 5$, where μ_0 is given by (4.64). The general behaviour of the numerical $\bar{X}_z$ curves is consistent with that of the exact model. However, as expected, for any particular Z, the numerical $\bar{X}_z$ is greater than the corresponding exact $\bar{X}_z$. This is because there is no region of negative mean velocity in the numerical model so that material at any Z can only have been transported from the region $x \geq 0$. This is unlike the situation in the exact model where material may have been transported from the region $x<0$. For example, from Fig. 4.10 we see that in the exact model, for $Z=1$ and $T \leq 10$, $\bar{X}_z$ is negative whereas in the numerical model $\bar{X}_z$ is always positive. At $T=250$, the magnitude of the difference between the numerical and exact results, expressed as a percentage of the exact value, ranges from ~2.5% at $Z=301$ to 7% at $Z=1$.

As discussed by Chatwin (1968), the centre of mass of material at any fixed Z eventually lags behind the centre of mass of the whole cloud, $\bar{X}(t)$. Figure 4.11 illustrates this by comparing the development with T of the numerically derived values for $\bar{X}_z(z,t)$ at various fixed Z and $\bar{X}(t)$, both non-dimensionalised by dividing by ku_*t. Of the $\bar{X}_z(z,t)$ shown, and within the range of T considered, those for $Z=1$, 41 and 101 do lag behind $\bar{X}(t)$ for all or part of the time whilst those for $Z=201$ and 301 always remain ahead of $\bar{X}(t)$.

Figure 4.12 compares the exact expression (B6) and the numerically calculated downwind coordinate of the centre of mass of the cloud, $\bar{X}(t)$, non-dimensionalised as for the previous figure. The comparison is good. The fact that $\bar{X}(t)$ as calculated by the numerical model is always positive and greater than the exact $\bar{X}(t)$

is a reflection of the results discussed for $\bar{X}_z(z,t)$, (Fig. 4.10).

Turning to the measures of spread of the cloud for which analytic expressions are available, the only known exact expression for $\sigma_x(z,t)$, given by (4.21b), is for the spread of material at ground-level (Z=0) from a ground-level source (H=0), (B9b). Figure 4.13 compares the numerically calculated downwind spread of the cloud, $\sigma_x(z,t)$, non-dimensionalised as for the other figures, at various fixed $Z>1$ and the exact expression (B9b). As expected, at each Z, the numerically derived spread is less than the constant exact value for all T. This is not surprising since, compared to the numerical model, the exact value will be augmented by the region of negative mean velocity below Z=1 and, for elevated Z, the exact value is only valid as $T \to \infty$ (Chatwin 1968). Hence we might expect the numerical model to have an asymptotic value for $\sigma_x(z,t)$ smaller than the exact $\sigma_x(0,t)$. Within the range of times considered here, from the numerically derived curves in Fig. 4.13, it is interesting to note that for each fixed $z>z_0$ (i.e. Z>1), z_1 say, there exists a time, t_p say, such that for t greater than t_p, $\sigma_x(z_1,t)$ is greater than the spread at ground-level (i.e. $\sigma_x(z_0,t)$). This is presumably due to the effect of the positive gradient in the mean velocity, which eventually results in a greater stretching of the material at elevated Z in the downwind direction compared to that of the material at ground-level. However, the analogy, for the numerical model, of the approach of the exact $\sigma_x(z,t)$ to $\sigma_x(0,t)$ as $t \to \infty$, is that we would expect all the numerical curves for Z>1 in Fig. 4.13 to converge to that for Z=1 as $T \to \infty$.

Figure 4.14 compares the numerically calculated values and exact expression, (B9a), for the downwind spread of the whole cloud,

$\Sigma_x(t)$, non-dimensionalised as for the other figures. The diagram is consistent with the results discussed for $\sigma_x(z,t)$, (Fig. 4.13).

As emphasised at the beginning of the section, equality between the numerical and exact models considered above was not expected. However, the above comparisons do show that the numerical results are reasonable and, given the differences between the two models, are consistent with the known analytic expressions.

4.4.3 Comparison of Second and Lower Order Approximations to $\chi(x,z,t)$ Derived from the Analytic and Numerical Results

This subsection compares approximations to the ground-level distribution of χ, χ_p for $p\leq 2$, (4.19), (a) where the coefficients of the series, $A_n(Z,T)$, and the arbitrary functions $m(z,t)$ and $\sigma(z,t)$, once chosen suitably, have been calculated from the known analytic expressions for the 'exact' model (as represented by Equations 4.7-4.12), with (b) the analogous χ_p for the numerical model, that is where the coefficients and arbitrary functions have been calculated from the numerical results. The comparisons need only be considered briefly since, as will be shown below, they merely reflect the comparisons discussed in the previous subsection (Section 4.4.2) for the various measures of quantity, location and spread of the cloud. For the same reason, the comparisons are for the ground-level distribution from a ground-level source (so that distributions above ground-level are not considered), and the comparisons are made at a single fixed time, T=250, that is the latest time for which numerical calculations are available (Section 4.4.1).

The comparisons are illustrated in Figs. (4.15a-e). As in Section 4.3.2, the abscissa of each figure is x/ku_*t and the ordinate is some suitably chosen multiple of $(ku_*t)^2 \chi_p$. Each figure compares an analytically derived approximation with the analogous numerically derived approximation as follows. First, each figure is for a particular choice of m and σ, viz.

$$\begin{aligned}
&\text{(a)} \quad m=\bar{X}(t) \; ; \qquad \sigma=\Sigma_x(t) \\
&\text{(b)} \quad m=\bar{X}(t) \; ; \qquad \sigma=\sigma_x(z_G,t) \\
&\text{(c)} \quad m=\bar{X}(t) \; ; \qquad \sigma=s_x(z_G,t) \\
&\text{(d)} \quad m=\bar{X}_z(z_G,t) \; ; \quad \sigma=\Sigma_x(t) \\
&\text{(e)} \quad m=\bar{X}_z(z_G,t) \; ; \quad \sigma=\sigma_x(z_G,t)
\end{aligned} \tag{4.65}$$

where $t=250z_0/ku_*$ (i.e. $T=250$) and z_G denotes the ground-level value of z. For the approximations based on the exact model, $z_G=0$ (i.e. $Z=0$), whereas for those based on the numerical results, $z_G=z_0$ (i.e. $Z=1$), since the numerical scheme has been applied in the region $z \rightarrow z_0$ (i.e. $Z \rightarrow 1$, see Section 4.3.3, Equation 4.54). All of the combinations for m and σ in (4.65) have been considered in varying degrees of detail in earlier sections, and represent the main natural choices for m and σ (Sections 4.2.3 and 4.3.2). The 'exact' curve in each figure (indicated by a solid line, '——'), that is the curve based on A_n, m and σ derived from the analytic expressions, is the highest order approximation known for the given m and σ, namely χ_2. Each of these approximations has already been considered in detail (Section 4.3.2). The numerically derived curve in each figure (indicated by a dashed line '---') is the corresponding approximation based on A_n, and the same m and σ calculated from the numerical results. As described in Section 4.2.3,

some of the choices in (4.65) cause one or more of the coefficients, A_1 and A_2, to be identically zero for all Z and T, so that, in effect, the approximations shown in Figs. (4.15a-e) are as follows:

$$\begin{aligned}
&\text{(a)}\quad \times_2 \\
&\text{(b)}\quad \times_2 \\
&\text{(c)}\quad \times_1 \quad \text{(since } A_2=0, \text{ Equation 4.26)} \\
&\text{(d)}\quad \times_2 \quad \text{(where } A_1=0, \text{ Equation 4.27)} \\
&\text{(e)}\quad \times_0 \quad \text{(since } A_2=A_1=0, \text{ Equation 4.28)}
\end{aligned} \tag{4.66}$$

From Fig. 4.15 it is readily seen that the numerically based approximations are similar to the curves based on the exact expressions. This is not surprising given the comparisons discussed in Section 4.4.2. The main point to make is that the numerically based approximations reflect the larger $\bar{X}(t)$ and $\bar{X}_z(z,t)$, and smaller $\Sigma_x(t)$ and $\sigma_x(z,t)$, of the numerical model compared to the exact model (Section 4.4.2). Thus the location of the peak of each numerically based approximation is further downwind than that of the analytically based approximation. The spread and peak of the numerically based approximations are also smaller than those of the corresponding analytically based approximation. However, since these differences are relatively small, we can be confident that any higher order, numerically based approximation (i.e. $\times_p$, $p>2$) will reflect the correct behaviour in the sense that it will behave similarly to the corresponding analytically based approximation. We can therefore use such numerically based higher order approximations to examine the use of the Hermite series, (4.13), to approximate $\times$. This is done in the next subsection.

4.4.4 Third and Fourth Order Approximations to $\chi(x,z,t)$ Derived From the Numerical Results

Section 4.3.2 illustrated approximations to the horizontal distribution of χ, χ_p for $p \leq 2$, where the coefficients, $A_n(Z,T)$ and the arbitrary functions $m(z,t)$ and $\sigma(z,t)$ of the Hermite series, once suitably chosen, were derived from the known analytic expressions. Section 4.4.3 compared these analytically derived approximations with the analogous approximations derived from the numerical results. Because of the limited exact results available, these earlier sections have focussed on the distribution at ground-level from a ground-level source. Using the numerical results, this section examines approximations, χ_p, for the concentration distribution at ground-level and at elevated z, and for $p>2$. For the reasons given in Section 4.4.1, all of the results presented are for release from a ground-level source.

As discussed in Sections 4.3.1 and 4.3.2, we would expect χ_p, $p>2$, to provide a better approximation to χ than χ_p, $p \leq 2$, if χ is significantly different from the Gaussian. From the numerical results, values for the moments of the cloud $N_i(z,t)$, $i \leq 4$, are available (Section 4.4.1). Since the coefficient, $A_n(Z,T)$, of the Hermite series for χ depends on the $N_i(z,t)$, $i \leq n$ (Section 4.3.1, Equation 4.31), the available numerical results enable $A_p(Z,T)$, $p \leq 4$, and therefore approximations to χ, χ_p, $p \leq 4$, to be determined. If the horizontal distribution of χ displays significant skewness or kurtosis, we would then expect application of the complete set of numerical results to provide a better approximation to χ than χ_p, $p \leq 2$. Initially in this section, the numerically calculated skewness and kurtosis of the cloud are examined (Section 4.4.4.1). Then the

numerical results are used to examine approximations χ_p for $p>2$ (Section 4.4.4.2).

4.4.4.1 The Skewness and Kurtosis of the Horizontal Distribution for $\chi(x,z,t)$

Figure 4.16 shows the calculated skewness of the cloud in the downwind direction at various fixed Z, $\beta_3(z,t)$, and of the cloud as a whole, $B_3(t)$, as functions of T, where β_3 and B_3 are given by (Kendall and Stuart 1969)

$$\beta_3(z,t) = \frac{1}{\sigma_x^3} \frac{\int_{-\infty}^{\infty} (x - \bar{X}_z)^3 \chi \, dx}{\int_{-\infty}^{\infty} \chi \, dx}$$

$$= \frac{1}{\sigma_x^3} (N_0)^{-3} (N_3 (N_0)^2 - 3N_2 N_1 N_0 + 2(N_1)^3) \qquad (4.67)$$

$$B_3(t) = \frac{1}{\Sigma_x^3} \int_0^{\infty} \int_{-\infty}^{\infty} (x - \bar{X})^3 \chi \, dx dz \qquad (4.68)$$

and $\bar{X}_z(z,t)$, $\bar{X}(t)$, $\sigma_x(z,t)$, $\Sigma_x(t)$ and $N_i(z,t)$, are given by (4.20c, b), (4.21b, a) and (4.30), respectively. It should be noted that of the curves for $\beta_3(z,t)$, those for $Z \geq 21$ have not been extended back to $T=5$ (the smallest T for which results were available - see Section 4.4.1) since in the early stages of their development with T they exhibit erratic behaviour. This is due to the relative inaccuracy to which μ_0 (given by 4.64) was available for use in

subsequent calculations (Section 4.4.1), and to the dependence of β_3 on $(N_0)^{-3}$ and hence on $(\mu_0)^{-3}$. Indeed, $\beta_3(z,t)$ for Z=501 and 601 is somewhat erratic for all or the majority of the time range in Fig. 4.16.

Looking in more detail at the curves in the figure, as expected, (a) at Z=1, β_3 is always positive, in other words, the distribution at ground-level has a long "tail" in the downwind direction, and (b) at elevated Z, β_3 is initially negative (with an initial magnitude that decreases with increasing Z). At all Z, β_3 appears to be approaching a small positive value (~0.18-0.2) as $T \rightarrow \infty$. This behaviour is not inconsistent with Saffman's analysis (1962), discussed in Sections 4.2.2 and 4.4.3. However, the asymptotic value for β_3 obtained here is somewhat smaller than Saffman's value of ~1. This is presumably a reflection of the fact that Saffman used a wind profile linear in z, so that the effect of wind shear in his model will be greater than that for the logarithmic wind profile used here. It is also clear from Fig. 4.16 that at elevated Z, and - using the reciprocal theorem - at ground-level for an elevated source, the distribution of material has a negative skewness for some or all of the range of dispersion time shown. Indeed, extrapolating the results to later times, it would seem that for the more elevated Z, the distribution will be negatively skewed for a significant proportion of the dispersion time.

Turning to the curve for the skewness of the cloud as a whole about $\bar{X}(t)$, $B_3(t)$, shown in Fig. 4.16, it would seem that it is dominated by the material at elevated Z. The approach to a small negative value (approximately -0.1 to -0.15), at least within the range of T considered, is due to the interaction of two main conflicting factors. First, as noted above, the skewness of the material at the more elevated Z is negative, and $\bar{X}_z(z,t)$ is greater than $\bar{X}(t)$

(Section 4.4.2). Hence the skewness of material at such Z, when measured about $\bar{X}(t)$ will be even more negative. Conversely, in the lower layers of the cloud, the skewness of the distribution at fixed Z is positive and $\bar{X}_z(z,t)$ eventually lags behind $\bar{X}(t)$. Hence, at these Z, the skewness measured about $\bar{X}(t)$ will be even more positive. The resulting curve for $B_3(t)$ is consistent with the numerical calculations of Atesmen (1972). He used a model slightly different to the one considered here in that longitudinal diffusion was included and diffusion was limited in the vertical by an inversion height. Because of these differences, and because Atesmen non-dimensionalised his results differently to the approach used here, a direct comparison with his results is not possible. Nonetheless the behaviour of Atesmen's $B_3(T_n)$, where $T_n = ku_*t/z_n$ and z_n is the height of the inversion layer, before the effects of the inversion layer are felt, is consistent with Fig. 4.16 in that $B_3(T_n)$ decreases from -0.5 to zero in the range of times shown ($0 < T_n < 0.1$) and appears to be continuing to decrease.

Figures (4.17a,b) show the calculated kurtosis of the cloud in the downwind direction at various fixed Z, $\beta_4(z,t)$, and of the cloud as a whole, $B_4(t)$, where $\beta_4(z,t)$ and $B_4(t)$ are given by

$$\beta_4(z,t) = \left\{ \frac{1}{\sigma_x^4} \frac{\int_{-\infty}^{\infty} (x - \bar{X}_z)^4 \times dx}{\int_{-\infty}^{\infty} \times dx} \right\} - 3$$

$$= \frac{1}{\sigma_x^4} (N_0)^{-4} (N_4 (N_0)^3 - 4N_3 N_1 (N_0)^2 + 6N_2 (N_1)^2 N_0 - 3(N_1)^4)$$

$$-3 \qquad (4.69)$$

$$B_4(t) = \left\{ \frac{1}{\Sigma_x^4} \int_0^{\infty} \int_{-\infty}^{\infty} (x - \bar{X})^4 \times \, dxdz \right\} - 3 \qquad (4.70)$$

and $\bar{X}_z(z,t)$, $\bar{X}(t)$, $\sigma_x(z,t)$, $\Sigma_x(t)$ and $N_i(z,t)$ are given by (4.20c,b), (4.21b,a) and (4.30), respectively. For the corresponding Gaussian distribution, $\beta_4(z,t)$ or $B_4(t)$ is equal to zero (Kendall and Stuart 1969). Similarly to $\beta_3(z,t)$ and $B_3(t)$, we would expect $\beta_4(z,t)$ at fixed Z and $B_4(t)$ to approach constant values as $T \to \infty$. Two separate figures are shown in Fig. 4.17 simply because a single diagram including all the curves is too cluttered for easy interpretation. As for Fig. 4.16, the curves for larger Z are not extended back to $T=5$ because of their erratic behaviour. Note from (4.69) that β_4 depends on $(N_0)^{-4}$ and therefore on $(\mu_0)^{-4}$, (4.64). As a result, the curves are relatively more erratic than the corresponding curves for the skewness in Fig. 4.16. Although the erratic nature of the curves for $\beta_4(z,t)$ for larger Z ($Z>401$) makes them unsuitable for determining reliable values for $\beta_4(z,t)$ for these Z, it is clear that at all Z, as T increases, $\beta_4(z,t)$ approaches a small negative value in the range -0.3 to -0.4. In other words, the distribution at any fixed Z is eventually flatter than the Gaussian, i.e. is platykurtic. Turning to the curve for the kurtosis of the cloud about $\bar{X}(t)$, $B_4(t)$, it is not clear that it is approaching a particular value. This is interesting since comparison with Atesmen's (1972) calculations for the cloud kurtosis and the comparison made above with his result for the cloud skewness, $B_3(t)$ (Fig. 4.16), would suggest that the approach of $B_4(t)$ to its asymptotic value should be observed in Fig. 4.17. Atesmen's results show $B_4(T_n)$, T_n as given above,

approaching a value of ~0.4 at T_n ~0.1. There appears to be no obvious explanation for this discrepancy.

4.4.4.2 Third and Fourth Order Approximations to $\chi(x,z,t)$

From the previous subsection (Section 4.4.4.1) it is clear that whilst deviations from the Gaussian are evident in the horizontal distribution of $\chi(x,z,t)$ as $t \to \infty$, these deviations are rather smaller than might have been expected from Saffman's analysis (1962) of the simpler dispersion model with a power-law wind profile. The table below summarises the numerically derived values of various measures of location, spread and shape of the distribution for $\chi^{(G)}(x,z,t)$ at T=250, the latest time for which results are available (Section 4.4.1):

	Z=1	Z=41	Z=101	Z=201	Z=301
$(ku_*t)^{-1}\ \bar{X}_z(z,t)$	19.85	21.81	23.64	25.67	27.13
$(ku_*t)^{-1}\ \sigma_x(z,t)$	3.37	3.59	3.65	3.58	3.47
$\beta_3(z,t)$	0.22	0.14	0	-0.14	-0.22
$\beta_4(z,t)$	-0.31	-0.40	-0.44	-0.36	-0.31

(4.71a)

$(ku_*t)^{-1}\ \bar{X}(t)$	25.48
$(ku_*t)^{-1}\ \Sigma_x(t)$	4.79
$B_3(t)$	-0.07
$B_4(t)$	-0.25

(4.71b)

All of these values are drawn from results presented in Sections 4.4.2 and 4.4.4.1, and have been selected to illustrate the range of values at T=250 for skewness, $\beta_3(z,t)$, and kurtosis, $\beta_4(z,t)$, of the distribution at any fixed height that can be determined reliably

from the numerical results (i.e. are not unduly influenced by inaccurately known μ_0, Section 4.4.1). Given these ranges, in turning to third and fourth order approximations to $\times$, it is reasonable to focus on the distribution of material at Z=1, 101 and 301. The values of skewness and kurtosis at these Z provide sets of values representative of the different types of deviations from Gaussianity displayed by $\times$ at fixed Z. For the reasons given earlier, the focus will also be on approximations to $\times$ for the five pairs of choices for m and σ given in (4.65).

Figures (4.18a-e) illustrate fourth and lower order approximations to $\times^{(G)}(x,z,t)$ at Z=1. Each figure is for a fixed choice of m and σ. Figure 4.18a corresponds to the choice given in Equation (4.65a) (i.e. $m=\bar{X}(t)$, $\sigma=\Sigma_X(t)$), Fig. 4.18b corresponds to the choice (4.65b), and so on. One of the main conclusions that can be drawn from the figures is that, for the horizontal distribution at (Z,T)=(1,250), and for fixed m and σ, the effect on the approximation of the inclusion of the third and fourth order terms of the Hermite series, varies in significance depending on the choice for m and σ. In particular, for the <u>most</u> natural of all the choices for m and σ, that is $m=\bar{X}_z(z,t)$, $\sigma=\sigma_X(z,t)$, the effects are the least significant (Fig. 4.18e). This is clearly a reflection of the relatively small deviation of the actual distribution from the Gaussian, which has a skewness and kurtosis of 0.22 and -0.31, respectively, (4.71a). Note that for this choice of m and σ, as expected, the fourth order approximation, $\times_4$, compared to the second order approximation, $\times_2$, is both positively skewed and flatter. On the other hand, for other choices of m and/or σ (Figs. 4.18a, c and d), $\times_4$ is peakier than the corresponding $\times_3$ and $\times_4$.

Apart from Fig. 4.18b, all of the approximations are of reasonable general shape, although, subjectively speaking, the negative values in the case of $m=\bar{X}(t)$, $\sigma=\Sigma_X(t)$ (Fig. 4.18a) and $m=\bar{X}(t)$, $\sigma=s_X(z,t)$ (Fig. 4.18c) are unsatisfactory. As has already been noted (Section 4.3.2), choosing $m=\bar{X}(t)$, $\sigma=\sigma_X(z,t)$ (Fig. 4.18b) also results in significant negative values for $\times_2$. Including the third and fourth order terms in the approximation for any of these three choices for m and σ, whilst reducing the significance of the negative values, does not seem to result in an acceptable approximation for $\times$. This confirms the observation made in Section 4.3.2 that choosing m and/or σ significantly different from the actual mean or spread of the material, respectively, at the chosen Z, can result in an approximation with unacceptable negative values. In particular, the negative values in Figs. (4.18a-c) appear to be a result of attempting to approximate $\times$ by a series with $m=\bar{X}(t)$, rather than the more natural $m=\bar{X}_z(z,t)$ when the difference between $\bar{X}(t)$ and $\bar{X}_z(z,t)$, at ~28% (expressed as a percentage of $\bar{X}_z(z,t)$, see 4.71), is relatively large.

From Fig. 4.18d, it might at first seem surprising that approximating $\times$ by a series with $m=\bar{X}_z(z,t)$ but with a σ ~42% greater than the actual spread of material at $Z=1$ (i.e. $\sigma=\Sigma_X(t)=4.79ku_*t$ compared with $\sigma_X(z,t)=3.37ku_*t$, see (4.71)) only results in negligible negative values for $\times$, $2<p<4$. However, it will be recalled from Section 4.3.2 (Fig. 4.4b) that $\times_2$ for $m=\bar{X}_z(z,t)$ but for a σ much smaller than the actual spread of the material does contain unacceptable negative values for $\times_2$. Considering the main role of σ in the series (i.e. as the spread of the Gaussian first term) it seems reasonable that choosing $m=\bar{X}_z$ but σ much larger than the actual σ does not result in significant

negative values for $\times_p$ (but clearly will result in an unrealistically large spread for $\times_p$), whereas, for the same choice of m, choosing σ much smaller than the actual spread does result in unacceptable negative values for $\times_p$.

To enable a different comparision, Figs. (4.19a-c) regroup the curves of Figs. (4.18a-e) to compare approximations of the same order for the different choices of m and σ. Figure 4.19a compares $\times_2$ for the choices (4.65a-e), Figs. (4.19b,c) compare $\times_3$ and $\times_4$, respectively, for the same choices. Not surprisingly, it is clear from Figs. (4.19a-c) that the differences in the shape, spread and location of the second order approximations for different m and σ (Fig. 4.19a), which were observed in the corresponding exact curves (Section 4.3.2), are also a feature of the third and fourth order approximations (Figs. 4.19b and c, respectively). For example, in Fig. 4.19c, there is a ~30% difference between the peak value of $\times_4$ for $m=\bar{X}(t)$, $\sigma=\Sigma_x(t)$ and that for $m=\bar{X}(t)$, $\sigma=s_x(z,t)$ (expressed as a percentage of the latter).

Figures (4.20a-e) and (4.21a-e) show $\times_p$, $2\leq p\leq 4$, for Z=101 and Z=301, respectively, analogous to those already considered for Z=1 (Figs. 4.18a-e), i.e. for the same choices of m and σ. For Z=101 (Figs. 4.20a-e), $\beta_3(z,t)=0$ and $\beta_4(z,t)=-0.44$ whilst for Z=301 (Figs. 4.21a-e), $\beta_3(z,t)=-0.22$ and $\beta_4(z,t)=-0.31$, (see Equation 4.71a). For both sets of figures, and unlike the case for Z=1 (Figs. 4.18a-e), for each of the chosen m and σ, the negative values for any $\times_p$, $2\leq p\leq 4$, if they exist at all, are negligible. In the cases of $m=\bar{X}(t)$, $\sigma=\Sigma_x(t)$, $\sigma_x(z,t)$ or $s_x(z,t)$ (Figs. 4.20a-c and 4.21a-c), this is probably a result of the fact that the differences between $\bar{X}(t)$ and $\bar{X}_z(z,t)$ at Z=101 and Z=301 (7% and 6%, respectively, when expressed as a percentage of $\bar{X}_z(z,t)$, see

4.71), are relatively small compared to the 28% difference at Z=1. In the case of $m=\bar{X}_z(z,t)$, $\sigma=\Sigma_x(t)$ (Figs. 4.20d and 4.21d), the same negligible negative values were found for Z=1 (Fig. 4.18d). Given that the difference between $\Sigma_x(t)$ and $\sigma_x(z,t)$ at Z=101 or 301 is positive and, in both percentage and absolute terms, of the same order as that at Z=1 (31% and 37%, respectively, when expressed as a percentage of $\sigma_x(z,t)$, compared to 42% at Z=1), it is not surprising that $\times_p$ for $2<p<4$, like those at Z=1 do not possess significant negative values.

Although there are no significant negative values in Figs. (4.20a-e and 4.21a-e), as was the case for Z=1, some of the $\times_4$, namely those for $m=\bar{X}(t)$, $\sigma=\Sigma_x(t)$ or $s_x(z,t)$ and $m=\bar{X}_z(z,t)$, $\sigma=\Sigma_x(t)$ (Figs. 4.19 and 4.20, a, c and d, respectively) are peakier rather than flatter than the corresponding $\times_2$. However, for $m=\bar{X}_z(z,t)$ and $\sigma=\sigma_x(z,t)$, $\times_3$ and $\times_4$ possess all the expected properties. At Z=101 (Fig. 4.20e), $\times_3$ is identical to $\times_2$, reflecting the zero skewness at this Z, whilst at Z=301 (Fig. 4.21e), $\times_3$ is slightly negatively skewed compared to $\times_2$. In both cases, $\times_4$ is flatter than $\times_2$ and $\times_3$.

4.5 Summary and Conclusions

As explained at the beginning of this chapter (Sections 4.2.2 and 4.2.3), the main aim of this investigation has been to examine the use of the first few terms of the Hermite series (4.13) to approximate $\times$, and in particular to approximate the expected deviations from the Gaussian of the horizontal distribution of $\times$ as $t \to \infty$. For several reasons (Section 4.4.1), this has been achieved by focussing on the behaviour of the horizontal distribution of

material released from a ground-level source, $\chi^{(G)}(x,z,t)$, for various natural choices for the arbitrary functions of the series $m(z,t)$ and $\sigma(z,t)$, and at $T=ku_*t/z_0=250$ (i.e. the latest time for which calculations were available), for various fixed $Z(=z/z_0)$. There are several main conclusions that can be drawn.

First, as t increases, the skewness and kurtosis of the horizontal distribution of χ at any fixed Z appear to be approaching values in the range ~0.18 to 0.2 and -0.3 to -0.4, respectively (Section 4.4.4.1). In other words, the distribution at any fixed Z eventually is more positively skewed (i.e. has a longer tail in the downwind direction) and flatter than the Gaussian. The result for the skewness is consistent with Saffman's analysis (1962) of dispersion in a velocity field linear in z. The numerically calculated skewness and kurtosis at T=250 and at various fixed Z, provided values ranging from approximately -0.22 to 0.22 and -0.3 to -0.45 respectively, (4.71a), and so were suitable for examining the use of the series to approximate the horizontal distribution of χ as $t \to \infty$.

Whilst no attempt has been made to quantify what constitutes an acceptable approximation to χ, examination of the use of the first five terms, or less, of the Hermite series for a ground-level source (i.e. $\chi_p^{(G)}(x,z,t)$ for $p\leq 4$), for various choices of m and σ, has shown that (Section 4.4.4.2):

(a) choosing m and σ equal to the mean, $\bar{X}_z(z,t)$, and spread, $\sigma_x(z,t)$, of the material at the corresponding Z, respectively, consistently (i.e. at various Z and therefore for various values of skewness and kurtosis) gives the best approximation for χ in the sense that, compared to other

choices for m and σ, $\times_p$ for $2<p<4$ (i) had only negligible negative values, and (ii) correctly reflected the actual skewness and kurtosis at the chosen Z.

(b) For the same m and σ, given the magnitude of the deviations of the horizontal distribution of $\times$ from the Gaussian as $t \to \infty$, evidence from other applications of a Hermite series approximation (Barton and Dennis 1952; Kendall and Stuart 1969) would suggest that, for the chosen model (4.7)-(4.12), the series (4.13) will be of practical use.

(c) Other choices for m and σ can result (i) in - what subjectively appear to be - unacceptable negative values for $\times_p$, $2<p<4$, and (ii) in $\times_4$ which are peakier rather than flatter than the corresponding $\times_2$ and which therefore do not reflect either the negative kurtosis at the particular Z, $\beta_4(z,t)$, or of the cloud as a whole, $B_4(t)$.

(d) In addition to the effects outlined in (c) above, compared to the choice $m=\bar{X}_z(z,t)$, $\sigma=\sigma_x(z,t)$, other choices for m and σ can result in significantly different locations for the maximum and spread of the horizontal distribution of $\times_p$, $p<4$.

There appear to be two main ways of continuing to develop the application of a Hermite series to dispersion in the atmosphere. The first is to continue with the adopted simplified model of dispersion, (4.7)-(4.12), and quantify (i) what is meant by "unacceptable" and "significant" (as used in (c) and (d) above), and (ii) when choices for m and σ other than $\bar{X}_z$ and σ_x,

respectively, result in unacceptable approximations for χ. This could be done by applying the series (4.13) for various choices of m and σ but for a wider range of values for the measures of location, spread and shape of the distribution for χ than used here. It should then be possible to derive rules governing when choices other than $m=\bar{X}_Z$ and $\sigma=\sigma_X$ are adequate. Ideally, these rules should be in terms of parameters appropriate to dispersion in the atmosphere (for example, time since and height of release). As far as the use of the series with $m=\bar{X}_Z$ and $\sigma=\sigma_X$ is concerned, a limited amount of qualitative and quantitative guidance on when χ can be approximated by χ_4 is available from studies of the application of Hermite series to other problems (Barton and Dennis 1952; Kendall and Stuart 1969). However, this evidence is in terms of the skewness and kurtosis of the distribution under consideration. For our problem, it would valuable to quantify when, for example, χ_4 is of use in terms of parameters appropriate to dispersion in the atmosphere. Again this should be possible by applying the series to a wide range of values for the measures of location, spread and shape of the distribution for χ. One final point concerning the application of the Hermite series (4.13) to the model (4.7)-(4.12), it would be of interest to compare the use of the Edgeworth series with that of the Gram-Charlier series (Section 2.2.1) to approximate χ.

This chapter has shown that a Hermite series can be used to represent the distribution of mean concentration based on a <u>particular</u> simplified model of dispersion in the atmosphere, (4.7)-(4.12). As discussed earlier (Section 4.2.2), the model is somewhat restricted in its range of application. The second way of proceeding to develop the application of a Hermite series to dispersion in the atmosphere, is to investigate the application to

less simplified models. For example, since completing this work the author has been made aware of a series of papers (Sullivan 1983a and b; Sullivan and Yip 1985, 1987) describing work, begun independently, which applies a three dimensional Hermite series to a model applicable, inter alia, to dispersion in the atmosphere. In the model, in particular, the principal axes of the eddy diffusivity tensor K_{ij} do not coincide with the coordinate axes (x,y,z of Section 4.2), the significance of which is discussed by Monin and Yaglom 1971, p.666-669 and Sullivan and Yip 1985. The results of this chapter clearly indicate that such work should prove to be of practical use.

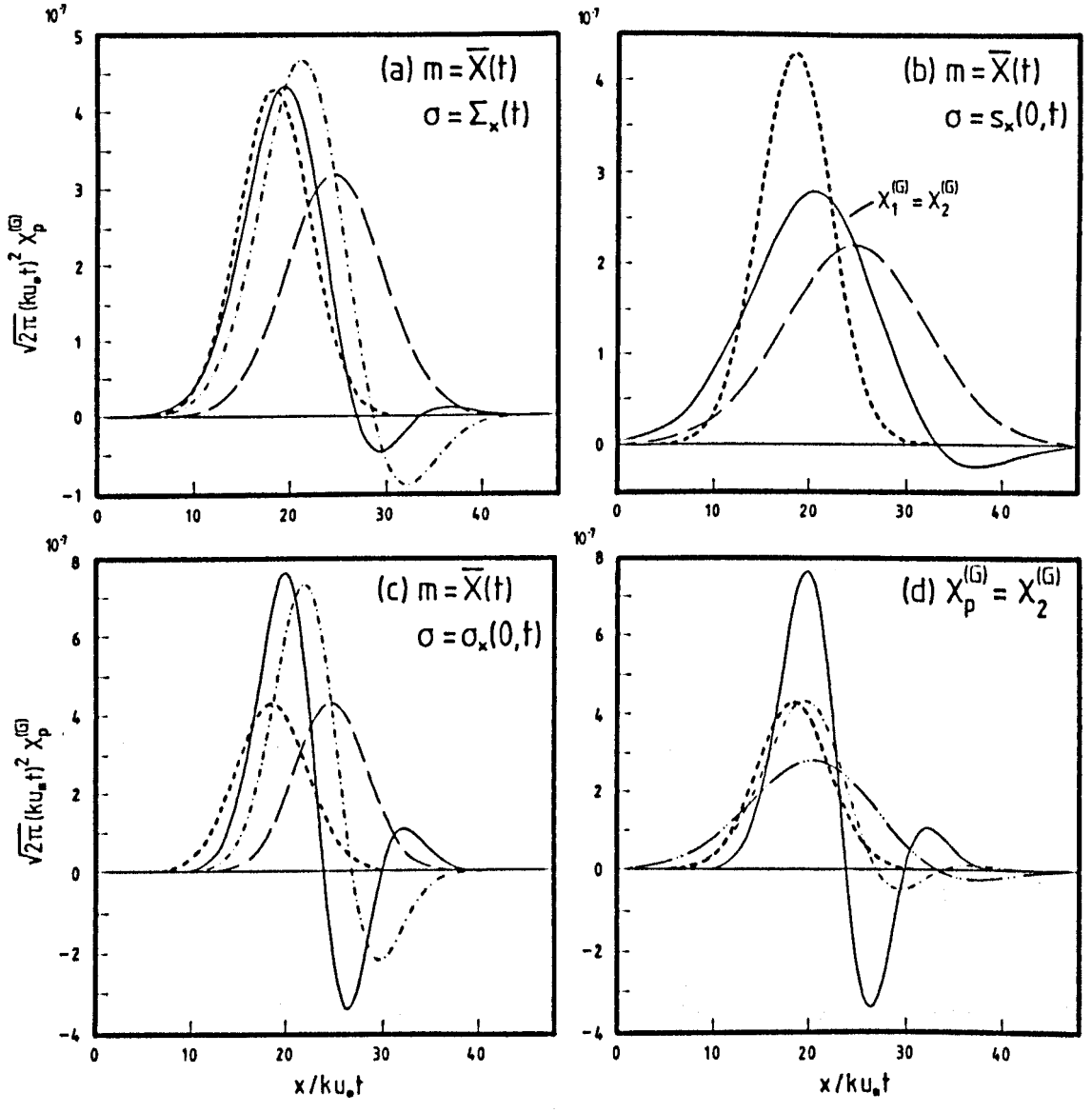

Key: (a), (b) and (c) –

$\chi_0^{(G)}$

$\chi_1^{(G)}$

$\chi_2^{(G)}$

(d) –

m	σ
$\bar{X}(t)$	$\Sigma_x(t)$
$\bar{X}(t)$	$s_x(0,t)$
$\bar{X}(t)$	$\sigma_x(0,t)$

all figures –

$\chi_2^{(G)} = \chi_1^{(G)} = \chi_0^{(G)}$ for $m = \bar{X}_z(0,t)$, $\sigma = \sigma_x(0,t)$

Fig.4.1 Second and Lower Order Approximations to the Ground-Level Concentration Downwind of a Ground-Level Point Source, T=250

Derived from Exact Results

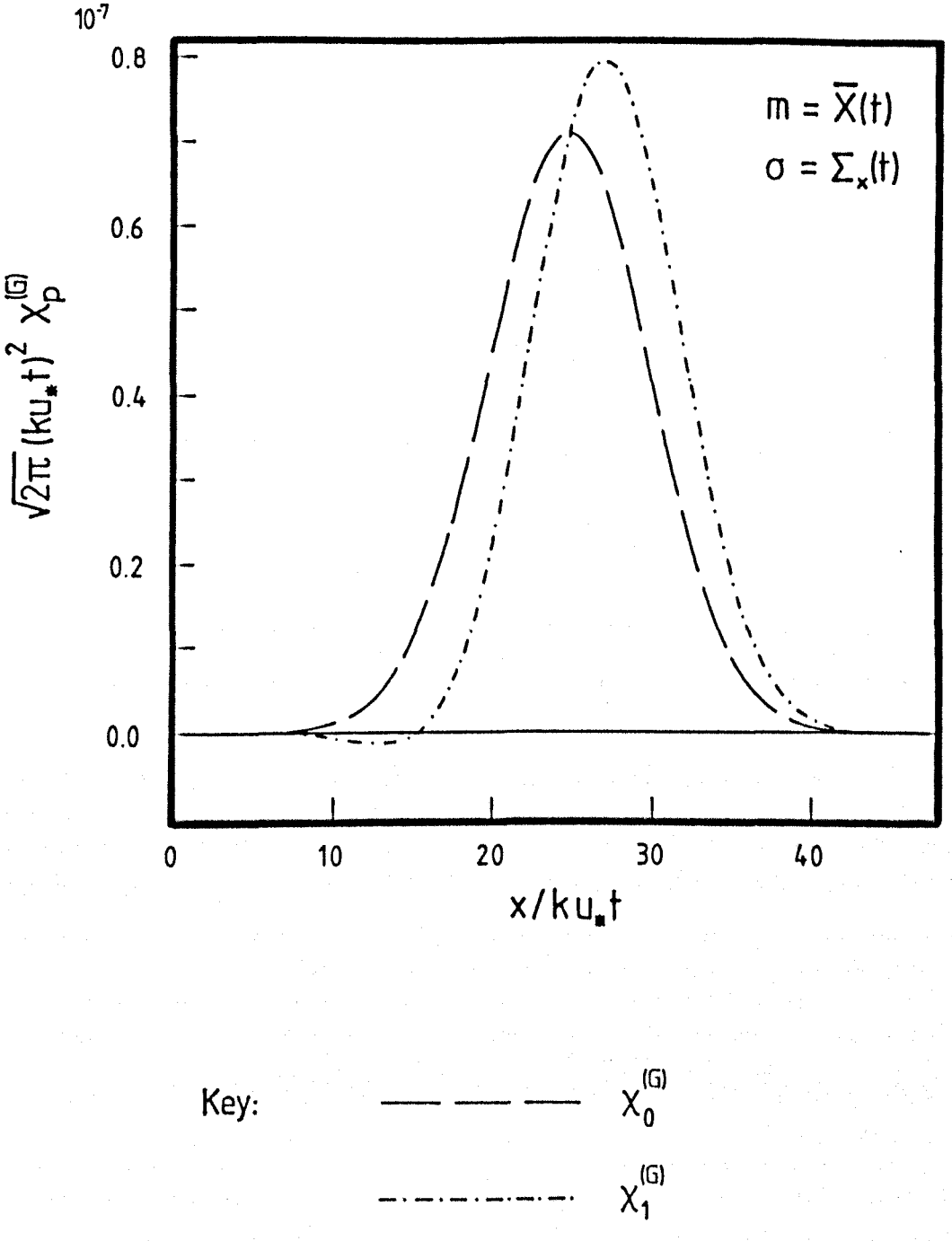

Fig.4.2 Zeroth and First Order Approximations to the Horizontal Downwind Concentration from a Ground-Level Point Source at Z=375, T=250

Derived from Exact Results

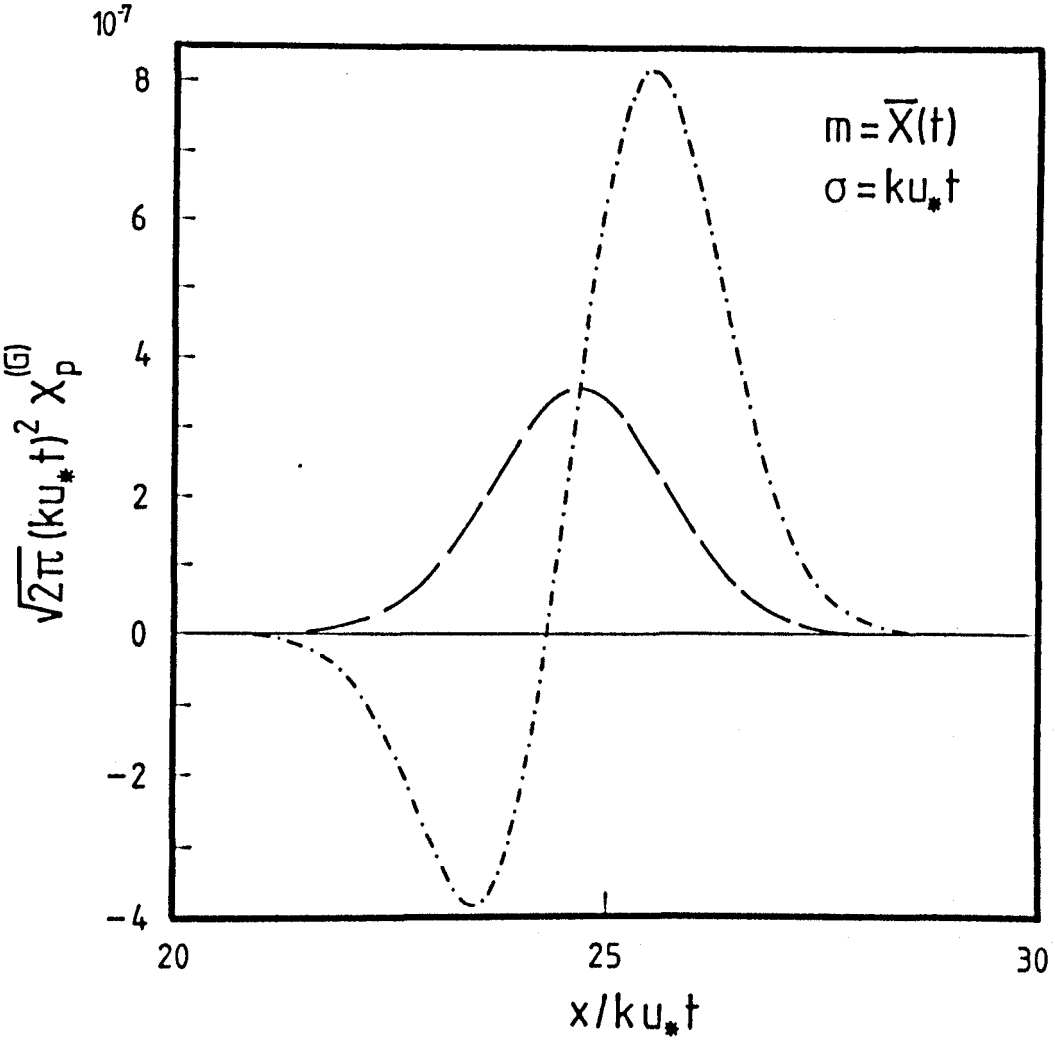

Key: — — — $X_0^{(G)}$

-·-·-·-·- $X_1^{(G)}$

Fig.4.3 Zeroth and First Order Approximations to the Horizontal Downwind Concentration from a Ground-Level Point Source at Z=375, T=250

Derived from Exact Results

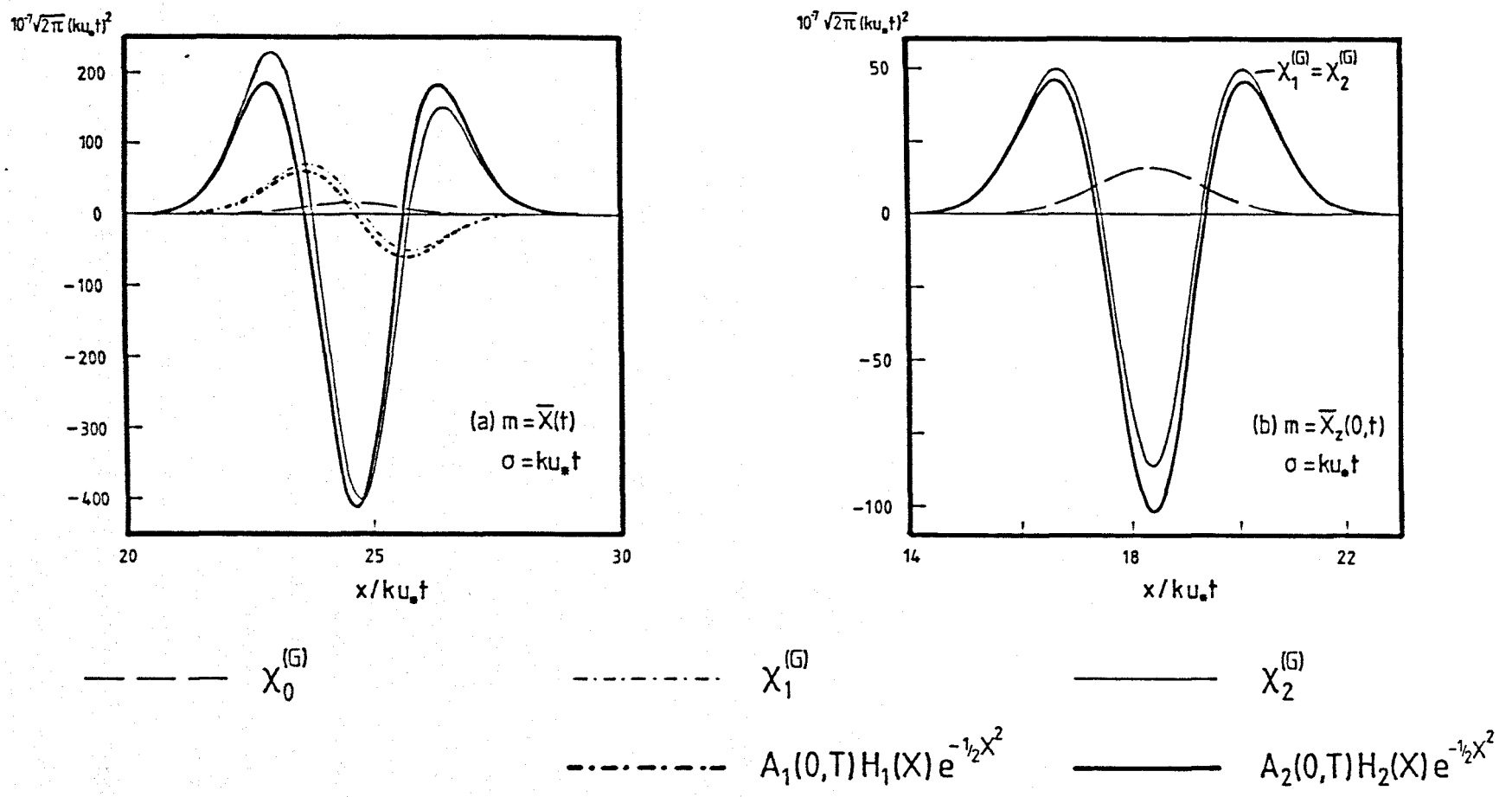

Fig.4.4 Second and Lower Order Approximations, and Contributions to the Approximations, to the Ground-Level Concentration Downwind of a Ground-Level Point Source at $T=250$

Derived from Exact Results

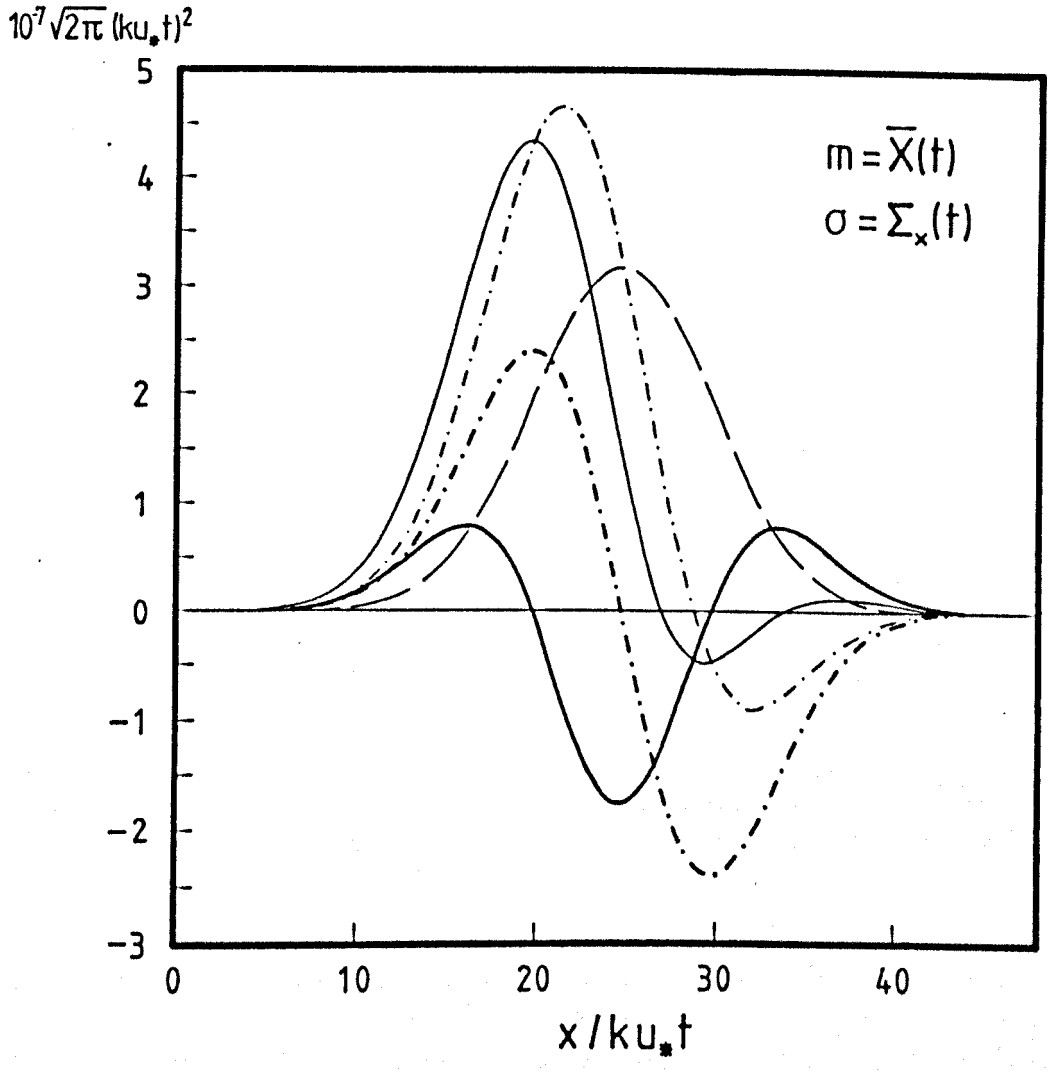

Key:

$\chi_0^{(G)}$

$\chi_1^{(G)}$

$\chi_2^{(G)}$

$A_1(0,T)H_1(X)e^{-\frac{1}{2}X^2}$

$A_2(0,T)H_2(X)e^{-\frac{1}{2}X^2}$

Fig.4.5 Second and Lower Order Approximations, and Contributions to the Approximations, to the Ground-Level Concentration Downwind of a Ground-Level Point Source at T=250

Derived from Exact Results

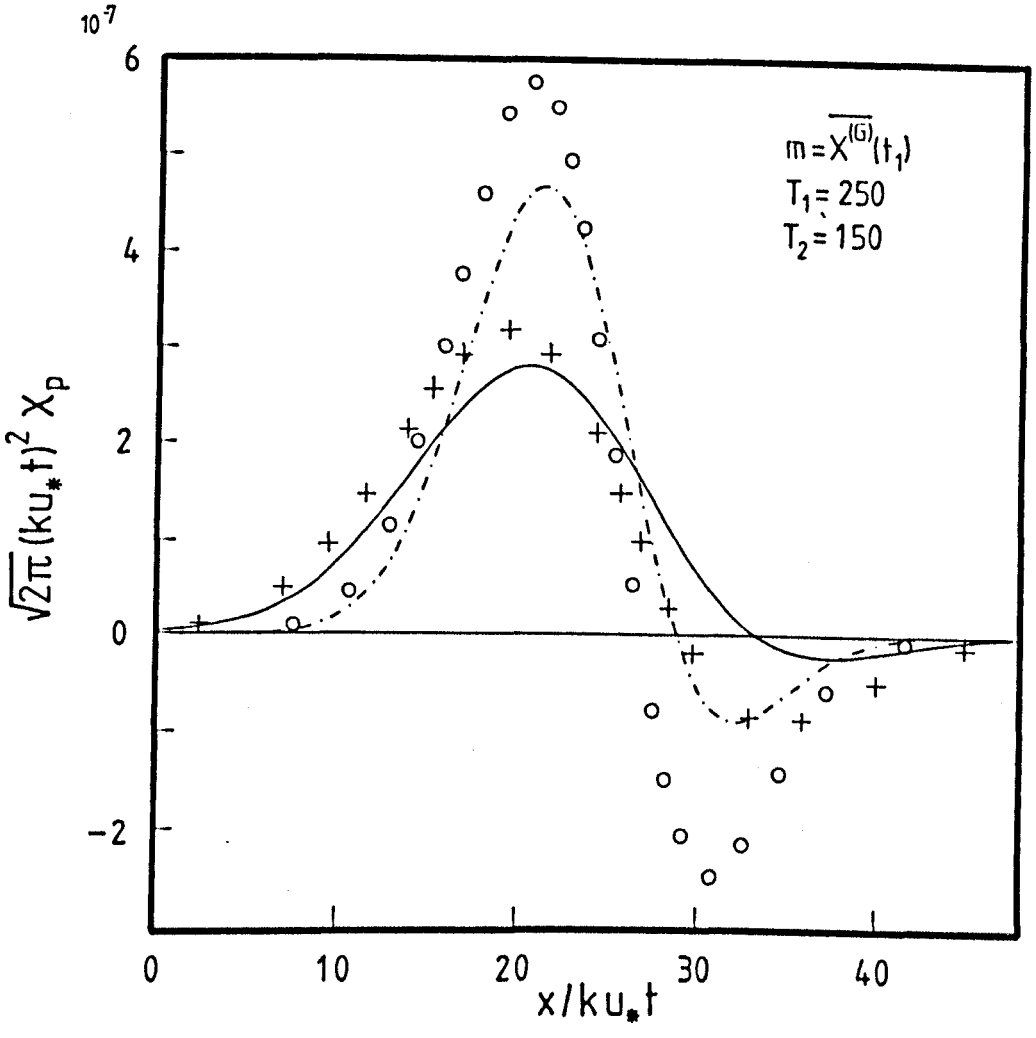

Key: $T_i = ku_* t_i / z_o$, $i = 1, 2$

-·-·-·-·-	$\chi_1^{(G)}(x,0,t_1)$	$\sigma = \Sigma_x^{(G)}(t_1)$
o	$\chi_1^{(E)}(x,0,t_2)$, $H = 100$	
———	$\chi_1^{(G)}(x,0,t_1)$	$\sigma = s_x^{(G)}(0,t_1)$
+	$\chi_1^{(E)}(x,0,t_2)$, $H = 100$	

Fig.4.6 Comparison Between Approximations to the Ground-Level Concentration Downwind of a Ground-Level and Elevated Point Source

Derived from Exact Results

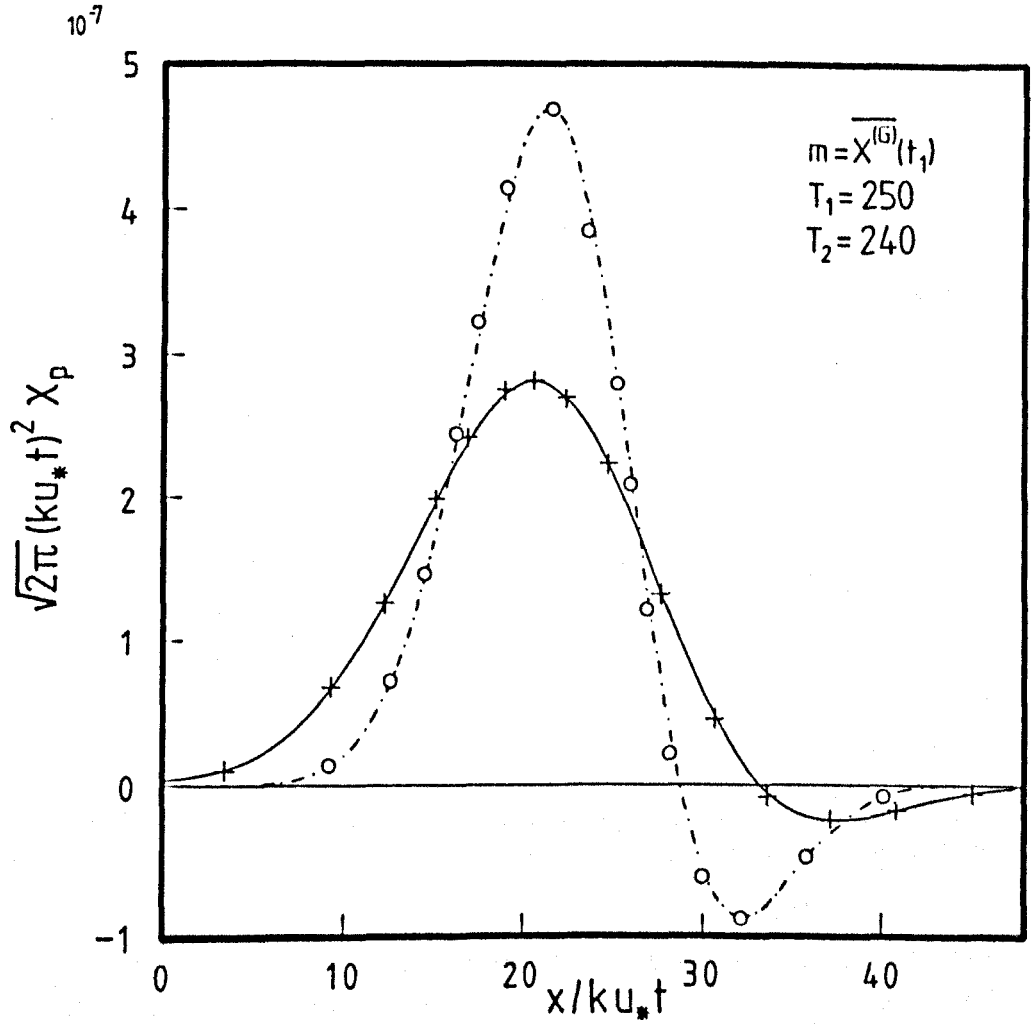

Key: $T_i = ku_* t_i / z_o$, $i = 1, 2$

-----	$X_1^{(G)}(x,0,t_1)$	$\sigma = \Sigma_x^{(G)}(t_1)$
o	$X_1^{(E)}(x,0,t_2)$, $H=10$	
———	$X_1^{(G)}(x,0,t_1)$	$\sigma = s_x^{(G)}(0,t_1)$
+	$X_1^{(E)}(x,0,t_2)$, $H=10$	

Fig.4.7 Comparison Between Approximations to the Ground-Level Concentration Downwind of a Ground-Level and Elevated Point Source

Derived from Exact Results

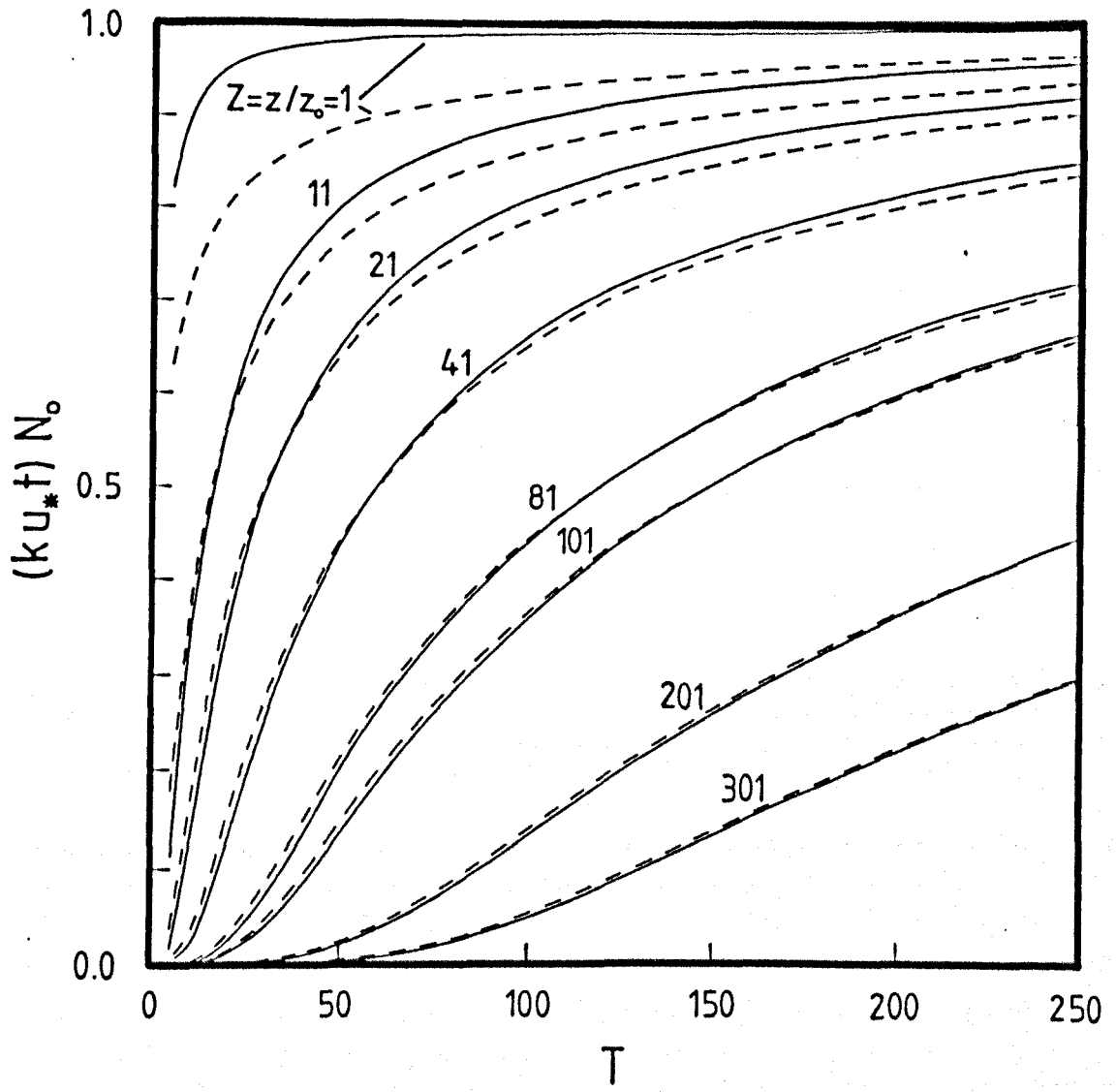

Fig.4.8 Proportion of Material, $N_o(z,t)$, at Various Fixed Heights Above the Ground

Comparison Between Exact (——) and Numerical (- - -) Results

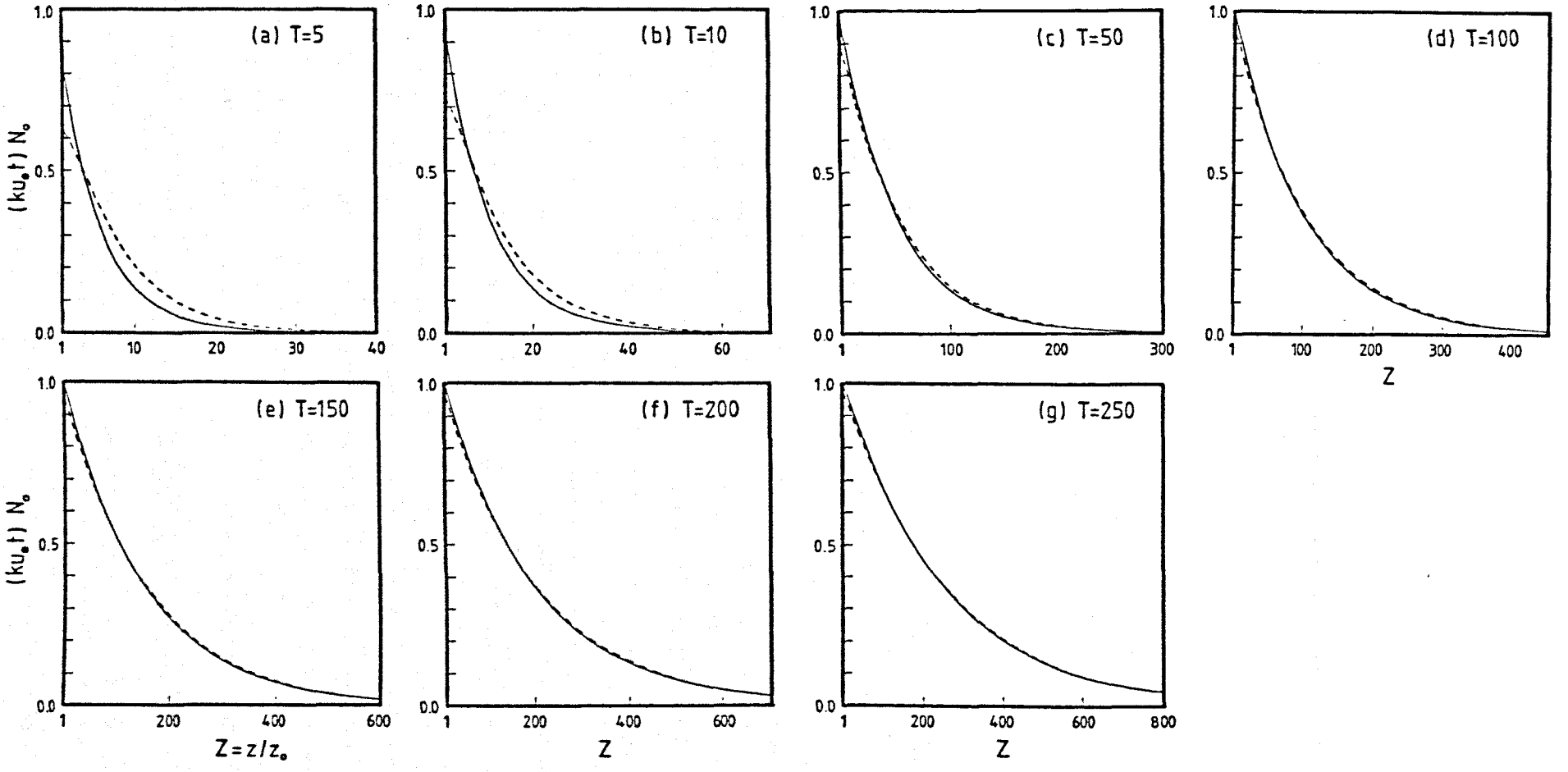

Fig.4.9 Proportion of Material, $N_o(z,t)$, at Various Fixed Times
Comparison Between Exact (——) and Numerical (- - - -) Results

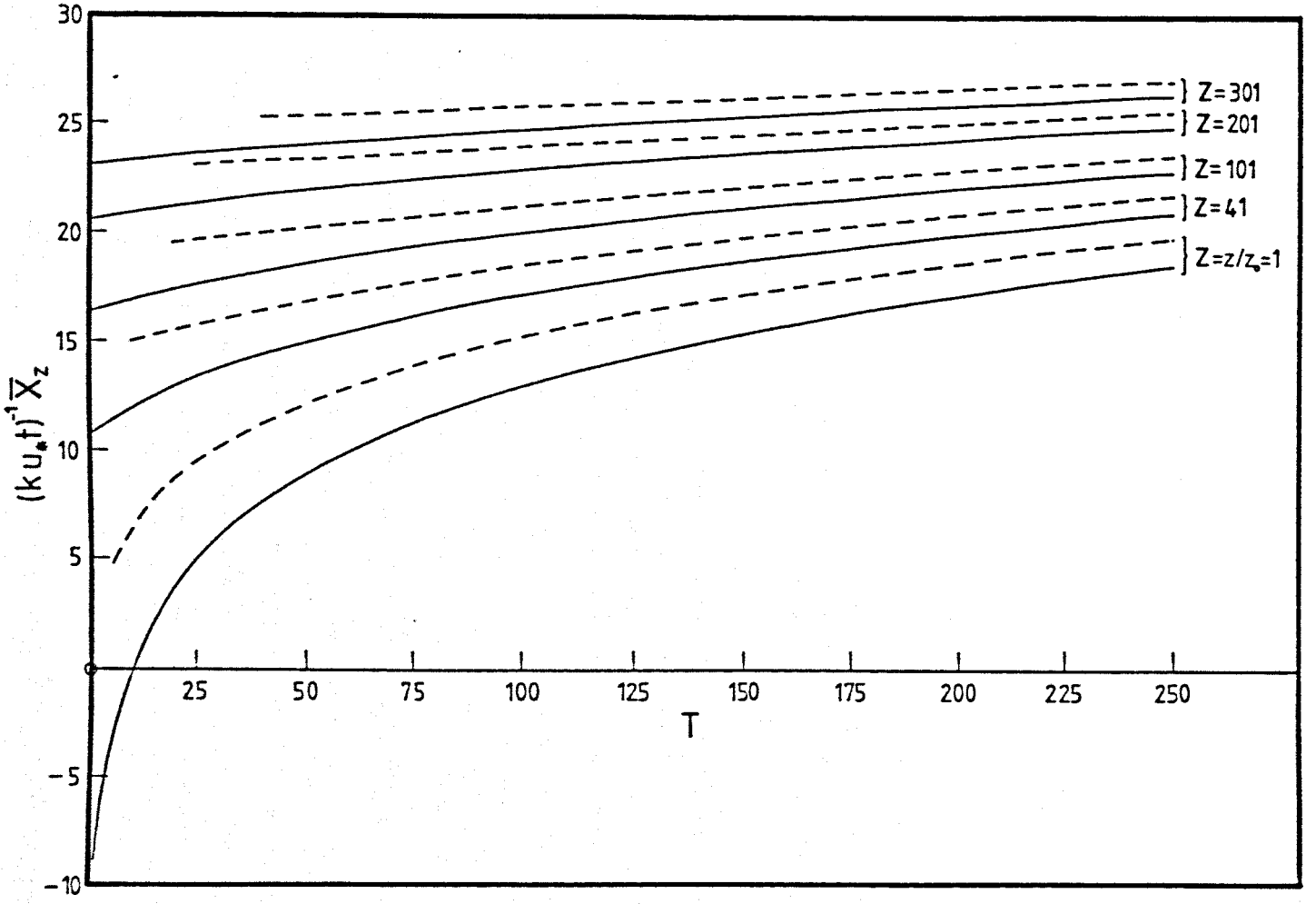

Fig.4.10 Downwind Coordinate of the Centre of Mass of Material at Various Fixed Heights Above the Ground, $\overline{X}_z(z,t)$ Comparison Between Exact (——) and Numerical (– – –) Results

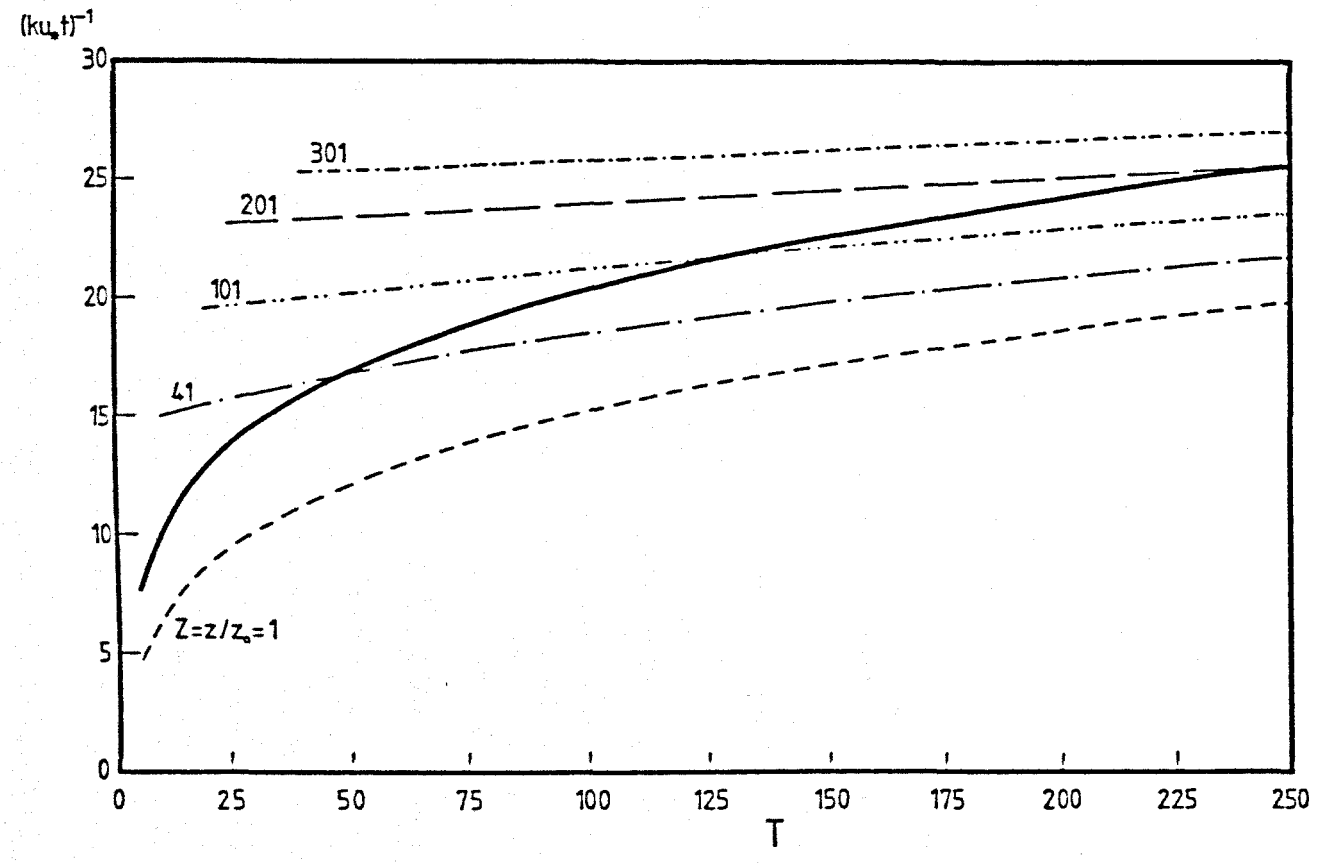

Key: $\overline{X}_z(z,t)$ – broken lines, heights as indicated $\overline{X}(t)$ – solid line (——)

Fig.4.11 Downwind Coordinate of the Centre of Mass of Material at Various Fixed Heights Above the Ground, $\overline{X}_z(z,t)$, and of the Cloud, $\overline{X}(t)$

Derived from Numerical Results

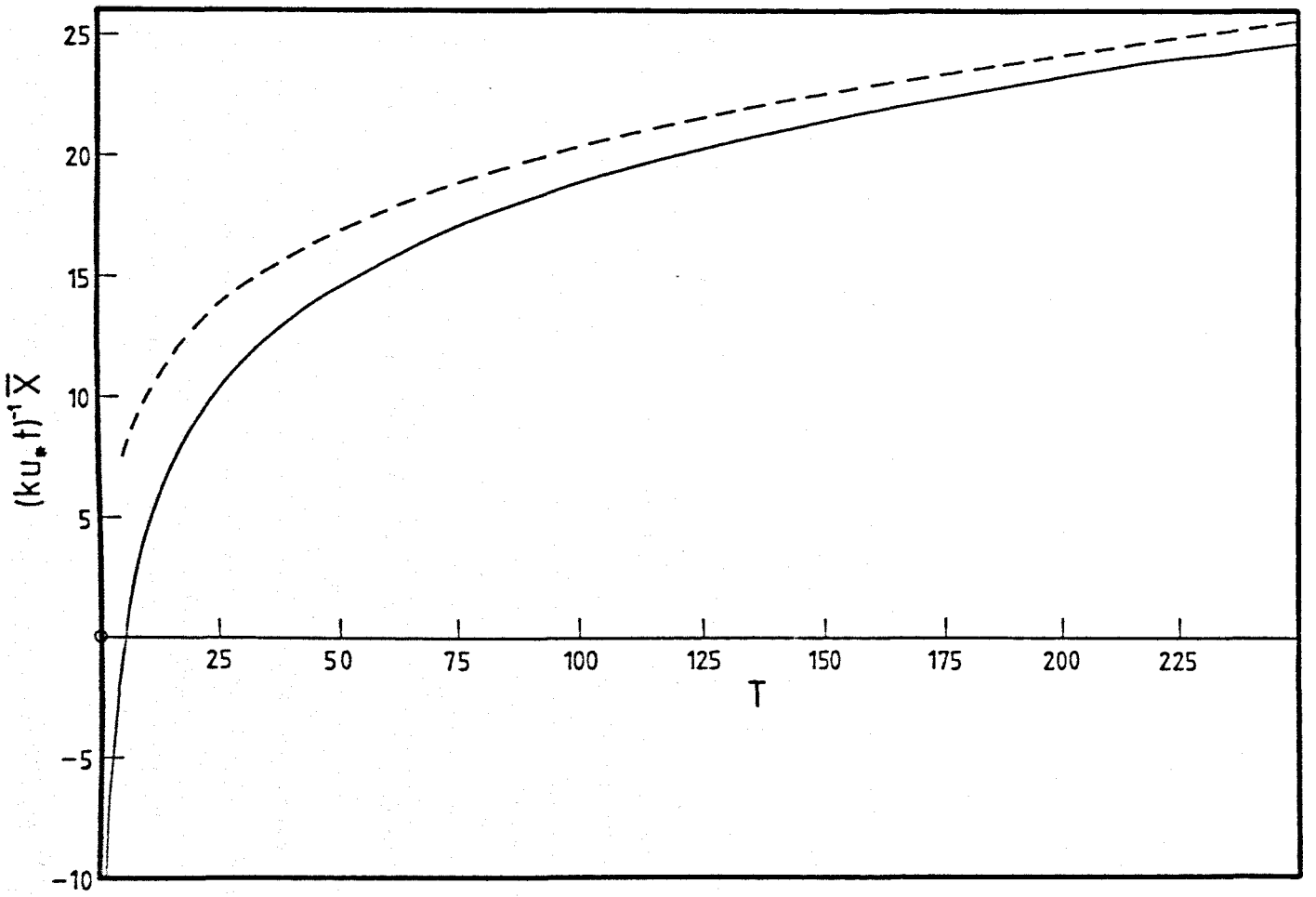

Fig.4.12 Downwind Coordinate of the Centre of Mass of the Cloud, $\overline{X}(t)$
Comparison Between Exact (——) and Numerical (– – –) Results

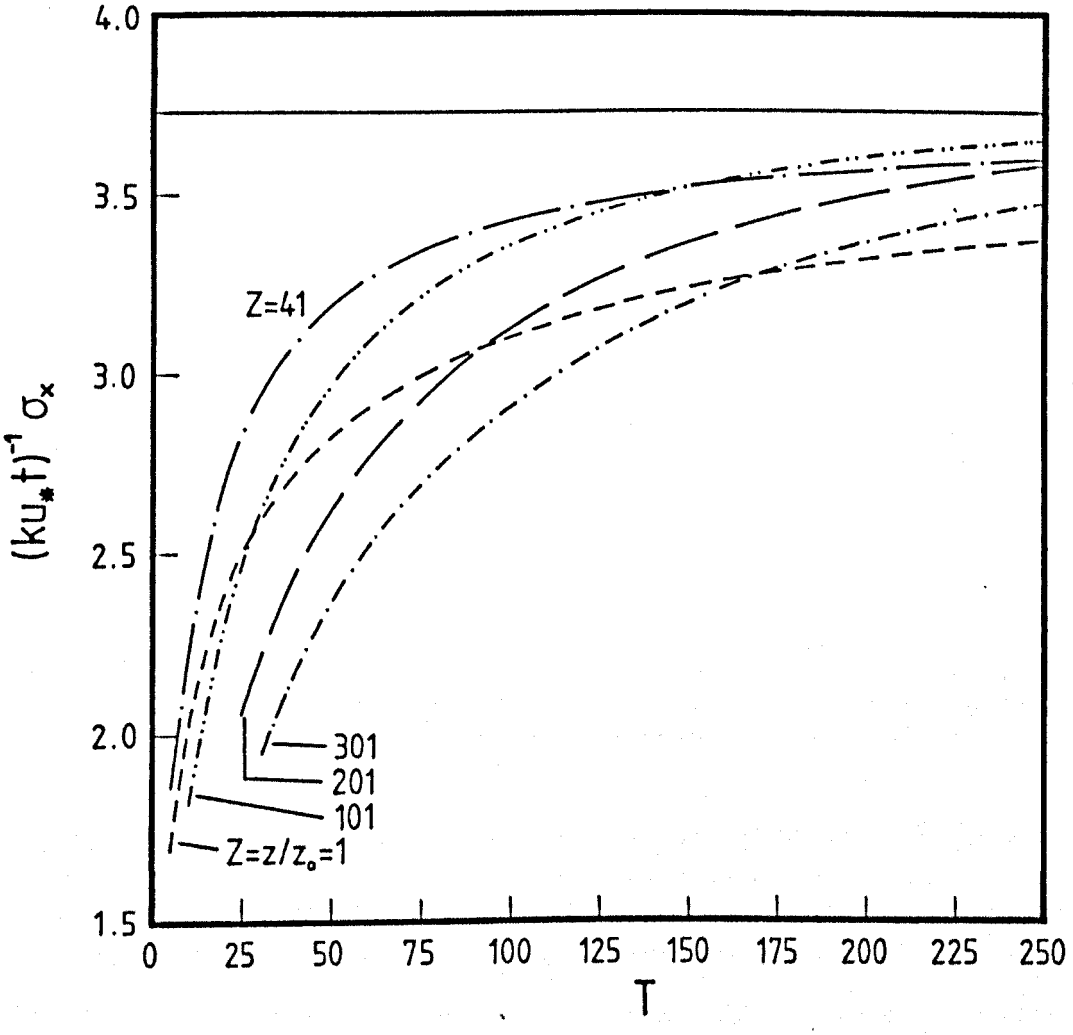

Key: numerical results - broken lines, heights as indicated
exact result - solid line (——), Z = 0

Fig.4.13 Downwind Standard Deviation of Material at Various Fixed Heights Above the Ground, About the Centre of Mass of Material at the Same Height, $\sigma_x(z,t)$

Comparison Between Exact and Numerical Results

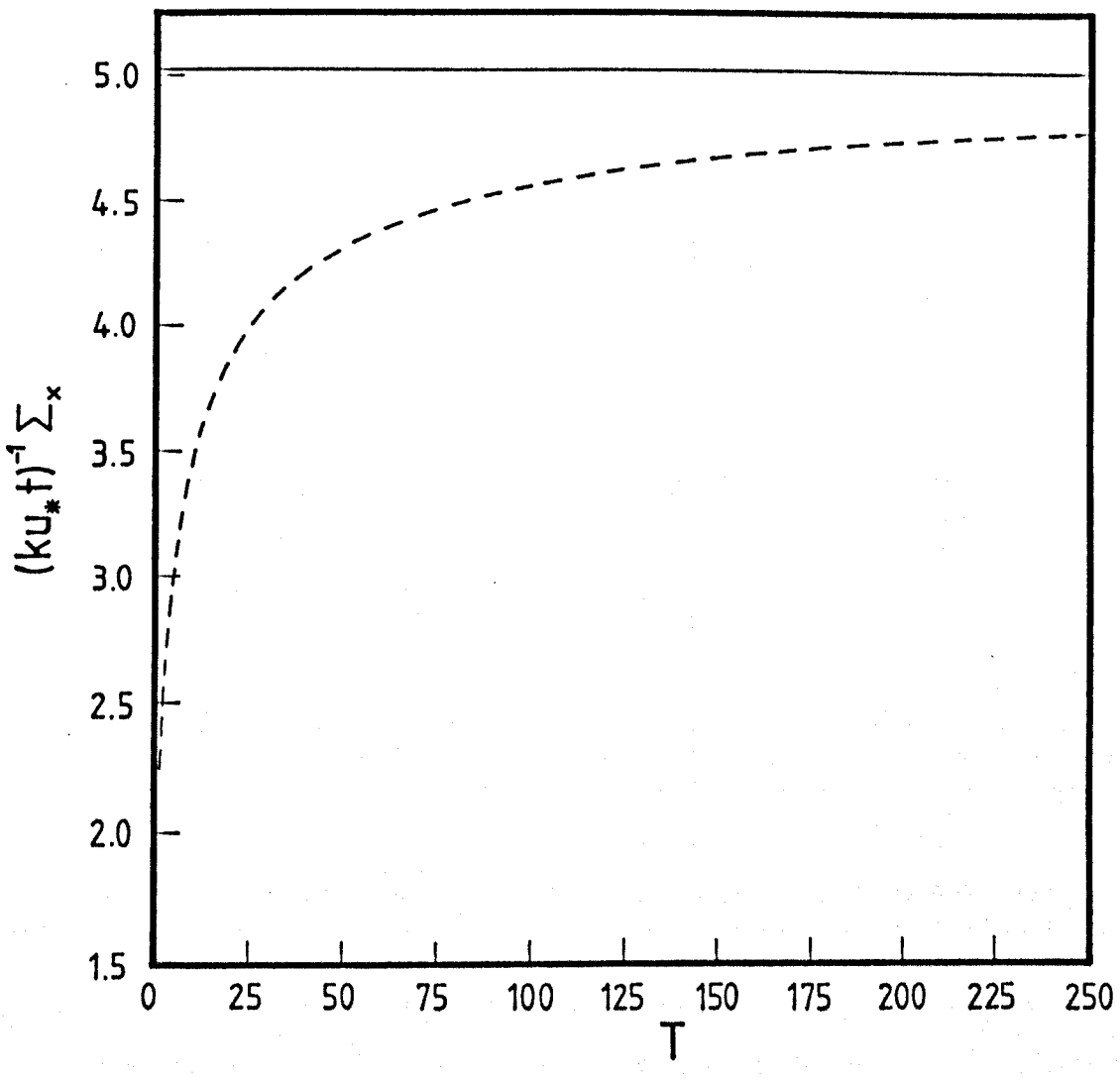

Fig.4.14 Downwind Standard Deviation of the Cloud About its Centre of Mass, $\Sigma_x(t)$

Comparison Between Exact (——) and Numerical (---) Results

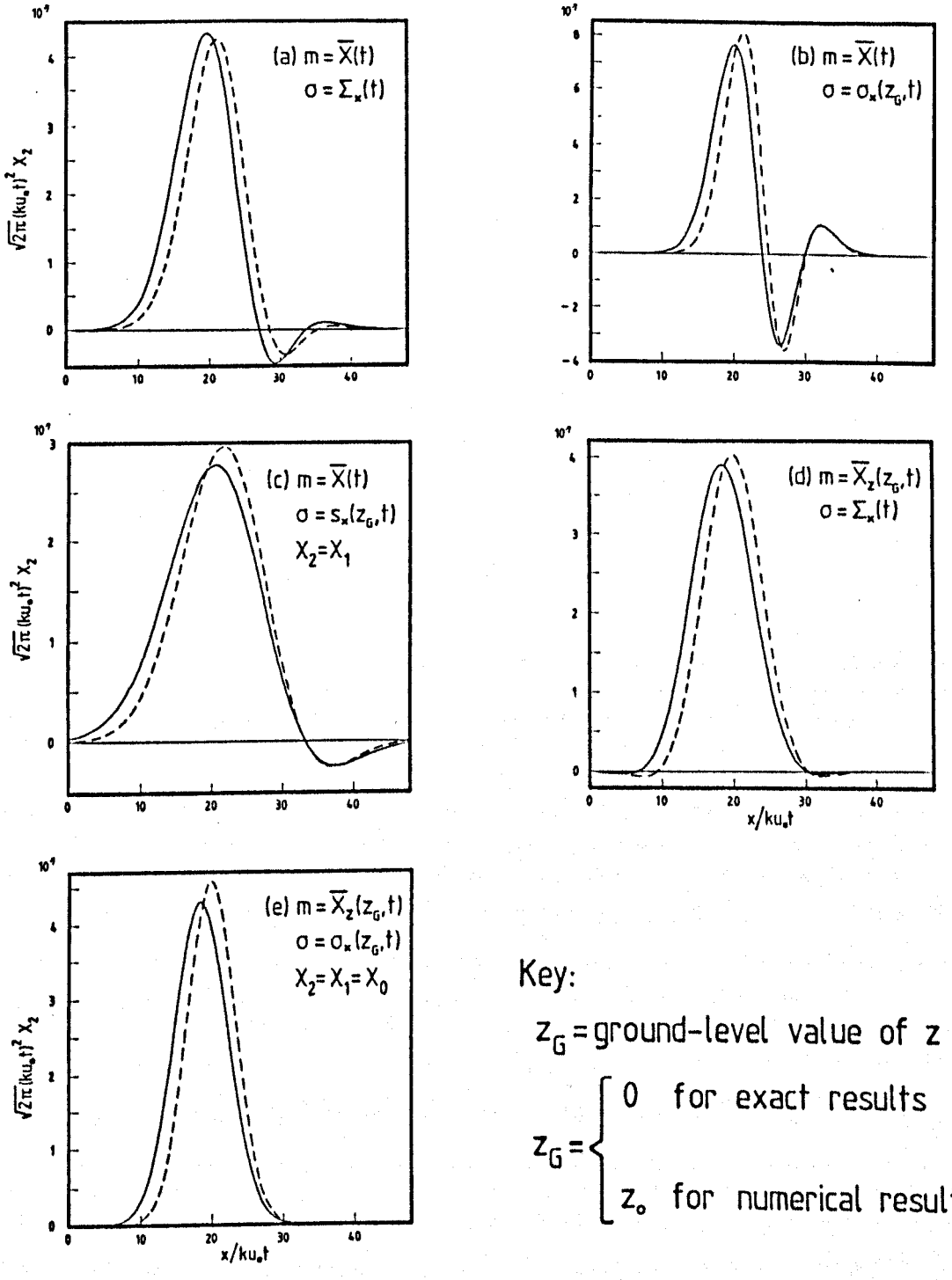

Fig.4.15 Second Order Approximations to the Ground-Level Concentration Downwind of a Ground-Level Point Source at T = 250

Comparison Between Exact (——) and Numerical (– – –) Results

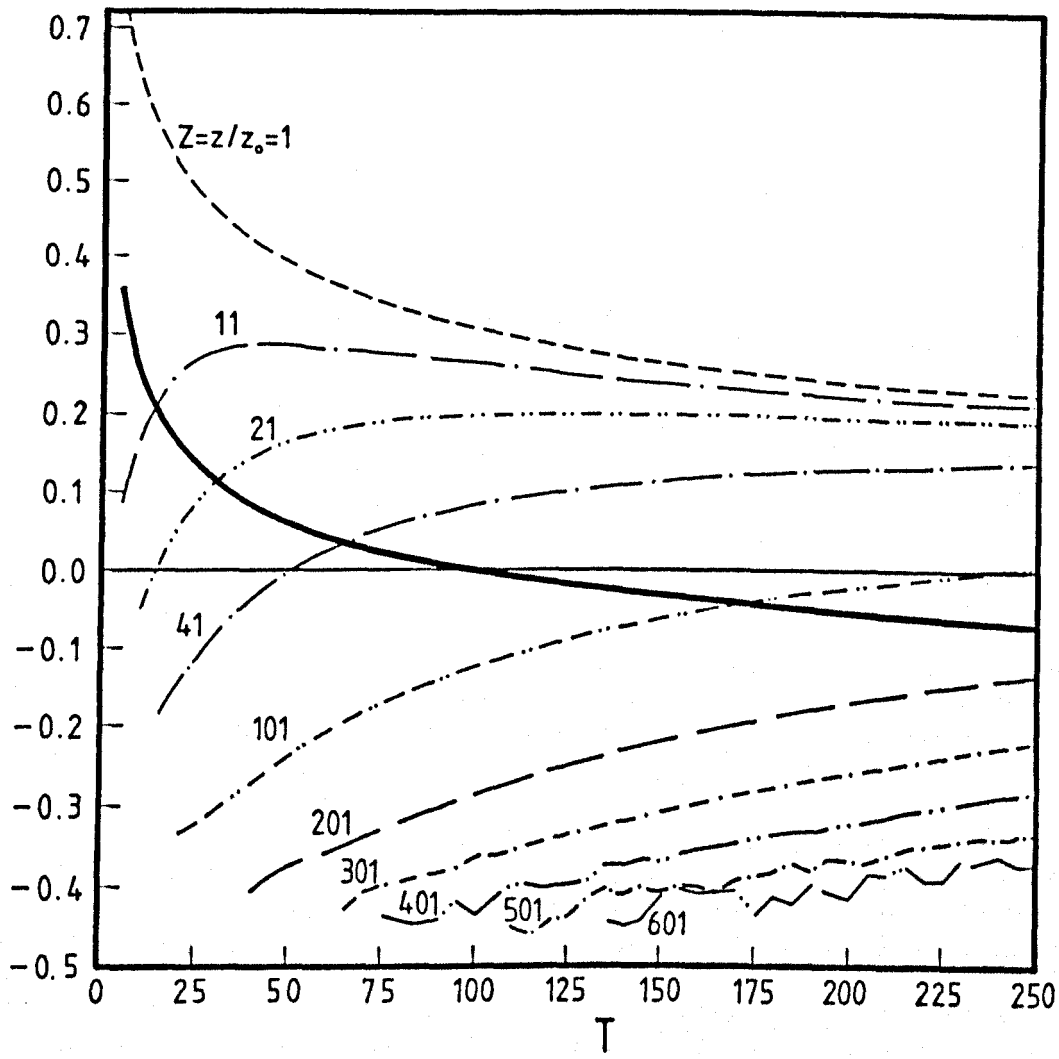

Key: $\beta_3(z,t)$ - broken lines, heights as indicated

$B_3(t)$ - solid line (——)

Fig.4.16 Downwind Skewness of Material at Various Fixed Heights Above the Ground, $\beta_3(z,t)$, and of the Cloud, $B_3(t)$

Derived from Numerical Results

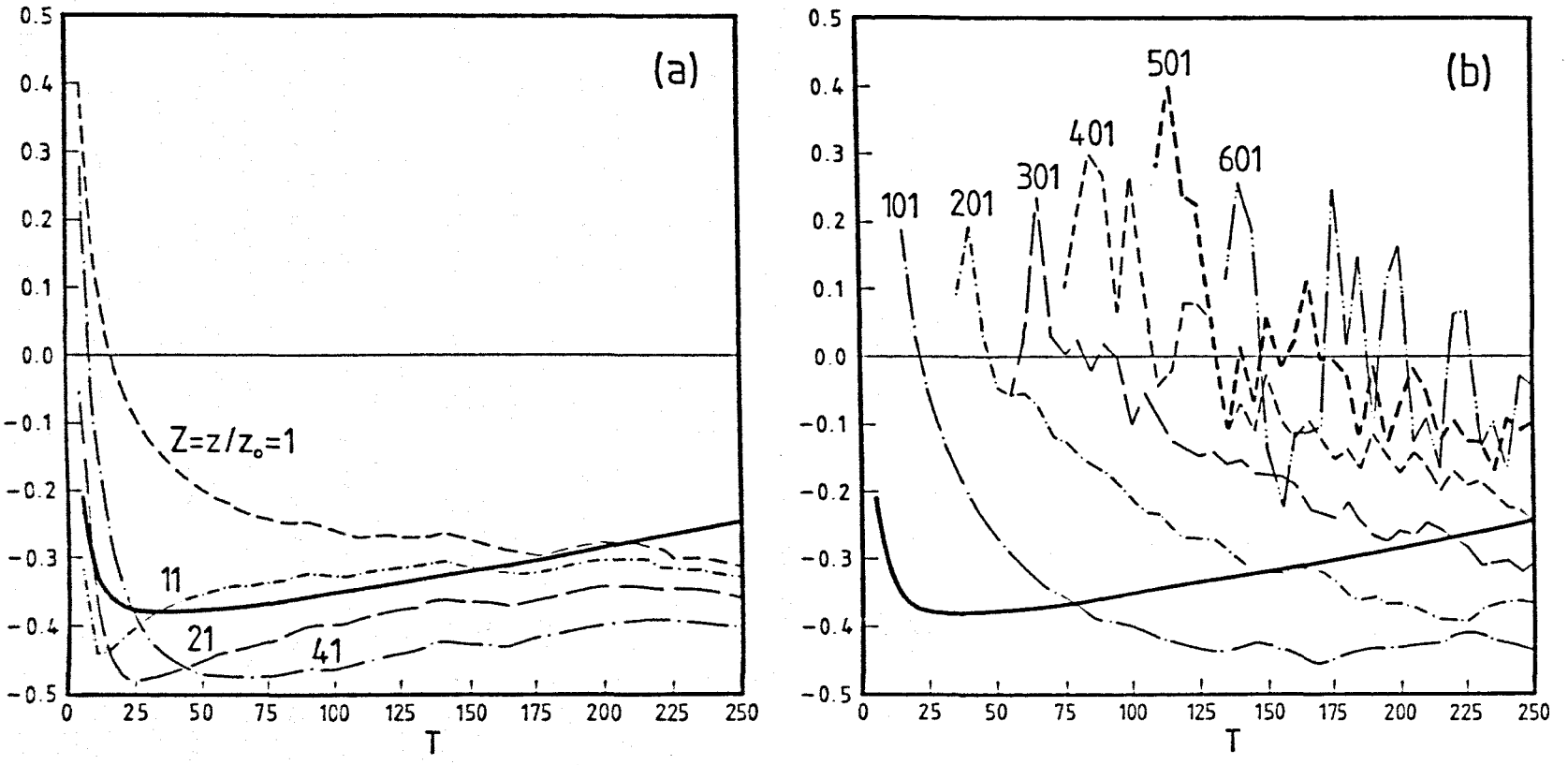

Key: $\beta_4(z,t)$ - broken lines, heights as indicated $B_4(t)$ - solid line (——)

Fig.4.17 Downwind Kurtosis of Material at Various Fixed Heights Above the Ground, $\beta_4(z,t)$, and of the Cloud, $B_4(t)$ Derived from Numerical Results

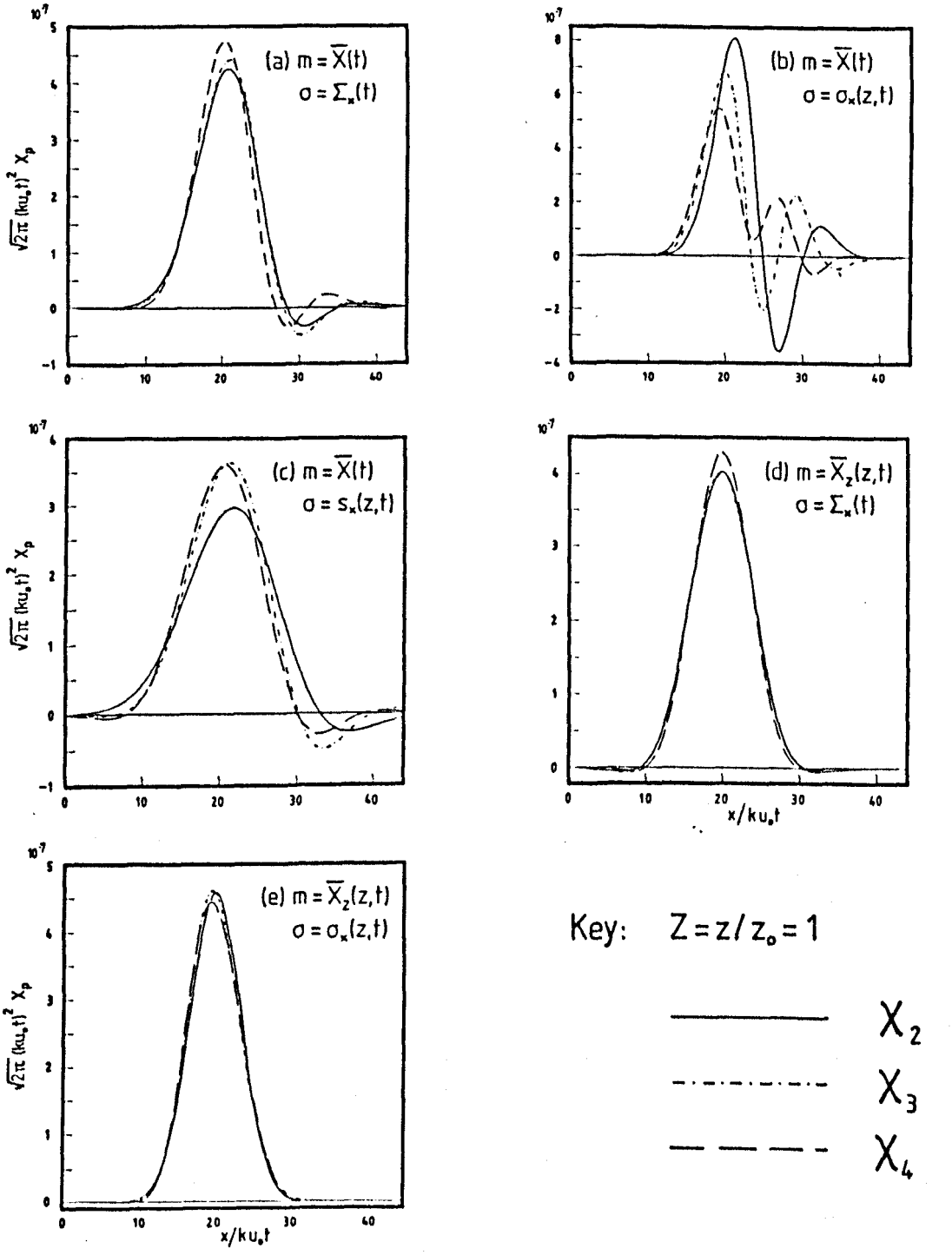

Fig.4.18 Second, Third and Fourth Order Approximations to the Ground-Level Concentration Downwind of a Ground-Level Point Source at T = 250

Derived from Numerical Results

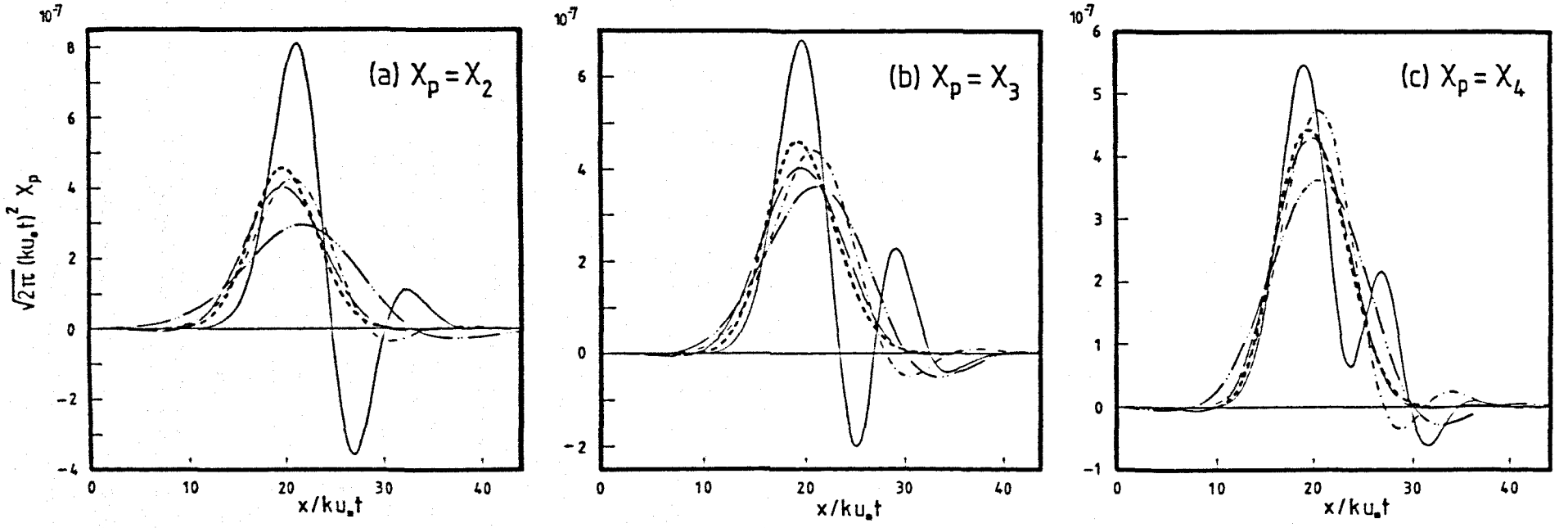

Key: $Z = z/z_o = 1$,

	m	σ		m	σ		m	σ
-·-·-·-·-	$\overline{X}(t)$	$\Sigma_x(t)$	—··—··—	$\overline{X}(t)$	$s_x(z,t)$	- - - - - - -	$\overline{X}_z(z,t)$	$\sigma_x(z,t)$
————	$\overline{X}(t)$	$\sigma_x(z,t)$	— — —	$\overline{X}_z(z,t)$	$\Sigma_x(t)$			

Fig.4.19 (a) Second, (b) Third, and (c) Fourth Order Approximations to the Ground-Level Concentration Downwind of a Ground-Level Point Source at $T = 250$

Derived from Numerical Results

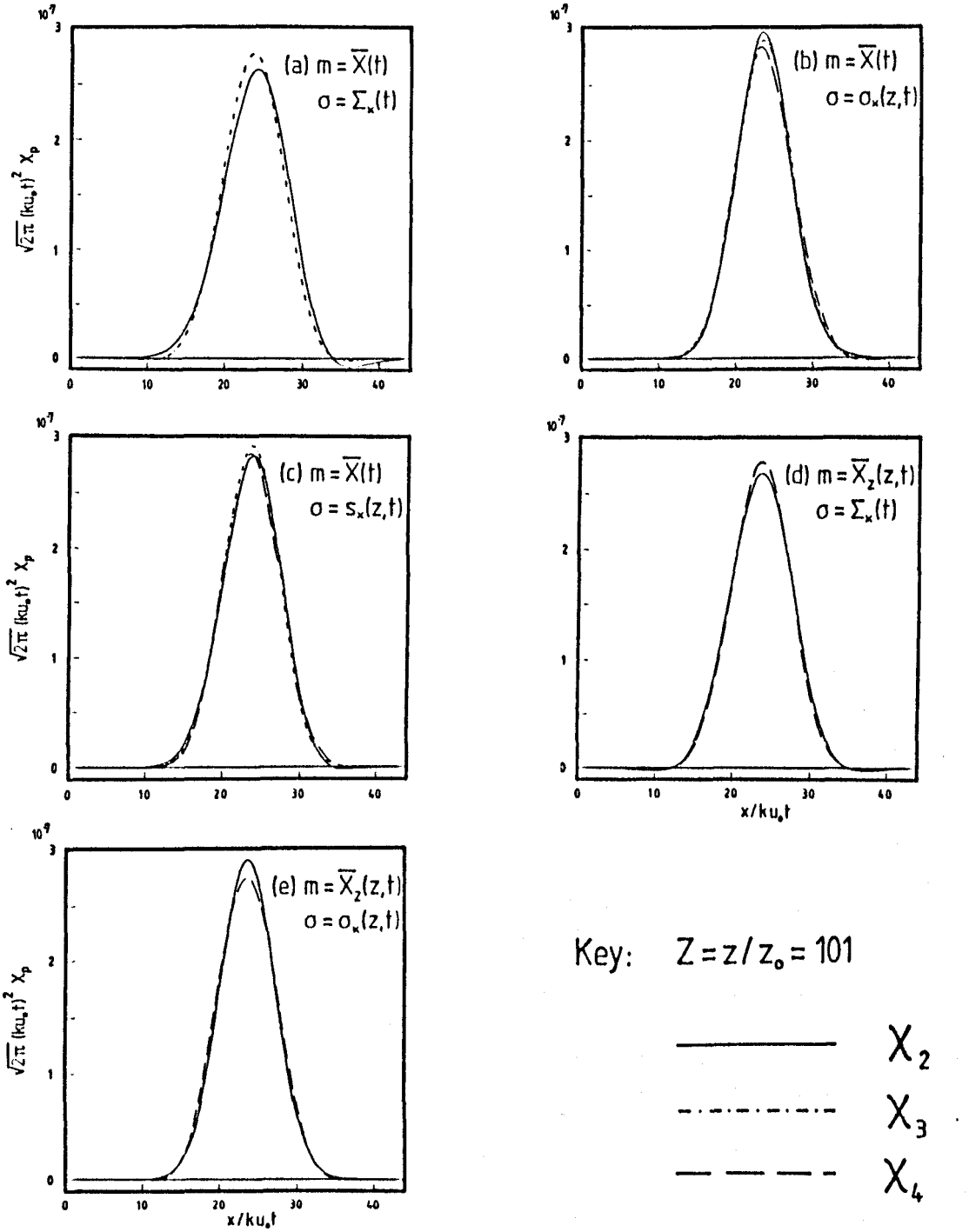

Fig.4.20 Second, Third and Fourth Order Approximations to the Elevated Horizontal Concentration Downwind of a Ground-Level Point Source at Z = 101, T = 250

Derived from Numerical Results

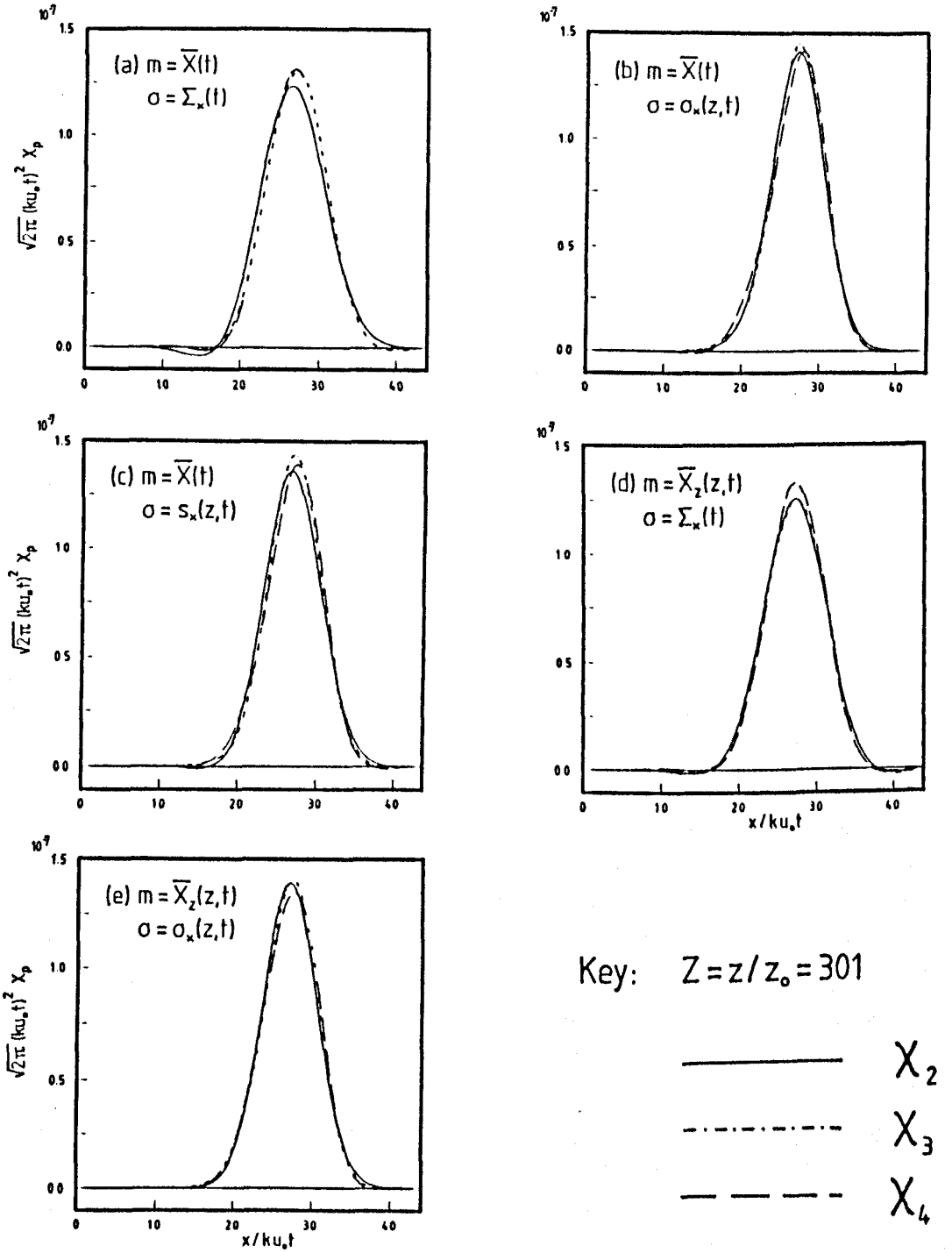

Fig.4.21 Second, Third and Fourth Order Approximations to the Elevated Horizontal Concentration Downwind of a Ground-Level Point Source at Z = 301, T = 250

Derived from Numerical Results

References

Abramowitz, M. and Stegun, I.A. (Editors), 1965, "Handbook of Mathematical Functions", U.S. National Bureau of Standards.

Aris, R., 1956, Proc. Roy. Soc. A, 235, 67-77.

Atesmen, K.M. 1972, Int. J. Heat and Mass Transfer, 15, 2271-2291.

Barton, D.E. and Dennis, K.E. 1952, Biometrika, 39, 425-427.

Batchelor, G.K. 1952, Proc. Camb. Phil. Soc., 48, 345-362.

Batchelor, G.K. 1959, J. Fluid Mech., 5, 113-133.

Batchelor, G.K. 1964, Arch. Mech. Stosowanej 3, 16, 661-670.

Batchelor, G.K. 1970, "An Introduction to Fluid Dynamics", Cambridge University Press.

Birch, A.D., Brown, D.R., Dodson, M.G. and Thomas, J.R. 1978, J. Fluid Mech., 88, 431-449.

Carn, K.K. and Chatwin, P.C. 1985, J. Haz. Mat., 11, 281-300.

Chambers, J.M. 1967, Biometrika, 54, 367-383.

Chatwin, P.C. 1968, Quart. J. Roy. Met. Soc., 94, 350-360.

Chatwin, P.C. 1970, J. Fluid, Mech., 43, 321-352.

Chatwin, P.C. 1980, J. Hydraulics Division, ASCE, 106, No.HY1, Proc. Paper 15150, 71-83.

Chatwin, P.C. 1982, J. Haz. Mat., 6, 213-230.

Chatwin, P.C. and Sullivan, P.J. 1978, "How Some New Fundamental Results on Relative Turbulent Diffusion Can be Relevant in Estuaries and Other Natural Flows", in Hydrodynamics of Estuaries and Fjords (ed. J.C.J. Nihoul), Elsevier, 233-242.

Chatwin, P.C. and Sullivan, P.J. 1979a, J. Fluid Mech., 91, 337-355.

Chatwin, P.C. and Sullivan, P.J. 1979b, J. Fluid Mech., 94, 83-101.

Chatwin, P.C. and Sullivan, P.J. 1979c, Proc. 5th Biennial Symposium on Turbulence, Rolla, Missouri, (eds. J.L. Zakin and G.K. Paterson), Scientific Press, Princeton, 211-216.

Chatwin, P.C. and Sullivan, P.J. 1980a, J. Fluid Mech., 97, 405-416.

Chatwin, P.C. and Sullivan, P.J. 1980b, Proc. 13th AIAA Fluid and Plasma Dynamics Conference, Snowmass, Colorado, Paper No. AIAA-80-1335.

Chatwin, P.C. and Sullivan, P.J. 1981, Proc. 3rd Symposium on "Turbulent Shear Flows", Sacramento, California, 9.1-9.6.

Corrsin, S. 1959, J. Geophys. Res., 64, 2134-2150.

Cramer, H.E. 1946, "Mathematical Methods of Statistics", University Press, Princeton, N.J.

Csanady, G.T. 1973 (reprinted 1980), "Turbulent Diffusion in the Environment", D. Reidel.

Erdélyi, A. (Editor) 1953, "Higher Transcendental Functions", vol.2, McGraw-Hill.

Fackrell, J.E. and Robins, A.G. 1982, J. Fluid Mech., 117, 1-26.

Frost, W. and Moulden, T.H. (Editors) 1977, "Handbook of Turbulence", vol. 1, Plenum.

Hanna, S.R. 1984a, Boundary-Layer Met., 29, 361-375.

Hanna, S.R. 1984b, Atmos. Environ., 18, 1091-1106.

Kampé de Fériet, J. 1966, David Taylor Model Basin Report 2013, Naval Ship Research and Development Center, Washington D.C.

Kendall, M.G. and Stuart, A. 1969, "The Advanced Theory of Statistics", vol.1, Griffin.

Kowe, R. 1982, The Probability Density Function of Concentration In a Turbulent Shear Flow, Ph.D. Thesis, University of Liverpool.

Kowe, R. and Chatwin, P.C. 1983, Proc. 8th Australasian Fluid Mechanics Conference, Newcastle, NSW, 3A.5-3A.8.

Kowe, R. and Chatwin, P.C. 1985, J. Engineering Mathematics, 19, 217-231.

Lockwood, F.C. and Naguib, A.S. 1975, Comb. and Flame, 24, 109-124.

Lumley, J.L. 1970, "Stochastic Tools in Turbulence", Academic Press.

Lupini, R. and Tirabassi, T. 1983, Atmos. Environ., 17, 965-971.

Mihaila, I.M. 1968, Rev. Roum. Math. Pures et Appl., 13, 803-813.

Monin, A.S. and Yaglom, A.M. 1971, "Statistical Fluid Mechanics", vol.1 (ed. J.L. Lumley), MIT Press.

Monin, A.S and Yaglom, A.M. 1975, "Statistical Fluid Mechanics", vol.2 (ed. J.L. Lumley), MIT Press

Panofsky, H.A. and Dutton, J.A. 1984, "Atmospheric Turbulence", Wiley-Interscience.

Pasquill, F. and Smith, F.B. 1983, "Atmospheric Diffusion" (3rd ed.) Ellis Horwood.

Reynolds, O. 1894, Phil. Trans. Roy. Soc. Lond., 186, 123-161.

Richardson, L.F. 1926, Proc. Roy. Soc. A, 110, 709-737.

Richtmyer, R.D. and Morton, K.W. 1967, "Difference Methods for Initial-Value Problems" (2nd ed.), Interscience.

Saffman, P.G. 1960, J. Fluid Mech., 8, 273-283.

Saffman, P.G. 1962, Quart. J. Roy. Met. Soc., 88, 382-393.

Saffman, P.G. 1963, J. Fluid Mech., 16, 545-572.

Sawford, B.L. and Hunt, J.C.R. 1986, J. Fluid Mech., 165, 373-400.

Sawford, B.L. and Stapountzis, H. 1986, Boundary-Layer Met., 37, 89-105.

Smith, F.B. 1957, J. Fluid Mech., 2, 49-76.

Smith, R. 1978, J. Fluid Mech., 88, 323-337.

Smith, R. 1982a, J. Fluid Mech., 123, 131-142.

Smith, R. 1982b, Q.J. Mech. Appl. Math., 35, 345-366.

Smith, R. 1982c, IMA J. Appl. Mathematics, 28, 149-160.

Smith, R. 1985, J. Fluid Mech., 152, 217-233.

Sullivan, P.J. 1971, J. Fluid Mech., 47, 601-607.

Sullivan, P.J. 1975, Mem. Soc. Roy. Sci. Liège, 6^{e} Serie, 7, 253-260.

Sullivan, P.J. 1976, ZAMP, 27, 727-732.

Sullivan, P.J. 1983a, Proc. 7th Biennial Symposium on Turbulence (eds. J.L. Zakin and G.K. Paterson), Univ. of Miss. Press, 92-98.

Sullivan, P.J. 1983b, "Mathematical Modelling in Science and Technology", Proc. 4th ICMM, Zurich, Switzerland, 622-626.

Sullivan, P.J. and Yip, H. 1985, ZAMP, 36, 596-608.

Sullivan, P.J. and Yip, H. 1987, ZAMP, 38, 409-423.

Sykes, R.I., Lewellen, W.S. and Parker, S.F. 1984, J. Fluid Mech., 139, 193-218.

Taylor, G.I. 1921, Proc. Lond. Math. Soc. (2), 20, 196-212.

Taylor, G.I. 1953, Proc. Roy. Soc. A, 219, 186-203.

Taylor, G.I. 1954a, Proc. Roy. Soc. A, 223, 446-468.

Taylor, G.I. 1954b, Proc. Roy. Soc. A, 225, 473-477.

Townsend, A.A. 1951, Proc. Roy. Soc. A, 209, 418-430.

Wilson, D.J., Robins, A.G. and Fackrell, J.E. 1985, Atmos. Environ. 19, 1053-1064.

Yaglom, A.M. 1976, Fluid Mech. Sov.-Res., 5, 73-87.

APPENDIX A

A Generalised Three Dimensional Hermite Series Representation

This appendix summarises some relevant properties of three dimensional Hermite polynomials and derives expressions for the coefficients of a generalised three dimensional Hermite series representation. Many of the equations are applicable to n-dimensional Hermite polynomials, further details are given by Erdélyi (1953).

Define positive-definite, symmetric, quadratic forms $\phi(\underline{w},\underline{\underline{\Psi}})$ and $\Phi(\underline{W},\underline{\underline{\Psi}})$

$$\phi(\underline{w},\underline{\underline{\Psi}}) = \Psi_{ij}w_iw_j \; ; \quad \Psi_{ij} = \Psi_{ji} \; ; \quad \Psi_{ii} > 0$$

$$\Phi(\underline{W},\underline{\underline{\Psi}}) = \Psi_{ij}W_iW_j \; ; \quad \Psi_{ij} = \Psi_{ji} \; ; \quad \Psi_{ii} > 0$$

such that

$$\left.\begin{aligned} W_i &= \frac{1}{2}\frac{\partial\phi}{\partial w_i} = \Psi_{ij}w_j \\ w_i &= \frac{1}{2}\frac{\partial\Phi}{\partial W_i} = \Psi_{ij}W_j \end{aligned}\right\} \Psi_{ij}\Psi_{jk} = \delta_{ik}$$

so that

$$\phi(\underline{w},\ \underline{\underline{\Psi}}) = \Phi(\underline{W},\underline{\underline{\Psi}})$$

The complete biorthogonal set of Hermite polynomials $\left\{H^{(n)}_{ij\ldots k}(\underline{w},\underline{\underline{\Psi}}),\ G^{(n)}_{ij\ldots k}(\underline{w},\underline{\underline{\Psi}});\ \ n=1,2,\ldots\right\}$ is defined by

$$H^{(n)}_{ij\ldots k}(\underline{w},\underline{\underline{\Psi}}) = (-1)^n \exp\left\{+\frac{1}{2}\Phi(\underline{w},\underline{\underline{\Psi}})\right\} \frac{\partial^n}{\partial w_i \partial w_j \ldots \partial w_k} \exp\left\{-\frac{1}{2}\Phi(\underline{w},\underline{\underline{\Psi}})\right\} \tag{A1}$$

$$G^{(n)}_{ij\ldots k}(\underline{w},\underline{\underline{\Psi}}) = (-1)^n \exp\left\{+\frac{1}{2}\Phi(\underline{W},\underline{\underline{\Psi}})\right\} \frac{\partial^n}{\partial W_i \partial W_j \ldots \partial W_k} \exp\left\{-\frac{1}{2}\Phi(\underline{W},\underline{\underline{\Psi}})\right\} \tag{A2}$$

where n represents the number of subscripts $i,j,\ldots,k$. Although not conventional, on the left hand side of (A1) and (A2) it is important for this work to denote the functional dependency of the polynomials on the tensor $\underline{\underline{\Psi}}$.

The expressions for the first few polynomials are

$$H^{(0)} = G^{(0)} = 1$$

$$H^{(1)}_i = \Psi_{ij} w_j = W_i \; ; \quad G^{(1)}_i = \Psi_{ij} W_j = w_i$$

$$H^{(2)}_{ij} = \Psi_{ip}\Psi_{jq} w_p w_q - \Psi_{ij} = W_i W_j - \Psi_{ij} \tag{A3}$$

$$G^{(2)}_{ij} = \Psi_{ip}\Psi_{jq} W_p W_q - \Psi_{ij} = w_i w_j - \Psi_{ij}$$

$$H^{(3)}_{ijk} = W_i W_j W_k - (\Psi_{ij} W_k + \Psi_{ik} W_j + \Psi_{jk} W_i)$$

$$G^{(3)}_{ijk} = w_i w_j w_k - (\Psi_{ij} w_k + \Psi_{ik} w_j + \Psi_{jk} w_i)$$

$$H^{(4)}_{ijkl} = W_iW_jW_kW_l - (\Psi_{ij}W_kW_l + \Psi_{ik}W_jW_l + \Psi_{il}W_jW_k + \Psi_{jk}W_iW_l + \Psi_{jl}W_iW_k + \Psi_{kl}W_iW_j) + (\Psi_{ij}\Psi_{kl} + \Psi_{ik}\Psi_{jl} + \Psi_{il}\Psi_{jk})$$

(A3)(contd.)

$$G^{(4)}_{ijkl} = w_iw_jw_kw_l - (\Psi_{ij}w_kw_l + \Psi_{ik}w_jw_l + \Psi_{il}w_jw_k + \Psi_{jk}w_iw_l + \Psi_{jl}w_iw_k + \Psi_{kl}w_iw_j) + (\Psi_{ij}\Psi_{kl} + \Psi_{ik}\Psi_{jl} + \Psi_{il}\Psi_{jk}) .$$

The polynomials are symmetric in their subscripts and

$$G^{(n)}_{ij\ldots k}(\underline{w},\underline{\Psi}) = H^{(n)}_{ij\ldots k}(\underline{W},\underline{\Psi}) .$$

The biorthogonal property of the polynomials may be written

$$n(\underline{\Psi}) \int H^{(n)}_{ij\ldots k}(\underline{w},\underline{\Psi})\, G^{(m)}_{pq\ldots r}(\underline{w},\underline{\Psi})\, \exp\left\{-\frac{1}{2}\phi(\underline{w},\underline{\Psi})\right\} dV(\underline{w})$$

$$= \begin{cases} n! & \text{if } n=m \text{ and } ij\ldots k \text{ is a permutation of } pq\ldots r \\ 0 & \text{otherwise} \end{cases} \qquad \text{(A4)}$$

where

$$n(\underline{\Psi}) = (2\pi)^{-3/2}\,[\Delta(\underline{\Psi})]^{1/2} \qquad \text{(A5)}$$

and $\Delta(\underline{\Psi})$ is the determinant of $\underline{\Psi}$, i.e.

$$\Delta(\underline{\Psi}) = \frac{1}{6}\,\varepsilon_{ijk}\varepsilon_{pqr}\,\Psi_{ip}\Psi_{jq}\Psi_{kr} \qquad \text{(A6)}$$

where ε_{ijk} is the Levi-Civita density or permutation symbol.

Consider any well behaved function $\Lambda(\underline{w})$ with moments of all orders defined by

$$S^{(n)}_{ij\ldots k} = \int w_i w_j \ldots w_k \, \Lambda(\underline{w}) \, dV(\underline{w}) \, . \tag{A7}$$

Represent $\Lambda(\underline{w})$ by the following generalised three dimensional Hermite series

$$\Lambda(\underline{w}) = n(\underline{\Psi}) \sum_{m=0}^{\infty} C^{(m)}_{ij\ldots k} H^{(m)}_{ij\ldots k}(\underline{w},\underline{\Psi}) \exp\left\{-\frac{1}{2}\phi(\underline{w},\underline{\Psi})\right\} \, . \tag{A8}$$

Multiplying both sides of (A8) by $G^{(n)}_{pq\ldots r}(\underline{w},\underline{\Psi})$, integrating over $\underline{w}$ and using (A4), the following expression for the coefficients $C^{(n)}_{ij\ldots k}$, n=1,2,...., of the series is obtained

$$C^{(n)}_{ij\ldots k} = \frac{1}{n!} \int G^{(n)}_{ij\ldots k}(\underline{w},\underline{\Psi}) \, \Lambda(\underline{w}) \, dV(\underline{w}) \, . \tag{A9}$$

For example, using (A3) and (A7)

$$C^{(0)} = S^{(0)} \tag{A10}$$

$$C^{(1)}_i = S^{(1)}_i \tag{A11}$$

$$C^{(2)}_{ij} = \frac{1}{2}\left\{S^{(2)}_{ij} - \Psi_{ij} S^{(0)}\right\} \tag{A12}$$

$$C^{(3)}_{ijk} + \frac{1}{3!}\left\{S^{(3)}_{ijk} - (\Psi_{ij} S^{(1)}_k + \Psi_{ik} S^{(1)}_j + \Psi_{jk} S^{(1)}_i)\right\} \, . \tag{A13}$$

APPENDIX B

Analytic Expressions for Some Measures of Location and Spread of the Cloud

Using the model for dispersion in the atmospheric surface layer detailed in Chapter 4, this appendix summarises the expressions available for the measures of location and spread of a cloud of material.

Chatwin (1968) has shown that $\bar{Z}(t)$ defined by (4.71a) is given by

$$\bar{Z}(t) = ku_* t \left[1 + \frac{H}{T}\right] \tag{B1}$$

and that $\bar{X}(t)$ defined by (4.71b) satisfies

$$\frac{d\bar{X}}{dt} = \frac{u_*}{k} \left\{\log_e H + E_1\left[\frac{H}{T}\right]\right\} \tag{B2}$$

where $E_1(x)$ is the exponential integral function defined for all positive x by (Abramowitz and Stegun 1965, p228)

$$E_1(x) = \int_x^\infty \frac{\exp(-t)}{t}\, dt = -\gamma - \log_e x + \sum_{n=1}^{\infty} \frac{(-1)^n x^n}{n.n!} \tag{B3}$$

and γ is Euler's constant given by

$$\gamma = \lim_{m\to\infty} \left(1 + \frac{1}{2} + \frac{1}{3} + \ldots + \frac{1}{m} - \log_e m\right) = 0.5772\ldots . \tag{B4}$$

Equation (B2) may be integrated by parts to give

$$\bar{X}(t) = \frac{u_* t}{k} \left\{ E_1\left[\frac{H}{T}\right] \left[1 + \frac{H}{T}\right] + \log_e\left[\frac{H}{T}\right] - \exp\left[-\frac{H}{T}\right] \right\} \qquad (B5)$$

which for a ground-level source simplifies to

$$\bar{X}^{(G)}(t) = \frac{u_* t}{k} \left\{ \log_e T - (\gamma + 1) \right\} \qquad (B6)$$

consistent with Chatwin (1968). For a ground-level source $\bar{X}_z(z,t)$ defined by (4.71c) is given by (Chatwin 1968, Equations (23), (29), (30) and (37))

$$\bar{X}_z^{(G)}(z,t) = \frac{u_* t}{k} \left\{ E_1\left[\frac{Z}{T}\right] \exp\left[\frac{Z}{T}\right] + \log_e Z - 2 \right\} . \qquad (B7)$$

Thus using the reciprocal theorem (Smith 1957) which shows that the horizontal distribution of material at the ground from an elevated source, height h, is the same as the horizontal distribution of material at height h from a ground-level source

$$\bar{X}_z^{(E)}(0,t) = \frac{u_* t}{k} \left\{ E_1\left[\frac{H}{T}\right] \exp\left[\frac{H}{T}\right] + \log_e H - 2 \right\} . \qquad (B8)$$

In (B7) and (B8) the superscripts (G) and (E) have been used, as they are in Chapter 4, to denote ground-level and elevated sources respectively.

Lastly, for Σ_x, σ_x and s_x defined by (4.72), the following results for a ground-level source are available (Chatwin 1968)

$$\Sigma_x^{(G)}(t) = \frac{u_* t}{k} \sqrt{\left(\frac{\pi^2}{6} - 1\right)}$$

$$\sigma_x^{(G)}(0,t) = \frac{u_* t}{k} \sqrt{\left(2 - \frac{\pi^2}{6}\right)} \qquad \text{(B9)}$$

$$s_x^{(G)}(0,t) = \frac{u_* t}{k} \sqrt{\left(3 - \frac{\pi^2}{6}\right)} \ .$$